1998

# I. Metabolic modeling of glucose metabolism in Rhizopus oryzae and II. The effect of transcription on starvation-induced mutations in Escherichia coli

Angelika Longacre
*The University of Montana*

# INFORMATION TO USERS

This manuscript has been reproduced from the microfilm master. UMI films the text directly from the original or copy submitted. Thus, some thesis and dissertation copies are in typewriter face, while others may be from any type of computer printer.

**The quality of this reproduction is dependent upon the quality of the copy submitted.** Broken or indistinct print, colored or poor quality illustrations and photographs, print bleedthrough, substandard margins, and improper alignment can adversely affect reproduction.

In the unlikely event that the author did not send UMI a complete manuscript and there are missing pages, these will be noted. Also, if unauthorized copyright material had to be removed, a note will indicate the deletion.

Oversize materials (e.g., maps, drawings, charts) are reproduced by sectioning the original, beginning at the upper left-hand corner and continuing from left to right in equal sections with small overlaps. Each original is also photographed in one exposure and is included in reduced form at the back of the book.

Photographs included in the original manuscript have been reproduced xerographically in this copy. Higher quality 6" x 9" black and white photographic prints are available for any photographs or illustrations appearing in this copy for an additional charge. Contact UMI directly to order.

**UMI**

A Bell & Howell Information Company
300 North Zeeb Road, Ann Arbor MI 48106-1346 USA
313/761-4700 800/521-0600

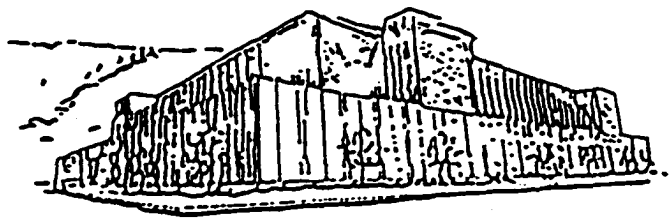

Maureen and Mike
# MANSFIELD LIBRARY

The University of **MONTANA**

---

# I. Metabolic Modeling of Glucose Metabolism in *Rhizopus oryzae*

# and

# II. The Effect of Transcription on Starvation-Induced Mutations in *Escherichia coli*

by

Angelika Longacre

B.S., Southwest Missouri State University 1988

M.S., Southwest Missouri State University 1990

Presented in partial fulfillment of the requirements for the degree of

Doctor of Philosophy

The University of Montana

1998

Approved by

Barbara P. Wright

Chair, Board of Examiners

5/15/98

Date

Dean, Graduate School

Longacre, Angelika, Ph. D., May,1998 Biochemistry

I. Metabolic Modeling of Glucose Metabolism in *Rhizopus oryzae*

Director: Barbara E. Wright BEW

A flux analysis of glucose metabolism in the filamentous fungus *Rhizopus oryzae* was achieved using a specific radioactivity curve-matching program, TFLUX. Glycolytic and tricarboxylic acid cycle intermediates labeled through the addition of extracellular [U-$^{14}$C]glucose and [U-$^{14}$C]acetate were isolated and purified for specific radioactivity determinations. This information, together with pool sizes and the rates of glucose utilization and end product production, provided input for flux maps of the system under two different experimental conditions. Based upon the understanding of this system gained through modeling, a mutant of *R. oryzae* with higher lactate and lower ethanol yields than the parent was sought for and found.

II. The Effect of Transcription on Starvation-Induced Mutations in *Escherichia coli*

Director: Barbara E. Wright BEW

When *Escherichia coli* is deprived of an essential amino acid the accumulation of uncharged tRNAs triggers the accumulation of ppGpp (the Stringent Response) which inhibits macromolecular synthesis and activates promoters of amino acid biosynthetic operons. During leucine starvation, a positive correlation has been established between reversion rates of a chromosomal *leuB*$^{-}$ allele and the concentration of ppGpp in *E. coli* (Wright, 1996, Mol. Microbiol. **19:**213-219; Wright & Minnick, 1997, Microbiology **143:**847-854), indicating that the selective gene activation triggered by amino acid starvation and enhanced by ppGpp leads to higher mutation rates of the transcribed genes. Further evidence indicates a correlation between *leuB* mRNA levels and reversion rates. It is known that ssDNA (exposed during transcription) is more vulnerable to mutagenesis than dsDNA.

To determine whether increased transcription of the *leuB*$^{-}$ allele, regardless of stringent control, can account for the increase in mutation rate of that allele, the *leu* promoter was replaced by the *tac* promoter in *E. coli* K12 strains CP78 (*relA*$^{wt}$, so ppGpp$^{+}$) and CP79 (*relA2*, so ppGpp$^{def}$). The chromosomal *leu* promoter was replaced with the *tac* promoter by double-crossover homologous recombination of a 3.6 kb fragment of dsDNA containing a kanamycin cassette and the *tac* promoter flanked by sequences homologous to regions of the *E. coli* chromosome both upstream and downstream of the *leu* promoter. A fragment beginning upstream of the 3.6 kb fragment and ending inside the *leuB* gene (downstream of the *leuA* gene) was PCR amplified from each recombinant and confirmed replacement of the *leu* with the *tac* promoter. Experiments indicate a significant effect of IPTG addition on *leuB*$^{-}$ reversion rates and *leuB* mRNA levels.

## ACKNOWLEDGMENTS

Barbara Wright has been more than an advisor to me, she has been a mentor, a friend and an example. Her dedication to research has made it possible for me to envision a long life filled with the thrill of scientific research. Not only have I made friends in her laboratory, I have also established collaborations that I look forward to continuing. I will always appreciate what Barbara has given me. I am thankful for the energetic and informative discussions I've had with George Card and Scott Manning - they helped me see parts of my project more clearly. I respect most their thorough knowledge of biochemistry and molecular biology and their insightfulness. I am grateful also to my fellow graduate students with whom I had many hours of enjoyable conversations. Most importantly, I thank my husband, Bart whose love, devotion and encouragement made graduate school not only bearable but enjoyable.

I could not have completed this work without Jackie Reimers, she not only taught me many of the techniques I employed, but she also developed and performed the RNA nuclease protection assays. Jackie Reimers and Judie Bernards performed many of the assays for the modeling experiments. Judie Bernards and Dr. Wright are responsible for the mutation rate data described in the introduction of Part II. Jackie Reimers and Dr. Wright collected the ppGpp concentration data also described in the introduction of Part II. Kris Zouhar collected the RNA for my assays and she performed a few mutation rate experiments for me. To all these people, I dedicate this dissertation.

## TABLE OF CONTENTS

## LIST OF TABLES

## LIST OF FIGURES

# Part I

## Metabolic Modeling of Glucose Metabolism in *Rhizopus oryzae*

# GENERAL INTRODUCTION

Lactic acid in its pure form will polymerize to form a completely degradable plastic. It has been used for many years in the manufacture of thin plastic films, but production costs at the current time prevent companies from utilizing poly(lactic acid) to a greater extent. If an inexpensive way to produce lactic acid in sufficient quantities can be found, affordable plastics products that are completely degradable can be manufactured.

Currently, *Lactobacillus* species are used to produce lactic acid. They are very efficient organisms and will convert 85-90% of the glucose they consume, to lactic acid. However, Lactobacilli can not convert starch directly to lactate and enzymatic breakdown of starch to glucose is costly. In addition, these organisms require an organic nitrogen source usually provided by corn steep liquor which adds many impurities that must be removed, adding to the expense and making recovery of lactate difficult. Another problem with the current procedure is that the lactate that is produced is in its calcium salt form and has to be treated with sulfuric acid in order to recover the lactic acid. Because these organisms grow best at pH 6.5, there is the added costs for buffers and for prevention of contamination.

The filamentous fungus *Rhizopus oryzae* provides an alternative to the Lactobacillus process that could reduce the expense of lactic acid production. *R. oryzae* can be grown in liquid culture and directly ferments starch and many agricultural products (e.g. rice, wheat and barley) to lactic acid. The fungus requires only a simple nitrogen source - ammonium sulfate, thus reducing impurities and resulting in a clear fermentation broth.

An advantage of the *Rhizopus* process is that the fungus thrives at low pH, eliminating the need for expensive buffers and also maintaining the lactate in its acidic form, making recovery easier. At the present time however, the *Rhizopus* process does not compete economically with the Lactobacillus process because of the relatively low yield of lactate per mole of glucose consumed (50-60%).

The premise of the project described here is that if lactate yields in *R. oryzae* can be increased to 75-85%, the *Rhizopus* process would result in the inexpensive production of lactic acid that could be used to manufacture affordable, degradable plastics.

## SPECIFIC AIMS

1) In order to understand the metabolism involved in lactate production in *R. oryzae*, radiolabel *R. oryzae* grown under conditions that result in lactate yields of about 60% by exposing the cultures to [U-$^{14}$C]glucose. Then based upon the results of the radiolabeling experiment, model glucose metabolism in this fungus.
2) Compare the metabolism modeled in (1) to a model of glucose metabolism in *R. oryzae* under optimized conditions that result in lactate yields of about 70%. From this, develop predictions about ways to further enhance lactate production.
3) Label the system with [$^{14}$C]acetate to test the prediction that this labeling would result in higher specific radioactivities of exclusively mitochondrial intermediates and lower specific radioactivities of metabolites with both cytosolic and mitochondrial pathways for production (opposite of the results obtained by using [U-$^{14}$C]glucose).

4) Test the prediction that a high lactate producing mutant would produce less ethanol and/or chitin (cell mass), by UV irradiating *R. oryzae* and selecting and characterizing a mutant with high lactate yields.

To that end, a flux analysis of glucose metabolism in the filamentous fungus *Rhizopus oryzae* was achieved using a specific radioactivity curve-matching program, TFLUX. Glycolytic and tricarboxylic acid cycle intermediates labeled through the addition of extracellular [U-$^{14}$C]glucose and [U-$^{14}$C]acetate were isolated and purified for specific radioactivity determinations. This information, together with pool sizes and the rates of glucose utilization and end product production, provided input for flux maps of the metabolic network under two different experimental conditions. Based upon the flux analysis of this system, a mutant of *R. oryzae* with higher lactate and lower ethanol yields than the parent was sought for and found.

This work was published in the form of the two manuscripts that follow: Chapter 1, Flux Analysis of Glucose Metabolism in *Rhizopus oryzae* for the Purpose of Increasing Lactate Yields, A. Longacre, J.M. Reimers, J.E. Gannon, and B.E. Wright. 1997. Fungal Genetics and Biology **21**:30-39; and Chapter 2, Models Of Metabolism In ***Rhizopus Oryzae***, B. E. Wright, A. Longacre and J. Reimers. 1996. J. theor. Biol. **182**:453-457.

# CHAPTER 1

## Flux Analysis of Glucose Metabolism in *Rhizopus oryzae* for the Purpose of Increasing Lactate Yields

A. Longacre, J.M. Reimers, J.E. Gannon, and B.E. Wright. 1997. Fungal Genetics and Biology 21:30-39

## INTRODUCTION

Filamentous fungi of the genus *Rhizopus* are important organisms in industrial fermentations. They are currently used to produce fumarate, other organic acids and some foodstuffs (Suntornsuk and Hang, 1994a). A renewed interest in the microbial production of lactic acid has emerged with the growth of "degradable" plastic technology. Production of poly(lactic acid) requires a highly purified, preferably L(+)-lactic acid anhydrous monomer. The current approach to the production of polymer-grade lactic acid, on a commercial scale, appears to be fermentation of whey lactose or starch-derived glucose by a homolactic lactobacillus. The primary advantage of the lactobacillus process is the high yield (80-90%); however, a serious disadvantage is the difficulty in removing impurities, making recovery and purification imperfect and costly. In contrast, *Rhizopus oryzae* has the ability to ferment starch directly in minimal medium using an inexpensive ammonium salt as the sole nitrogen source, producing a clear non-colored fermentation broth. The primary limitation of the *Rhizopus* process is in the relatively poor yield of lactate per mole of glucose consumed. The purpose of the present investigation was to improve lactic acid

yields through the development of flux maps of glucose metabolism in *R. oryzae* and through the creation and selection of specific mutants.

Flux maps of glucose metabolism in *R. oryzae* under two different environmental conditions were constructed to simulate *in vivo* conditions and provide kinetic frameworks for making predictions about the system and for testing the relevance of *in vitro* data to metabolism *in vivo*. The models were developed using TFLUX, a specific radioactivity curve-matching program (Sherwood *et al.*, 1979). TFLUX is used for modeling steady-state systems where pool sizes and fluxes remain constant over the labeling period. Steady-state carbohydrate metabolism in the slime mold *Dictyostelium discoideum* was successfully modeled using TFLUX (Kelley *et al.*, 1979; Wright and Reimers, 1988), resulting in many predictions which were later substantiated experimentally (Wright and Kelly, 1981; Wright and Albe, 1994).

In this work, *R. oryzae* cells were exposed to exogenous [U-$^{14}$C]glucose under the following two conditions: (A) 42 mM glucose at 32°C in the presence of 30 mM $Na_2CO_3$; (B) 286 mM glucose at 25°C in the presence of 10 mM $Na_2CO_3$. It was anticipated that such different environmental conditions would result in significant variations in pool sizes, reaction rates and relative concentrations of end products; however, the models simulating each data set should have the same basic structure, e.g., reaction pathways and compartmentation of metabolites. For both experiments, extracellular and intracellular metabolites were isolated and their concentrations, based on packed cell volume, were determined enzymatically. The metabolites were also purified to homogeneity for specific radioactivity determinations. The rate of glucose utilization as well as the rates of

pyruvate, lactate, ethanol, fructose-6-phosphate, glucose-6-phosphate, malate and fumarate production were determined based on changes in concentration in the medium during the growth period. The rate of chitin synthesis was measured separately and an average rate utilized during model development. All of this information was then integrated into steady state flux maps of glucose metabolism. The flux maps were used as the basis for three predictions which were substantiated experimentally: first, that fumarate and malate specific radioactivities after [U-$^{14}$C]glucose labeling should be intermediate between that of exclusively glycolytic and exclusively citric acid cycle intermediates; second, that a mutant producing higher amounts of lactic acid would produce less ethanol; third, that labeling the system with [$^{14}$C]acetate should give rise to a citrate pool with significantly higher specific radioactivity than the malate and fumarate pools. The first and second predictions are the subject of this work, and substantiation of the third prediction was described previously (Wright *et al.*, 1996).

## MATERIALS AND METHODS

### *Fungal strain and spore preparation*

*Rhizopus oryzae* (NRRL 1510) was grown on Sabouraud Dextrose Agar (Difco) for seven days at 32°C. Spores were harvested from the plates by gently shaving the spores with a sterile disposable razor into sterile water. The spore preparation was filtered through seven layers of sterile cheesecloth and stored at -20°C in 1% glycerol.

*Culture media*

Chemicals and enzymes, unless otherwise indicated, were purchased from Sigma Chemical Co., St. Louis, MO. The organism was grown in liquid culture in media consisting of 10, 20 or 30 mM $Na_2CO_3$, 12.2 mM $K_2HPO_4$, 88.7 mM $KH_2PO_4$, 1.0 mM $MgSO_4 \cdot 7H_2O$, 15.1 mM $(NH_4)_2SO_4$ and 300 mM glucose. In preparing the medium, it was critical that each component was added in the order listed and completely dissolved before the next was added, otherwise $CO_2$ would be lost. The glucose was sterilized separately and added to the salts before inoculation. Three hundred ml medium was inoculated with spores of varying concentrations as indicated. Cultures were incubated with shaking at 125 rpm at 25°C or 32°C, as indicated, for the specified time periods. Cells were harvested by filtration and a fraction of the cells was removed and lyophilized to determine dry weight. The remaining cell pellet was frozen at -50°C until perchloric acid extraction could be carried out. The filtered medium samples were frozen until metabolite assays could be performed.

*Effect of carbonate concentration on metabolite concentrations*

Sixteen flasks containing 300 ml medium with 4 each of 0, 10, 20 or 30 mM $Na_2CO_3$ were inoculated with $1 \times 10^5$ spores $ml^{-1}$. The flasks were incubated at 32°C for 70, 141, 215 or 285 h at which time the cells and media were harvested and assayed for metabolite concentrations.

*Radiolabeling experiment A*

Six flasks containing 300 ml medium with 30 mM $Na_2CO_3$ were inoculated with 6.8 x $10^4$ spores $ml^{-1}$. After a 46 h incubation at 32°C, cells were filtered through Whatman glass fiber filters (GF/F). Growth medium from each flask was analyzed for metabolite concentration by enzymatic assay as described below. Cells from one flask were placed in 30 ml of glucose-free medium; this flask became the cold companion. The remaining cells from five flasks were combined into 120 ml glucose-free medium with 1 ml [U-$^{14}$C]glucose (ICN; 1 mCi $ml^{-1}$, 273 mCi $mmole^{-1}$). One hundred µl of radioactive medium was analyzed for starting glucose concentration and specific radioactivity. The radioactive medium contained 42 mM glucose as a starting concentration, which was carry-over from the growth medium. These procedures were done as rapidly as possible and the cells were not washed, in order to perturb metabolism to a minimal extent. Both flasks were incubated at 32°C with shaking for 20 minutes. Cells from both flasks were filtered through disposable Nalgene filters (0.2 µm with extra holes, ~1mm, punched in them to facilitate filtration). The radiolabeled cells were washed once with 20 ml glucose-free medium to remove carry-over of extracellular metabolites. Washing results in the loss of about 2% of the intracellular metabolites. A portion of the cold companion cell mat was retained for dry weight determination. The remaining cold companion cells and the radiolabeled cells were frozen until they could be extracted with perchloric acid.

*Radiolabeling experiment B*

Fifteen flasks containing 300 ml medium with 10 mM $Na_2CO_3$ were inoculated with 2.9 x $10^4$ spores $ml^{-1}$. After a 49 h incubation at 25°C, cells from each of three groups of five flasks were collected by filtering through one Buchner funnel, without filter paper. The pooled growth medium from all 15 flasks was assayed for metabolite concentrations as described below. Combined cells from 5 flasks were resuspended in 60 ml total volume including cells, pooled growth medium and 1.2 ml [U-$^{14}$C]glucose (42.5% ICN; 1 mCi $ml^{-1}$, 200 mCi $mmole^{-1}$ and 57.5% ARC; 1 mCi $ml^{-1}$, 340 mCi $mmole^{-1}$). One hundred µl of radioactive medium from each of the three reaction flasks was analyzed for starting glucose concentration and specific radioactivity; the radioactive medium contained 286 mM glucose. The flasks were incubated at 25°C with shaking: one for 10 min, the second for 20 min and the third for 30 min. After incubation, the cells were filtered through disposable Nalgene filters (0.2 µm), washed with 5 ml glucose-free medium and frozen until perchloric acid extraction could be performed.

*Perchloric acid extraction*

All operations were carried out at 4°C. The frozen cells were extracted with 5 ml of 0.5 N perchloric acid per gram wet weight of cells and ground with 0.4 gram glass beads (450-500 micron) per gram wet weight of cells using a mortar and pestle. Cell debris was removed by centrifugation at 12,000 x g for 10 min. The pH of the supernatant was adjusted to 7.0 using a mixture containing 2 N KOH, 0.4 M KCl and 0.4 M imidazole base. Excess salt was allowed to precipitate on ice for 10 min and was removed by

centrifugation as above. The final supernatant was chromatographed as described below or directly assayed for the metabolites of interest.

*Metabolite purification for concentration and specific radioactivity determinations*

Portions of the perchloric acid extracts from radiolabeling experiment B were retained for ethanol purification by HPLC. The remainder of the perchloric acid extracts from experiment B and the perchloric acid extract and incubation medium from experiment A were separately layered onto a column of Bio-Rad AG1-X4 resin and the metabolites were separated as their borate complexes by anion exchange chromatography according to a modification of the procedure of Thompson (1979) as described by Wright *et al.* (1982). Lactate, glucose, glucose-6-phosphate and trehalose were eluted from the anion exchange column with a linear gradient of ammonium biborate (0.1-0.4 M). Citrate, malate, fumarate and fructose-1,6-bisphosphate were eluted with a linear gradient of NaCl (0.4-0.7 M).

Glucose, glucose-6-phosphate, trehalose, citrate, malate, fumarate and fructose-1,6-bisphosphate fractions from the anion exchange column were separately desalted through Dowex 50W-X8 columns and lyophilized. The remaining borate was removed from the lyophilized fractions and non-lyophilized lactate fractions by repeated methanol evaporation.

Lactate, glucose, citrate, malate and fumarate were identified enzymatically and purified by descending paper chromatography on Whatman 54 SFC (suitable for

chromatography) paper for 8 h in a solvent containing butanol:acetic acid:$H_2O$ (12:3:5 by volume), eluted and lyophilized before further purification by HPLC.

Glucose-6-phosphate was purified by descending paper chromatography on Whatman 54 SFC for 24 h in a solvent containing butanol:pyridine:water:formic acid (6:4:3:1.05), eluted from the paper and treated with 0.735 U alkaline phosphatase in 200 µl 50 mM Tris-HCl (pH 8.1) for 1 h at 37°C.

Fructose-1,6-bisphosphate was purified by descending paper chromatography on Whatman 54 SFC paper for 18 h in a solvent containing n-propyl acetate:formic acid:$H_2O$ (11:5:3) plus 0.05 g tetrasodium EDTA per ml, eluted from the paper, lyophilized and treated with 1.5 U alkaline phosphatase in 200 µl of 50 mM Tris-HCl (pH 8.1) for 1 h at 37°C. The liberated fructose was isolated by descending paper chromatography on Whatman 54 SFC for 5.5 h with a solvent containing ethyl acetate:pyridine:$H_2O$ (12:5:4), eluted and lyophilized before further purification by HPLC.

The lactate, glucose, citrate, malate, fumarate and non-phosphorylated glucose and fructose were further purified by HPLC using a Perkin Elmer Series 410 HPLC with a Bio-Rad HPX-87H column with an eluant of 0.005 M $H_2SO_4$.

Trehalose was further purified by HPLC through a Bio-Rad BioSil Amino 5S column with an eluant of 90% acetonitrile. The peak fractions (determined by anthrone assay) were collected and the solvent removed by methanol evaporation. The trehalose was then digested with trehalase as described by Killick (1985). The liberated glucose was

separated and purified by HPLC through a Bio-Rad BioSil Amino 5S column with an eluant of 90% acetonitrile.

Ethanol was purified through two HPLC steps. The perchloric acid extract was chromatographed through a Bio-Rad BioSil Amino 5S column with an eluant of 90% acetonitrile. The peak fractions (determined by enzymatic assay as described below) were then chromatographed through a BioRad HPX-87H column with an eluant of 0.01 N $H_2SO_4$.

After each purification step, an aliquot of the particular metabolite was counted and each concentration was determined spectrophotometrically by enzymatic assay. Citrate, glucose, malate and fructose were assayed according to methods described by Lowry and Passonneau (1972). Ethanol and fructose-1,6-bisphosphate were assayed according to Bergmeyer (1974). The assays for lactate and pyruvate were adapted from a Sigma diagnostic kit (number 826-A). Fumarate was assayed according to Bergmeyer (1974) except 2 mM NAD was substituted for acetylpyridine-adenine dinucleotide. Internal standards were used in all assays. Samples were counted in 3 ml of Aquasol-2 (DuPont-NEN). Metabolite concentrations were determined as μmole per ml of packed cell volume (mM packed cell volume) based on the determination of 280 mg dry weight per ml packed cell volume in these cells. Specific radioactivities were determined as cpm $\mu mole^{-1}$.

*Computer simulation using TFLUX*

Sixty-three percent of the model input parameters for experiment A and 72% of the parameters for experiment B (reaction rates, metabolite concentrations and exogenous

glucose specific radioactivities) were derived from experimental data obtained under the growth conditions indicated above. Final values for unknown pool sizes and fluxes were determined by best fit to the specific radioactivity data as a whole, using the computer program TFLUX (Sherwood *et al.*, 1979). Briefly, if we assume that the system is in steady state, then a set of linear differential equations can be used to describe the specific radioactivities of the metabolite pools over time. From the input, the program constructs a system of differential equations of the form $\dot{X} = Ax + b$ in which A is an n x n constant matrix, b is a constant n vector, and the n vector x contains the specific radioactivity of each of n pools. The program then computes each pool specific radioactivity as a function of time. The TFLUX user specifies the number of intracellular and extracellular pools by name, size (mM packed cell volume) and initial specific radioactivity. Connections between pools are specified as constant flux rates (mM packed cell volume per min). Use of equivalent concentrations in terms of packed cell volume for both internal and external metabolites simplifies the calculations and insures that conservation of mass is observed.

*Mutagenesis and selection*

A slightly modified version of the method described by Suntornsuk and Hang (1994b) was followed for UV mutagenesis and mutant selection. Five ml *R. oryzae* spores in 1% glycerol ($8.9 \times 10^6$ spores/ml) were mixed in a 50 ml flask with 5 ml liquid culture medium containing 10 mM $Na_2CO_3$. The spores were incubated at 32°C with shaking at 125 rpm for 6 h to induce germination and loss of the spore coat so the spores would be more susceptible to UV irradiation. The spores were then placed in a sterile petri dish on a

rotating platform, to keep them from settling in the petri dish, and exposed to UV radiation at 254 nm for 10 - 60 min at a distance of 12.5 cm. Irradiated and non-irradiated spores were diluted and spread on the following selective medium as described by Suntornsuk and Hang (1994b): 1% soluble starch, 0.1% peptone, 0.025% $MgSO_4 \cdot 7H_2O$, 0.1% $KH_2PO_4$, 0.15% Triton X-100, 0.02% bromocresol green and 2% agar in distilled water (pH 5.5).

Mutant colonies were observed to have larger rings of acid production and smaller colony size than the untreated controls (parent colonies). One such mutant colony was selected and replated for isolation on the selective medium. This step was necessary because when the spores were preincubated before UV irradiation they tended to clump. An isolated mutant colony was plated for spore collection as described above and a final concentration of $5.8 \times 10^4$ spores $ml^{-1}$ of mutant as well as parent spores were used as inoculum in liquid culture for comparison of lactate and ethanol yields. Growth conditions for five experiments were as follows: 1) 25°C, 10 mM $Na_2CO_3$, 460 h with intermittent shaking at 125 rpm; 2) 25°C, 10 mM $Na_2CO_3$, 355 h shaken at 125 rpm; 3) 25°C, 10 mM $Na_2CO_3$, 0.05 mM nitrilotriacetic acid (NTA), 355 h shaken at 125 rpm; 4) 25°C, 30 mM Na2CO3, 355 h shaken at 125 rpm; and 5) 32°C, 10 mM $Na_2CO_3$, 355 h shaken at 125 rpm. The following calculations were used: lactate yield = [(mM lactate produced)(3 carbons per molecule)]/[(mM glucose consumed)(6 carbons per molecule)] x 100; ethanol yield = [(mM ethanol produced)(2 carbons per molecule)]/[(mM glucose consumed)(6 carbons per molecule)] x 100.

# RESULTS

*Effect of carbonate concentration on metabolite concentrations*

In a number of experiments the observation was made that, to a variable extent, the addition of 10 mM $Na_2CO_3$ enhanced lactic acid production while reducing ethanol accumulation. One of these experiments is reported in Table 1. Intracellular and extracellular concentrations of lactate, ethanol, citrate, malate and fumarate were monitored at four successive times over a 285 h period in cells grown in four different concentrations of sodium carbonate. The data reported are for the extracellular metabolites measured at 141 h and 285 h only as all time points showed the same trends. Changes in intracellular metabolite concentrations mimicked the extracellular concentration changes (data not shown). The greatest yields of lactic acid were achieved at 10 mM $Na_2CO_3$ presumably because at higher carbonate levels malate and fumarate production was greatly enhanced, thereby reducing the amount of pyruvate available for lactate production.

*Computer simulation using TFLUX*

The modeling process began with the drawing of a realistic map of the metabolism known to take place in *R. oryzae*. Metabolism in *Rhizopus* has been studied for decades, and a number of mitochondrial and cytosolic enzymes have been described (Wegener and Romano, 1964; Osmani and Scrutton, 1985; Kenealy *et al.*, 1986; Peleg *et al.*, 1989; Yu and Hang, 1991). The presence of pyruvate carboxylase, NAD-malate dehydrogenase and

TABLE 1

*Rhizopus oryzae* extracellular metabolite concentrations (mM packed cell volume)

at varying concentrations of sodium carbonate

| $Na_2CO_3$ | Time (h) | Lactate | Ethanol | Citrate | Malate | Fumarate |
|---|---|---|---|---|---|---|
| 0 mM | 141 | 23000 | 7150 | 9.34 | 111.1 | 257.8 |
| | 285 | 48800 | 27900 | 22.3 | 134.4 | 162.4 |
| 10 mM | 141 | 27000 | 6980 | 28.7 | 184.0 | 727.3 |
| | 285 | 102000 | 18000 | 17.6 | 154.9 | 681.6 |
| 20 mM | 141 | 38800 | 5730 | 20.6 | 364.8 | 1861.3 |
| | 285 | 77500 | 1390 | 34.7 | 255.2 | 982.5 |
| 30 mM | 141 | 25600 | 5320 | 35.2 | 366.7 | 1751.8 |
| | 285 | 60300 | 4570 | 27.1 | 354.1 | 1541.1 |

fumarase in the cytosol led Osmani and Scrutton (1985) to propose a scheme of pyruvate metabolism in *Rhizopus* which involves a normal tricarboxylic acid cycle in the mitochondrion and a separate cytosolic pathway for fumarate formation. The present investigation supports and extends that scheme and provides a means of testing predictions about *Rhizopus* metabolism. Included in the proposed model of glucose metabolism is the strictly anaerobic production of lactate (Foster, 1949; Gibbs and Gastel, 1953). The lack of evidence for the existence of malic enzyme in this organism also supports a completely fermentative mode of lactate formation. Although it has been suggested (McCullough *et al.*, 1986), there is at this time no conclusive evidence for a mitochondrial malate transport system in *Rhizopus;* therefore, that exchange was not included in this model.

The TFLUX map and fluxes (experimentally determined or TFLUX generated) are presented in Fig. 1 and Table 2. The known and TFLUX generated pool sizes and specific radioactivities are listed in Tables 3, 4 and 5. Chitin was found to accumulate at a rate of about 20% of the rate of glucose uptake. Experimentally determined specific radioactivities are in good agreement with those generated by TFLUX (Tables 3 and 5). Thus, in experiment A (Table 3), input to the model of known metabolic pathways in *Rhizopus* consisted of 9 measured pool sizes and 9 specific radioactivity determinations (including the exogenous glucose starting specific radioactivity of $26.28 \pm 0.04 \times 10^4$ cpm $\mu mole^{-1}$). Input also included 9 fluxes (Table 2) based on glucose utilization and end product accumulation (chitin, pyruvate, fructose-6-phosphate, glucose-6-phosphate, ethanol, lactate, malate and fumarate) calculated as mM PCV $min^{-1}$: {[(μmole

FIG 1. **Map of glucose metabolism in *R. oryzae*. This map together with the fluxes indicated in Table 2 constitute the flux maps of glucose metabolism in *R. oryzae*.**

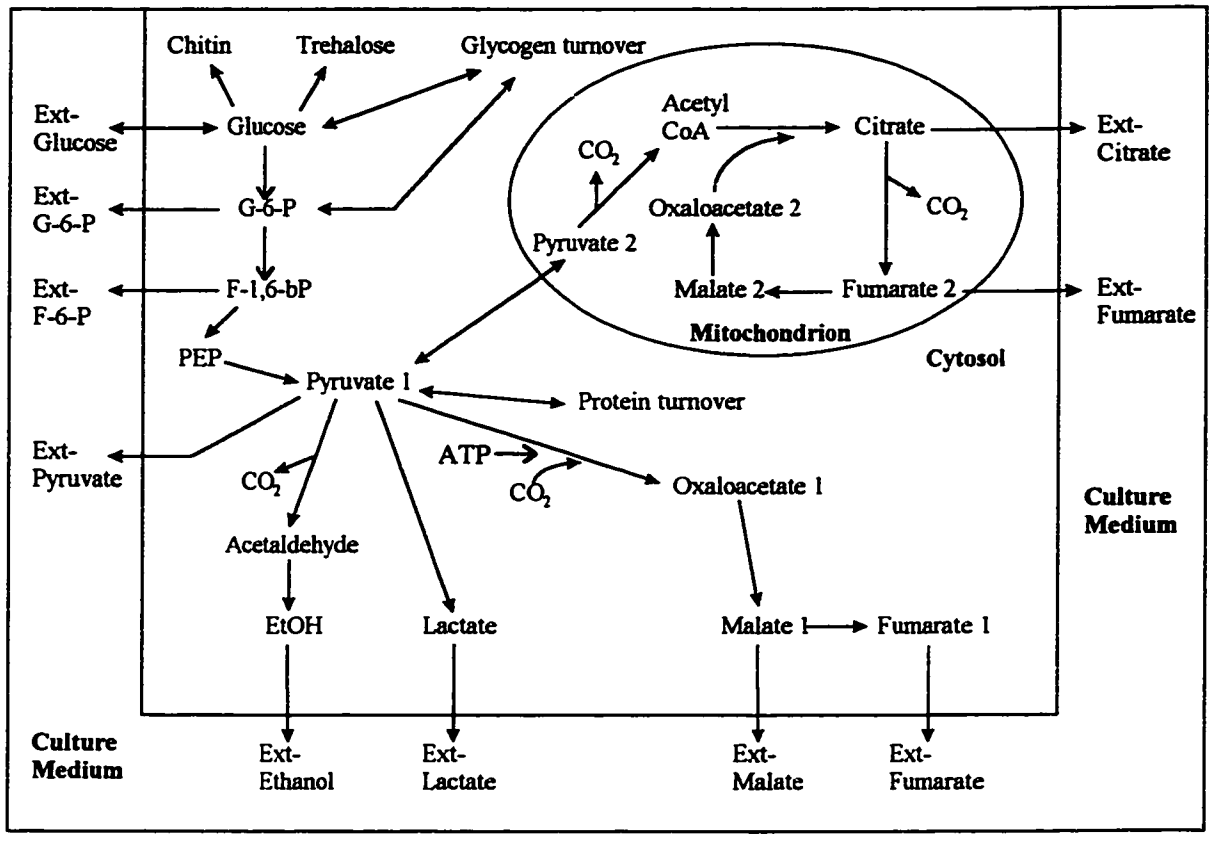

TABLE 2

Flux rates for *Rhizopus oryzae* radiolabeling experiments A and B and a comparison of the percentage of glucose uptake ((metabolite flux / net glucose uptake flux) x 100) for the production of some key metabolites in these two experiments

| Flux | Exp. A[a] Fluxes (mM PCV/min) | % of glucose uptake | Exp. B[b] Fluxes (mM PCV/min) | % of glucose uptake |
|---|---|---|---|---|
| Ext-Glucose → Int-Glucose | 11.224 | | 18.642 | |
| Int-Glucose → Ext-Glucose | 4.1 | | 9.0 | |
| Net Glucose Uptake* | 7.124 | 100 | 9.642 | 100 |
| Glucose → Chitin* | 1.425 | 20 | 1.928 | 20 |
| Glycogen Turnover at Glucose | 19.1 | | 5.0 | |
| Glucose → Trehalose* | 0.057 | 0.8 | 0.074 | 0.8 |
| Glucose → G-6-P | 5.642 | | 7.640 | |
| G-6-P → Ext-G-6-P* | 0.002 | | 0.002 | |
| Glycogen Turnover at G-6-P | 1.5 | | 2.7 | |
| G-6-P → F-6-P | 5.640 | | 7.638 | |
| F-6-P → Ext-F-6-P* | 0.002 | | 0.002 | |
| F-6-P → F-1,6-bP | 5.638 | | 7.636 | |
| F-1,6-bP → Phosphoenolpyruvate (PEP) | 5.638 | | 7.636 | |
| PEP → Pyruvate 1 | 5.638 | | 7.636 | |
| Cold Protein Turnover at Pyruvate 1 | 0.9 | | 13.0 | |
| Pyruvate 1 → Pyruvate 2 | 0.219 | | 0.132 | |
| Pyruvate 2 → Acetyl CoA & $CO_2$ | 0.219 | | 0.132 | |
| Flux through Citric Acid Cycle | 0.219 | 3 | 0.132 | 1.4 |
| Pyruvate 1 → Ext-Pyruvate* | 0.062 | 0.9 | 0.084 | 0.9 |
| Pyruvate 1 → Acetaldehyde, $CO_2$ & EtOH | 0.716 | | 0.762 | |
| EtOH → Ext-EtOH* | 0.716 | 10 | 0.762 | 7.9 |
| Pyruvate 1 → Lactate | 4.104 | | 6.465 | |
| Lactate → Ext-Lactate* | 4.104 | 58 | 6.465 | 67 |
| Pyruvate 1 & $CO_2$ → Oxaloacetate 1 | 0.537 | | 0.193 | |
| Oxaloacetate 1 → Malate 1 | 0.537 | | 0.193 | |
| Malate 1 → Ext-Malate* | 0.094 | 1.3 | 0.037 | 0.4 |
| Malate 1 → Fumarate 1 | 0.443 | | 0.156 | |
| Fumarate 1 → Ext-Fumarate* | 0.443 | 6.2 | 0.156 | 1.6 |

[a]Experiment A radiolabeling conditions: 30 mM $Na_2CO_3$, 42 mM glucose, 32°C
[b]Experiment B radiolabeling conditions: 10 mM $Na_2CO_3$, 286 mM glucose, 25°C
*These fluxes were determined experimentally as described in Materials and Methods

TABLE 3

Radiolabeling experiment A. TFLUX generated pool sizes (μmole per ml packed cell volume (mM PCV)) and specific radioactivities (SR x $10^4$ cpm per μmole) for a 20 minute simulation compared with those determined experimentally after a 20 minute incubation with [U-$^{14}$C]glucose

| Metabolite | Experimental Pool Size (mM PCV) | TFLUX Pool Size (mM PCV) | Experimentally Determined SR | TFLUX Generated SR |
|---|---|---|---|---|
| Extracellular Glucose | 703.0 | | 19.9 ± 0.6 | 20.0 |
| Intracellular Glucose | 8.5 | | 7.4 ± 0.1 | 7.4 |
| Fructose-1,6-bisphosphate | 0.6 | | 5.9 ± 0.1 | 5.9 |
| Citrate | 22.0 | | 0.46 ± 0.03 | 0.50 |
| Malate Mix[a] | 11.0 | | 0.68 ± 0.06 | 0.68 |
| Cytosolic Malate | | 1.3 | | 5.2 |
| Mitochondrial Malate | | 9.7 | | 0.07 |
| Fumarate Mix[a] | 1.0 | | 1.65 ± 0.05 | 1.6 |
| Cytosolic Fumarate | | 0.25 | | 5.3 |
| Mitochondrial Fumarate | | 0.75 | | 0.43 |
| Ethanol | 13.1 | | | 3.7 |
| Extracellular Lactate | 215.0 | | 1.75 ± 0.05 | 1.7 |
| Intracellular Lactate | 20.6 | | 5.3 ± 0.5 | 5.3 |
| Pyruvate Mix[a] | | 1.1 | | 5.1 |
| Cytosolic Pyruvate | | 1.0 | | 5.1 |
| Mitochondrial Pyruvate | | 0.1 | | 5.1 |

[a]The cytosolic and mitochondrial pools mix when extracted.

TABLE 4

Radiolabeling experiment B. Metabolite concentrations (pool sizes) in μmoles per ml packed cell volume (mM PCV) from cells incubated in the presence of [U-$^{14}$C]glucose

| Metabolite | Experimentally Determined Pool Size 10 min labeling | 20 min labeling | 30 min labeling | Average Pool Size | TFLUX Generated Pool Size |
|---|---|---|---|---|---|
| Glucose | 74.0 | 44.3 | 50.7 | 56.3 | |
| Glucose-6-phosphate | 0.48 | 0.44 | 0.32 | 0.41 | |
| Trehalose | 45.5 | 41.7 | 36.5 | 41.2 | |
| Fructose-1,6-bisphosphate | 1.8 | 1.6 | 1.2 | 1.5 | |
| Citrate | 20.3 | 18.0 | 14.4 | 17.6 | |
| Malate Mix[a] | 1.7 | 1.5 | 1.1 | 1.4 | |
| Cytosolic malate | | | | | 0.05 |
| Mitochondrial malate | | | | | 1.35 |
| Fumarate Mix[a] | 2.0 | 1.9 | 1.3 | 1.7 | |
| Cytosolic fumarate | | | | | 0.2 |
| Mitochondrial fumarate | | | | | 1.5 |
| Ethanol | 79.2 | 96.3 | 89.1 | 88.2 | |
| Lactate | 31.3 | 60.6 | 52.7 | 48.2 | |
| Pyruvate Mix[a] | | | | | 1.1 |
| Cytosolic pyruvate | | | | | 1.0 |
| Mitochondrial pyruvate | | | | | 0.1 |

[a]The cytosolic and mitochondrial pools mix when extracted.

TABLE 5

Radiolabeling experiment B. A Comparison of Experimentally Determined and TFLUX Generated Specific Radioactivities (SR x $10^4$ cpm per μmole)

| Metabolite | Minutes of labeling with [U-$^{14}$C]glucose | Experimental SR | TFLUX SR |
|---|---|---|---|
| Glucose | 10 | 8.56 ± 0.48 | 8.6 |
| | 20 | 8.47 ± 0.28 | 8.7 |
| | 30 | 8.79 ± 0.18 | 8.7 |
| Glucose-6-phosphate | 10 | 6.43 ± 0.06 | 6.4 |
| | 20 | 6.49 ± 0.08 | 6.5 |
| | 30 | 6.49 ± 0.11 | 6.4 |
| Trehalose | 10 | 0.12 ± 0.01 | 0.12 |
| | 20 | 0.31 ± 0.02 | 0.28 |
| | 30 | 0.38 ± 0.02 | 0.43 |
| Fructose-1,6-bisphosphate | 10 | 6.40 ± 0.08 | 6.4 |
| | 20 | 5.80 ± 0.22 | 6.5 |
| | 30 | 5.47 ± 0.20 | 6.4 |
| Citrate | 10 | 0.05 ± 0.00 | 0.06 |
| | 20 | 0.11 ± 0.01 | 0.14 |
| | 30 | 0.16 ± 0.01 | 0.22 |
| Malate Mix[a] | 10 | 0.10 ± 0.01 | 0.09 |
| | 20 | 0.11 ± 0.01 | 0.11 |
| | 30 | 0.18 ± 0.00 | 0.16 |
| Fumarate Mix[a] | 10 | 0.23 ± 0.02 | 0.28 |
| | 20 | 0.42 ± 0.08 | 0.34 |
| | 30 | 0.39 ± 0.06 | 0.40 |
| Ethanol | 10 | 0.28 ± 0.02 | 0.14 |
| | 20 | 0.40 ± 0.02 | 0.33 |
| | 30 | 0.25 ± 0.01 | 0.50 |
| Lactate | 10 | 1.65 ± 0.05 | 1.4 |
| | 20 | 2.15 ± 0.05 | 2.1 |
| | 30 | 2.35 ± 0.05 | 2.3 |

[a]The cytosolic and mitochondrial pools mix when extracted.

metabolite/ml medium)(ave ml medium/ave mg dry weight)(280 mg dry weight/ml packed cell volume)]/min}{# carbons per molecule/6 carbons per glucose molecule}. Since the metabolites measured are all derived from glucose metabolism their rates of accumulation were scaled to the number of carbons in the molecule relative to six carbons in each glucose molecule so that the rate of accumulation of each metabolite was a fraction of the rate of glucose utilization. The average volume of medium for experiment A was 285 ml and the average dry weight over the 46 h was 164.5 mg. For experiment B, the average volume of medium was 4275 ml and the average dry weight over the 49 h was 730.5 mg. A total of 27 independent parameters constituted input to the program for experiment A. Based on these data and the model, 7 unknown pool sizes (Table 3) and 9 fluxes (Table 2) were generated by best fit to the data as a whole. Therefore, the independent parameters represent 63% of the total number. For experiment B (Table 4), input consisted of 10 measured pool sizes (averages of 27 determinations plus exogenous glucose), 28 specific radioactivity determinations (including the exogenous glucose starting specific radioactivity of $11.14 \pm 0.91 \times 10^4$ cpm $\mu mole^{-1}$) and 9 fluxes (Table 2) based on glucose utilization and end product accumulation (as above), for a total of 47 independent parameters. Based on these data and the model, 7 unknown pool sizes (Table 4) and 11 fluxes (Table 2) were generated by best fit to the data as a whole. Thus, the independent parameters for experiment B represent 72% of the total number. In this experiment the lactate and glucose pool sizes were quite variable. However, changing them in the model over the ranges observed experimentally still gave a good fit to the specific radioactivity data (Table 5).

As 63% and 72% of the model parameters were determined empirically, this model is highly data-based. Pyruvate concentration and specific radioactivity were not obtained in the labeling experiments because pyruvate levels were too low to be detected by the methods utilized; however, the sizes of the two pyruvate pools were not highly constrained, i.e., changing their concentrations over a wide range did not affect the outcome of the model. The pool sizes of malate 1, malate 2, fumarate 1 and fumarate 2 could not be determined separately because the pools were mixed upon extraction due to the destruction of cellular integrity. Although these pool sizes (Tables 3 and 4) could not be determined empirically, their values were dictated by the known pool sizes and specific radioactivities of the mixed metabolites, and by the specific radioactivities of precursor and product pools. The sizes and specific radioactivities of the malate and fumarate pools were highly constrained; changing the compartmented sizes of the malate or fumarate pools by 15% resulted in specific radioactivities which were incompatible with the data. The model also predicts specific radioactivities for several metabolites that were not determined, but will be the subject of future experimentation.

*Mutant selection*

Under all conditions tested, the mutant exhibited higher lactate yields and lower ethanol yields per cell mass than the parent (Table 6). The mutant was also morphologically different from the parent: on selective plates the mutant rarely produced hyphae and the hyphae that did develop were shorter than those produced by the parent.

TABLE 6

Lactate and ethanol yields in a high lactate producing mutant compared with the parent, *Rhizopus oryzae* NRRL 1510

| | Mutant | | | | Parent | | | |
|---|---|---|---|---|---|---|---|---|
| Exp[a] | mg dry wt | EtOH yield | Lactate yield | lactate yield per mg dry wt | mg dry wt | EtOH yield | Lactate yield | lactate yield per mg dry wt |
| 1 | 122 | 5.1 | 75 | .61 | 169 | 9.2 | 60 | .36 |
| 2 | 199 | 6.4 | 79 | .40 | 396 | 13.2 | 48 | .12 |
| 3 | 156 | 3.2 | 76 | .49 | 242 | 7.9 | 70 | .29 |
| 4 | 190 | 4.3 | 85 | .45 | 304 | 6.2 | 78 | .26 |
| 5 | 207 | 2.0 | 86 | .42 | 313 | 10.0 | 72 | .23 |

[a]See Materials and Methods for experimental conditions. All values are the averages from at least two separate cultures.

Also, the mutant colonies usually developed a dark center and in liquid culture the mutant formed much smaller cell mats than the parent.

## DISCUSSION

Calcium carbonate is known to increase extracellular lactate and fumarate yields in *Rhizopus* (Lockwood *et al.*, 1936; Waksman and Foster, 1938; Foster and Waksman, 1939); however, the calcium interferes with lactate recovery and must be taken into account when determining dry weight. Therefore, in these studies, sodium carbonate was utilized instead of calcium carbonate. Sodium carbonate was found to enhance lactate, malate and fumarate yields as well as decrease ethanol production (Table 1). Since ethanol in *R. oryzae* is thought to be produced by the classical Embden-Meyerhoff pathway with reduction of acetaldehyde (Gibbs and Gastel, 1953), the enzyme pyruvate decarboxylase (EC 4.1.1.1), a $CO_2$ generating enzyme, is undoubtedly present. The effect of increased concentrations of sodium carbonate on extracellular metabolite accumulation (Table 1) may be due in part to the inhibition of pyruvate decarboxylase activity by carbonate and the stimulation of pyruvate carboxylase, which requires $CO_2$ as a substrate. If carbonate inhibits acetaldehyde and ethanol production, more pyruvate is available for lactate, malate and fumarate production. It should be noted that the greatest production of extracellular lactate occurred with 10 mM sodium carbonate, rather than 20 or 30 mM, although these concentrations also increased lactate production over controls with no carbonate. In contrast, extracellular malate and fumarate concentrations were substantially higher at 20 and 30 mM sodium carbonate compared to 10 mM. Intracellular

malate levels were also higher at 30 mM compared to 10 mM carbonate (data not shown). These findings are consistent with the effect of carbonate on end product production: at 10 mM carbonate, the higher pyruvate levels lead to enhanced lactate production, but at higher carbonate concentrations pyruvate carboxylase competes favorably for the available pyruvate and an increase in production of malate and fumarate is noted. This increase in extracellular malate and fumarate levels is thought to result from the cytosolic pathway, since citrate is exclusively a mitochondrial pool and extracellular citrate concentration does not increase in response to increased carbonate concentrations (Table 1). The increase in malate and fumarate levels in spite of the almost steady concentration of citrate provides further evidence for the existence of two separate pools of pyruvate, malate, fumarate and oxaloacetate in *R. oryzae*. The results of the two radiolabeling experiments confirmed the effects of $Na_2CO_3$ on this system (Table 2). That is, malate and fumarate as a percentage of glucose consumed was higher at 30 mM carbonate than at 10 mM and the lactate percentage was lower at 30 mM carbonate as compared to 10 mM carbonate.

Through the use of sodium carbonate, lactate yields were enhanced to about 65% of the glucose consumed; however, in order to make the *Rhizopus* process of lactate production better than the Lactobacillus process, the yield should be about 75-80%. Based upon the model it was clear that to significantly enhance lactate production, either flux through the citric acid cycle, or ethanol or chitin synthesis would have to be reduced. By growing *R. oryzae* in liquid culture and then transferring the culture to an anaerobic environment, flux through the citric acid cycle and cytosolic fumarate synthesis can be eliminated (Foster and Waksman, 1939); however, under anaerobic conditions ethanol

yield increases dramatically. Therefore, in order to significantly enhance lactate yields either ethanol or chitin synthesis would have to be reduced. This prediction led to the selection of a high lactate producing mutant (Table 6) with lactate yields of 75-86% (~30 g/L) accompanied by decreased ethanol and chitin (cell mass) synthesis .

## ACKNOWLEDGMENTS

This work was supported by NSF grant OSR-9350546 and the University of Montana.

We thank Judie Bernards and Virginia Miller for excellent technical assistance.

## REFERENCES

**BERGMEYER, H. U.** 1974. *Methods of Enzymatic Analysis*, Vol. 3. Academic Press, Inc., New York.

**FOSTER, J. W.** 1949. *Chemical Activities of Fungi*, pp. 282-295. Academic Press, Inc., New York.

**FOSTER, J. W., AND WAKSMAN, S. A.** 1939. The Production of Fumaric Acid by Molds Belonging to the Genus *Rhizopus*. *J. Am. Chem. Soc.* **61**:127-135.

**GIBBS, M., AND GASTEL, R.** 1953. Glucose Dissimilation by *Rhizopus*. *Arch. Biochem. Biophys.* **43**:33-38.

**KELLY, P. J., KELLEHER, J. K., AND WRIGHT, B. E.** 1979. The Tricarboxylic Acid Cycle in *Dictyostelium discoideum*. *Biochem. J.* **184**:589-597.

**KENEALY, W., ZAADY, E., DU PREEZ, J. C., STIEGLITZ, B., AND GOLDBERG, I.** 1986. Biochemical Aspects of Fumaric Acid Accumulation by *Rhizopus arrhizus*. *Appl. Environ. Microbiol.* **52**:128-133.

**KILLICK, K. A.** 1985. Trehalase from the Dormant Spore of *Dictyostelium discoidum* *Exptl. Mycol.* **9**:108-115.

**LOCKWOOD, L. B., WARD, G. E., AND MAY, O. E.** 1936. The Physiology of *Rhizopus oryzae*. *J. Agric. Res.* **53**:849-857.

**LOWRY, O. H., AND PASSONNEAU, J. V.** 1972. *A Flexible System of Enzymatic Analysis*, Academic Press, Inc., New York.

**MCCULLOUGH, W., ROBERTS, C. F., OSMANI, S. A., AND SCRUTTON, M. C.** 1986. Regulation of Carbon Metabolism in Filamentous Fungi. In *Carbohydrate Metabolism in Cultured Cells* (M. J. Morgan, Ed.), pp. 287-355. Plenum Press, New York.

**OSMANI, S. A., AND SCRUTTON, M. C.** 1985. The Sub-cellular Localisation and Regulatory Properties of Pyruvate Carboxylase from *Rhizopus arrhizus*. *Eur. J. Biochem.* **147**:119-128.

**PELEG, Y., BATTAT, E., SCRUTTON, M. C., AND GOLDBERG, I.** 1989. Isoenzyme Pattern and Subcellular Localisation of Enzymes Involved in Fumaric Acid Accumulation by *Rhizopus oryzae*. *Appl. Microbiol. Biotechnol.* **32**:334-339.

**SHERWOOD, P., KELLY, P., KELLEHER, J. K., AND WRIGHT, B. E.** 1979. TFLUX: A General Purpose Program for the Interpretation of Radioactive Tracer Experiments. *Comput. Programs Biomed.* **10**:66-74.

**SUNTORNSUK, W. AND HANG, Y. D.** 1994a. Efficacy of Chemicals for Controlling Colony Spread by *Rhizopus* species. *Lebensmittel-Wissenschaft & Technologie.* **27**:185-188.

**SUNTORNSUK, W. AND HANG, Y. D.** 1994b. Strain Improvement of *Rhizopus oryzae* for Production of L(+)-Lactic acid and Glucoamylase. *Lett. Appl. Microbiol.* **19**:249-252.

**THOMPSON, J.** 1979. Lactose Metabolism in *Streptococcus lactis*: Phosphorylation of Galactose and Glucose Moieties In Vivo. *J. Bacteriol.* **140**:774-785.

**WAKSMAN, S. A., AND FOSTER, J. W.** 1938. Respiration and Lactic Acid Production by a Fungus of the Genus *Rhizopus*. *J. Agric. Res.* **57**:873-899.

**WEGENER, W. S., AND ROMANO, A. H.** 1964. Control of Isocitrate Formation in *Rhizopus nigricans*. *J. Bacteriol.* **87**:156-161.

**WRIGHT, B. E., AND ALBE, K. R.** 1994. Carbohydrate Metabolism in *Dictyostelium discoideum*: I. Model Construction. *J. Theor. Biol.* **169**:231-241.

**WRIGHT, B. E., AND KELLY, P. J.** 1981. *Kinetic Models of Metabolism in Intact Cells, Tissues, and Organisms* In *Current Topics in Cellular Regulation* (B. L. Horecker and E. R. Stadtman, Eds.), Vol 19, pp. 103-158. Academic Press, Inc., New York.

**WRIGHT, B. E., LONGACRE, A., AND REIMERS, J. M.** 1996. Models of Metabolism in *Rhizopus oryzae. J. Theor. Biol. in press*

**WRIGHT, B. E., AND REIMERS, J. M.** 1988. Steady-State Models of Glucose-perturbed *Dictyostelium discoidium. J. Biol. Chem.* **263:**14906-14912.

**WRIGHT, B. E., THOMAS, D. A., AND INGALLS, D. J.** 1982. Metabolic Compartments in *Dictyostelium discoideum. J. Biol. Chem.* **257:**7587-7594.

**YU, R., AND HANG, Y. D.** 1991. Purification and Characterization of NAD-Dependent Lactate Dehydrogenase from *Rhizopus oryzae. Food Chem.* **41:**219-225.

# CHAPTER 2

## Models Of Metabolism In *Rhizopus Oryzae*

B. E. Wright, A. Longacre and J. Reimers. 1996. J. theor. Biol. **182:**453-457

## INTRODUCTION

Metabolic control theory (MCT) has been used to analyze realistic computer models of metabolism (Wright & Albe, 1994) (Albe & Wright, 1994). As there is a very poor correlation between enzymatic activity *in vivo* and *in vitro* (Wright & Kelly, 1981) (Albe, et al., 1990) we estimate this value within the framework of our highly data-based models. Thus, enzyme activity is calculated as the only unknown in each enzyme kinetic expression, knowing the reaction rate determined *in vitro* with tracers, as well as metabolite pool sizes, the kinetic mechanism and kinetic constants determined *in vitro*. This calculated value is called $V_{vivo}$ (Wright & Albe, 1990). Computer models nicely fulfill the requirements for MCT analysis, since steady state conditions prevail and since very small differential changes in enzyme activity can be made independently.

The work to be presented represents the first step in gathering the data required for the construction of a realistic metabolic model appropriate for MCT analysis. It is a flux analysis of glucose metabolism in the filamentous fungus *Rhizopus oryzae*. Under quasi-steady state conditions (i.e., during logarithmic growth) the organism was exposed for brief periods to radioactive tracers, such as [$^{14}$C]-glucose. Glycolytic and tricarboxylic acid cycle intermediates were then isolated and purified to homogeneity to determine their specific radioactivities (SRs). This information, together with pool sizes and the rates of

glucose utilization and end product production, provided input for flux maps of the system under various experimental conditions. We obtained evidence for the existence of two separately regulated pools of pyruvate in *Rhizopus oryzae*: a cytosolic pool channeled into ethanol, lactate, oxaloacetate, malate and fumarate synthesis, and a second pyruvate pool channeled into the tricarboxylic acid cycle. The model is shown in Figure 1.

## MATERIALS AND METHODS

Flux maps were constructed using TFLUX, a SR curve-matching program developed by Sherwood et al. (1979). TFLUX is used for a steady-state system where pool sizes and fluxes remain constant over the labeling period. Sixty-three percent of the model input parameters for experiment A and 72% of the parameters for experiment B were derived from experimental data under the growth and labeling conditions indicated for each experiment. These input parameters consisted of reaction rates, metabolite concentrations and the SR of the tracer [$^{14}$C]-glucose. Final values for unknown pool sizes and fluxes were determined by best fit to the SR data as a whole. Briefly, if we assume that the system is in steady state, then a set of linear differential equations can be used to describe the SRs of the metabolite pools over time. From the input, the program constructs a system of differential equations of the form $X = Ax + b$ in which A is an n x n constant matrix, b is a constant n vector, and the n vector x contains the specific radioactivity of each of n pools. The program then computes each pool SR as a function of time. The TFLUX user specifies the number of intracellular and extracellular pools by

FIG 1. Model of glucose metabolism in the filamentous fungus *Rhizopus oryzae*. Ext- stands for extracellular, G-6-P for glucose-6-phosphate, F-6-P for fructose-6-phosphate and F-1,6-bP for fructose-1,6-bisphosphate.

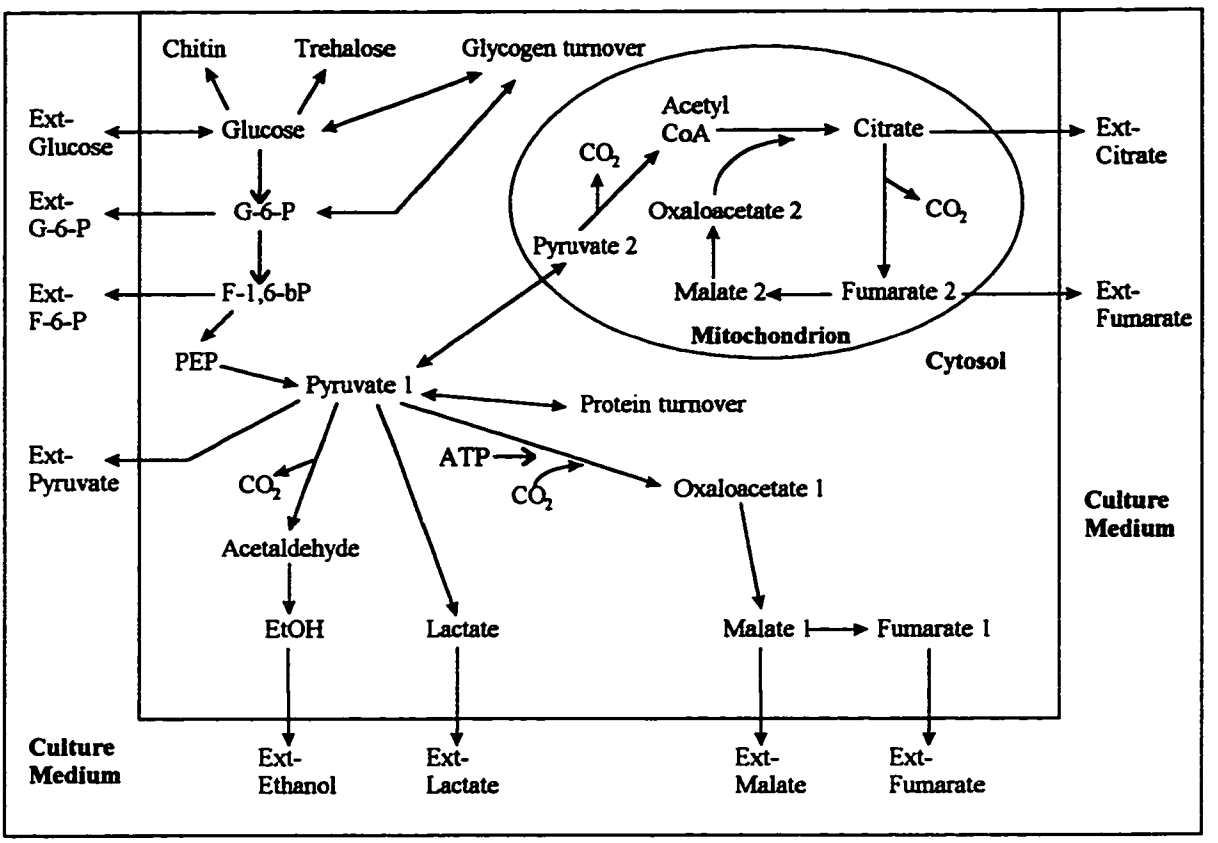

name, size (mM packed cell volume) and initial SR. Connections between pools are specified as constant flux rates (mM packed cell volume per min).

## RESULTS AND DISCUSSION

Three experiments were carried out with cells which had grown for 46-50 hours in a glucose-salts minimal medium at 27-32°C. They were removed from the growth medium by filtration and placed under the conditions specified for each experiment (Table 1). Cellular metabolite concentrations and SRs were determined in samples removed over a period of 20-30 min. These pool sizes for experiment A are listed in Table 2. Although the data and current thinking suggest that two separate intracellular pools of pyruvate, malate and fumarate exist in *Rhizopus oryzae* cells, when determining intracellular concentrations, the two pools are analyzed as one mixed pool due to the destruction of cellular integrity during the extraction procedure.

The growth media were analyzed for extracellular metabolite (see Figure 1) concentrations which were expressed in terms of mM packed cell volume (data not shown). These concentration data and the average dry weight over the incubation period were used to calculate average accumulation rates over the growth period (mM packed cell volume per min). The intracellular metabolite concentrations were expressed in terms of cell volume since that is where the metabolism being simulated occurs. As all parameters in the model must be expressed in the same terms, the extracellular concentrations and rates are also expressed in terms of cell volume. Moreover, in doing

Table 1. Unique conditions for each radiolabeling experiment in *Rhizopus oryzae*

| Condition | Experiment A | Experiment B | Experiment C |
|---|---|---|---|
| Label employed | [$^{14}$C]glucose | [$^{14}$C]glucose | [$^{14}$C]acetate |
| Glucose concentration (mM) | 42 | 286 | 291 |
| $Na_2CO_3$ concentration (mM) | 30 | 10 | 10 |
| Temperature (°C) | 32 | 27 | 27 |
| Labeling time (min) | 20 | 30 | 30 |

Table 2. *Rhizopus oryzae* radiolabeling experiment A, experimentally determined pool sizes (μmole per ml of packed cell volume) after a 20 minute incubation with [U-$^{14}$C]glucose and those generated by TFLUX for a 20 minute simulation

| Metabolite | Experimentally Determined Pool Size | TFLUX Generated Pool Size |
|---|---|---|
| Extracellular Metabolites | | |
| Glucose | 703.0 | |
| Lactate | 215.0 | |
| Intracellular Metabolites | | |
| Glucose | 8.5 | |
| Lactate | 20.6 | |
| Fructose-1,6-bisphosphate | 0.6 | |
| Citrate | 22.0 | |
| Ethanol | 13.1 | |
| Malate Mix[a] | 11.0 | |
| Cytosolic Malate | | 1.3 |
| Mitochondrial Malate | | 9.7 |
| Fumarate Mix[a] | 1.0 | |
| Cytosolic Fumarate | | 0.25 |
| Mitochondrial Fumarate | | 0.75 |
| Pyruvate Mix[a] | | 1.1 |
| Cytosolic Pyruvate | | 1.0 |
| Mitochondrial Pyruvate | | 0.1 |

[a]Mix indicates the metabolite concentration is a mixture of cytosolic and mitochondrial pools.

so, the measured amounts of extracellular end products over time were compatible with the intracellular rates responsible for their accumulation. The accumulation rates for experiments A and B are those fluxes for the metabolites which were expelled into the media and are designated in Table 3 as those rates for reactions leading to extracellular metabolite pools. The net rate of glucose uptake was determined in the same manner and is also indicated in Table 3.

All specific radioactivity values were determined in duplicate and the reported value is the mean, although in all cases the two values did not vary significantly. The SRs of metabolites for experiment A after the 20 min incubation are listed in Table 4 and are compared to the TFLUX-generated values. Thus, in experiment A, input to the model of known metabolic pathways in *Rhizopus* consisted of 9 measured pool sizes and 9 specific radioactivity determinations (including exogenous glucose starting SR). Input also included 9 fluxes based on glucose utilization and end product accumulation (chitin, pyruvate, fructose-6-phosphate, glucose-6-phosphate, ethanol, lactate, malate and fumarate), for a total of 27 independent parameters. Based on these data and the model, 7 unknown pool sizes and 9 fluxes were generated by best fit to the data as a whole (Tables 2 and 4). Thus, the independent parameters represented 63% of the total number.

One test of the validity of a model is to determine whether it can simulate the same metabolic system under perturbed conditions. Thus, in experiment B, exogenous glucose levels were raised to 286 mM, $Na_2 CO_3$ was lowered from 30 mM to 10 mM, and the cells were incubated at 27° rather than 32° C (Table 1). The reaction rates under these conditions are summarized in Table 3, and the match between experimental and TFLUX-

Table 3. Flux rates for *Rhizopus oryzae* radiolabeling experiments A and B

| Flux | Exp. A [$^{14}$C]glc; perturbed | Exp. B [$^{14}$C]glc |
|---|---|---|
| ext-glc → int-glc | 11.224 | 18.642 |
| int-glc → ext-glc | 4.1 | 9.0 |
| glc → chitin | 1.425 | 1.928 |
| glycogen turnover at glucose | 19.1 | 5.0 |
| glc → trehalose | 0.057 | 0.074 |
| glc → G-6-P | 5.642 | 7.640 |
| G-6-P → ext-G-6-P | 0.002 | 0.002 |
| glycogen turnover at G-6-P | 1.5 | 2.7 |
| G-6-P → F-6-P | 5.640 | 7.638 |
| F-6-P → ext-F-6-P | 0.002 | 0.002 |
| F-6-P → F-1,6-bP | 5.638 | 7.636 |
| F-1,6-bP → cytosolic pyr | 5.638 | 7.636 |
| cold protein turnover at cytosolic pyr | 0.9 | 13.0 |
| cytosolic pyr → mitochondrial pyr | 0.219 | 0.132 |
| mitochondrial pyr → acetyl CoA | 0.219 | 0.132 |
| Flux through Citric Acid Cycle | 0.219 | 0.132 |
| cytosolic pyr → ext-pyr | 0.062 | 0.084 |
| cytosolic pyr → EtOH | 0.716 | 0.762 |
| EtOH → ext-EtOH | 0.716 | 0.762 |
| cytosolic pyr → lactate | 4.104 | 6.465 |
| lactate → ext-lactate | 4.104 | 6.465 |
| cytosolic pyr → cytosolic OAA | 0.537 | 0.193 |
| cytosolic OAA → cytosolic malate | 0.537 | 0.193 |
| cytosolic malate → ext-malate | 0.094 | 0.037 |
| cytosolic malate → cytosolic fumarate | 0.443 | 0.156 |
| cytosolic fumarate → ext-fumarate | 0.443 | 0.156 |

Table 4. Experimental (Exp) and TFLUX generated specific radioactivities (x $10^4$ cpm per μmole) for *Rhizopus* oryzae radiolabeling experiments A - D

| Metabolite | Experiment A | | Experiment B | | Exp C |
|---|---|---|---|---|---|
| | Exp | TFLUX | Exp | TFLUX | Exp |
| Extracellular Metabolites | | | | | |
| Glucose | 19.9 | 20.0 | b | b | b |
| Lactate | 1.8 | 1.7 | b | b | b |
| Intracellular Metabolites | | | | | |
| Glucose | 7.4 | 7.4 | 8.6 | 8.6 | 0.0 |
| Lactate | 5.3 | 5.3 | 2.0 | 1.9 | <0.05 |
| Fructose-1,6-bisphosphate | 5.9 | 5.9 | 5.9 | 6.4 | <0.02 |
| Glucose-6-phosphate | b | | 6.5 | 6.4 | <0.01 |
| Trehalose | b | | 0.27 | 0.28 | 0.0 |
| Citrate | 0.46 | 0.50 | 0.10 | 0.14 | 15.3 |
| Ethanol | b | | 0.31 | 0.34 | <0.1 |
| Malate Mix[a] | 0.68 | 0.68 | 0.13 | 0.12 | 5.5 |
| Fumarate Mix[a] | 1.6 | 1.6 | 0.35 | 0.34 | 8.8 |

[a]Mix indicates the metabolite concentration is a mixture of cytosolic and mitochondrial pools.

[b]These values were not determined.

generated SRs is shown in Table 4. As might be expected, the rate of glucose utilization and flux through the glycolytic reactions increased. However, the rates of production of extracellular malate and fumarate were higher in experiment A, which had a higher concentration of sodium carbonate. This effect may in part be due to the inhibition of pyruvate decarboxylase activity by carbonate and the stimulation of pyruvate carboxylase, which requires $CO_2$ as a substrate. If carbonate inhibits acetaldehyde and ethanol production, more pyruvate is available for malate and fumarate production. It should be noted that the greatest production of extracellular lactate occurred with 10 mM sodium carbonate, rather than 20 or 30 mM (data not shown). In contrast, extracellular malate and fumarate concentrations were substantially higher at 20 and 30 mM sodium carbonate compared to 10 mM. Intracellular malate levels were also higher at 30 mM compared to 10 mM carbonate (data not shown). These findings were consistent with the following effect of carbonate on end product production: at 10 mM carbonate, the higher pyruvate levels lead to enhanced lactate production, but at higher carbonate concentrations pyruvate carboxylase competes favorably for the available pyruvate and an increase in production of malate and fumarate is noted. This increase in extracellular malate and fumarate levels is thought to result from the cytosolic pathway, since citrate, an exclusively mitochondrial pool, does not produce increased concentrations of extracellular citrate in response to increased carbonate concentrations.

We predicted that the specific radioactivities of the isolated (mixed) fumarate and the isolated (mixed) malate pools should be intermediate between those of the tricarboxylic acid cycle (e.g., citrate) and those of glycolysis (e.g., F-1,6-bP). This was

substantiated in experiments A and B (Table 4). If there is only one (mitochondrial) pool of citrate, and two pools (mitochondrial and cytoplasmic) of malate and fumarate, we predicted that labeling the system with [$^{14}$C]-acetate should give rise to a citrate pool with a significantly higher SR than the (mixed) malate and fumarate pools, which would in part be composed of unlabeled cytoplasmic pools. This was in fact observed (Table 4).

Having established the metabolite concentrations and flux patterns during glucose metabolism in *Rhizopus oryzae*, our next goal is the purification and kinetic characterization of key enzymes in this system. This information will allow the construction of a simple METASIM model (Wright & Kelly, 1981) for testing predictions and guiding experimental approaches. When this model has been expanded to a realistic level of complexity and has demonstrated predictive value, it will be subjected to MCT analysis (Wright, et al., 1992) (Albe & Wright, 1992) (Wright & Field, 1994) (Wright & Albe, 1994) (Albe & Wright, 1994).

## ACKNOWLEDGMENTS

This work was supported by NSF grant OSR-9350546 and The University of Montana.

## REFERENCES

**Albe, K.R. and Wright, B.E.** (1992). Systems Analysis of the Tricarboxylic Acid Cycle in *Dictyostelium discoideum*. *J. Biol. Chem.* **267**, 3106-3114.

**Albe, K.R. and Wright, B.E.** (1994). Carbohydrate metabolism in *Dictyostelium Discoideum*: II Systems' Analysis. J. *Theor Biol.* **169**, 243-251.

**Albe, K.R., Butler, M.H. and Wright, B.E.** (1990). Cellular concentrations of enzymes and their substrates. *J. Theor. Biol.* **143**, 163-195.

**Sherwood, P., Kelly, P., Kelleher, J.K., and Wright, B.E.** (1979). TFLUX a general purpose program for the interpretation of radioactive tracer experiments. *Comp. Prog. in Biomed.* **10**, 66-74.

**Wright, B.E.** (1968). An analysis of metabolism underlying differentiation in *Dictyostelium discoideum*. Annual Conference on Molecular Aspects of Differentiation, Oak Ridge National Laboratory. *J. Cell Physiol. Sup.*, 1, **72**, 145-160.

**Wright, B.E.** (1974). Kinetic models of cell differentiation. In: *Mathematic Models of Metabolic Regulation.* FEBS Advanced Course No. 27, Dobogoko, Hungary.

**Wright, B.E. and Park, D.J.M.** (1975). An analysis of the kinetic positions held by five enzymes of carbohydrate metabolism in *Dictyostelium discoideum*. *J. Biol. Chem.* **250**, 2219-2226.

**Wright, B.E.** (1973). *Critical Variables in Differentiation.* Prentice Hall, Inc., Englewood Cliffs, New Jersey. 109 pages.

**Wright, B.E.** (1970). The use of kinetic models to analyze differentiation. *Behavioral Science* **15**, No. 1, 37-45.

**Wright, B.E. and Albe, K.R.** (1994). Carbohydrate metabolism in *Dictyostelium* discoideum: I. Model construction. J. *Theor. Biol.* **169**, 231-241.

**Wright, B.E., Butler, M.H. & Albe, K.R.** (1992) Systems analysis of the tricarboxylic acid cycle in *Dictyostelium discoideum*. *J. Biol. Chem.* **267**, 3101-3105.

**Wright, B.E. and Field, R.J.** (1994). The tricarboxylic acid cycle in *Dictyostelium discoideum*. *J. Biol. Chem.* **269**, 19931-19932.

**Wright, B.E. and Kelly, P.J.** (1981) In: *Current Topics in Cellular Regulation.* (Horecker, B.L. and Stadtman, E.R., eds.) Vol. 19, pp. 103-158, Academic Press, Inc., New York.

**Wright, B.E. and Albe, K.R.** (1990). A new method for estimating enzyme activity and control coefficients *in vivo*. *Control of Metabolic Processes*, Il Ciocco, Italy (A. Cornish-Bowden, ed.), NATO ASI Series, Chapter 28, 317-328.

# Part II

# The Effect of Transcription on Starvation-Induced Mutations in *Escherichia coli*

# CHAPTER 3

## INTRODUCTION

When gram-negative bacteria are deprived of an essential nutrient, complex metabolic changes occur that enable the starving bacteria to maintain their viability - this process is known as the stringent response (Figs. 1 and 2; for a review see Cashel, et al., 1996). The major effector of the stringent response is the nucleotide derivative guanosine tetraphosphate (ppGpp; guanosine 3',5'-bis(diphosphate)). A general effect of ppGpp accumulation is that it down-regulates the synthesis of rRNA, tRNA, nucleotides and cell wall material thus sacrificing cell division for cell survival. In addition ppGpp stimulates the synthesis of RpoS, an alternative sigma factor ($\sigma^s$ or $\sigma^{38}$), which in turn stimulates the synthesis of about 40 proteins that protect the starving cell from extreme conditions, e.g. heat, oxidative damage and desiccation (Kolter, et al., 1993; Hengge-Aronis, 1996).

There are two known routes to ppGpp accumulation depending upon the limiting nutrient. In amino acid starved *Escherichia coli*, uncharged tRNAs accumulate and block translation, this sets up an idling reaction on the ribosome where the *relA* gene product converts ATP and GTP to (p)ppGpp. The RelA protein, (p)ppGpp synthetase I, is a ribosome-associated enzyme bound to about 1% of ribosomes. The enzyme responds to the ratio of charged to uncharged tRNAs rather than the concentration of either species of tRNA. Cells that lack RelA (*relA251*, Metzger, et al., 1989) or have decreased RelA expression (*relA1*,Metzger, et al., 1989; and *relA2*, Wright and Minnick, 1997) are inhibited in their ability to recover from starvation after the missing nutrient has been supplied (Cashel, et al., 1996) and they display a longer lag than wild-type cells when

FIG 1. The stringent response.

# THE STRINGENT RESPONSE

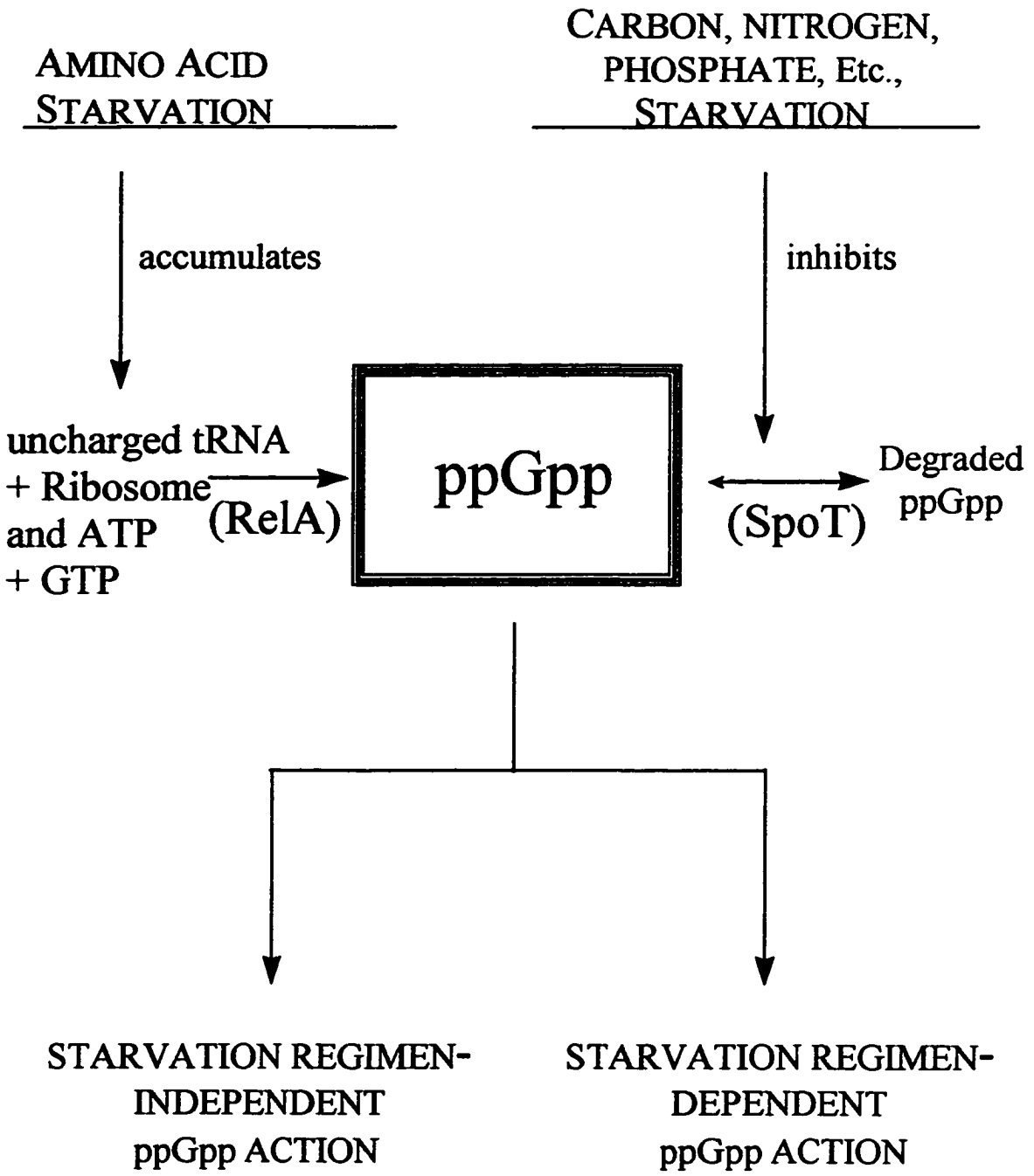

FIG 2. Guanosine tetraphosphate (ppGpp) action.


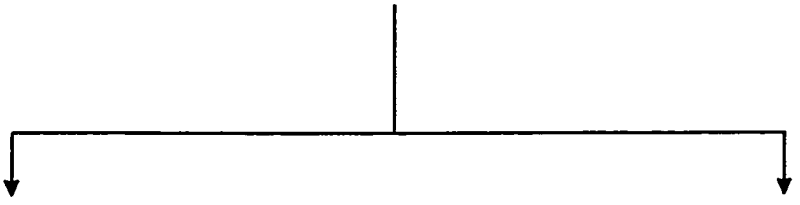

| STARVATION REGIMEN-INDEPENDENT | STARVATION REGIMEN-DEPENDENT |
|---|---|
| MAINTAIN VIABILITY BY: | POTENTIALLY able to address specific starvation problems by activating: |
| a) Inhibiting DNA, rRNA, tRNA, nucleotide and cell wall synthesis | a) Amino acid biosynthetic operons |
| b) Activating *rpoS* → $\sigma^s$ → protection from heat, oxidative damage, high osmolarity, desiccation, etc. | b) Proteolysis |
| | c) Carbon catabolic operons |
| | d) The *pho* regulon, etc. |

transferred from rich medium to minimal medium. However, the best characterized phenotype of these strains is that they continue to accumulate stable RNA (rRNA and tRNA) in amino acid limited cultures even after protein synthesis has stopped.

A second route to ppGpp accumulation occurs when growth is limited by starvation for carbon, nitrogen, or phosphate: (p)ppGpp accumulates because its degradation is inhibited by an as yet undiscovered mechanism. The *spoT* gene product is known to be the major effector of (p)ppGpp degradation so it is likely that the degratory activity of the SpoT protein is inhibited by carbon starvation. SpoT is a cytosolic enzyme with both (p)ppGpp degratory (3'-pyrophosphohydrolase) and synthetic (3'-pyrophosphotransferase) activities.

The mechanism by which ppGpp down-regulates some promoters and up-regulates others is not well understood; however, a discriminator sequence has been found in the -10 to the +1 region of the regulated promoters (Travers, 1984): promoters for rRNA, tRNA and ribosomal protein genes that are down-regulated by ppGpp have GC-rich discriminator sequences and the amino acid biosynthetic operons which are up-regulated have AT-rich discriminator sequences. Zacharias et al. (1989) demonstrated that putting a GC-rich discriminator sequence in a non-ppGpp-regulated promoter renders that promoter susceptible to down-regulation by ppGpp, but that making the *tac* discriminator GC-rich does not convert it to ppGpp-control. This suggests that other promoter features are involved in the mechanism of ppGpp control but are as yet undiscovered.

There is another consequence of the stringent response that until recently (Wright, 1996; Wright and Minnick, 1997; Wright, 1997) has gone undemonstrated. During

starvation for a particular nutrient, operon specific mechanisms result in the derepression of only those genes most likely to alleviate the stress. For example, in wild-type *E. coli*, when leucine is abundant, an attenuator mechanism inhibits transcription of the leucine biosynthetic operon genes; however when leucine levels decrease, the operon is derepressed, leucine biosynthetic genes are transcribed and translated and leucine is synthesized. The second manifestation of the stringent response is that ppGpp serves to further enhance transcription of those operons already derepressed by the specific starvation regimen (Fig. 2). Wright, et al. (in preparation) have recently shown this by measuring the level of *leuB* mRNA in two isogenic strains of *E. coli* K12 differing only in *relA*; CP78 is *relA*-wild-type (*relA*$^{wt}$; ppGpp$^{+}$) and CP79 is *relA2* which exhibits reduced ppGpp accumulation upon amino acid starvation (ppGpp-deficient or ppGpp$^{def}$).

Transcript levels were measured during log growth and after 60 min starvation for either leucine, arginine or arginine then leucine. It is clear from Figure 3 that during log growth when neither strain has elevated ppGpp concentration, *leuB* mRNA levels are low; then during leucine deprivation the *leu* operon is derepressed about 5-fold in the ppGpp$^{def}$ strain but in the *relA*$^{wt}$ strain the operon is derepressed about 20-fold due to both derepression and ppGpp enhancement. When the wild-type cells are starved for arginine (or threonine), ppGpp accumulates in the *relA*$^{wt}$ strain and there does appear to be some derepression of the leucine operon; however the levels are nowhere near the levels reached during leucine starvation as evidenced by the increase in *leuB* mRNA when arginine starvation is followed by leucine starvation. So, ppGpp alone activates the *leu* operon ~5-fold and leucine starvation alone derepresses the *leu* operon ~5-fold, but

FIG 3. CP78(ppGpp$^{+}$) and CP79 (ppGpp$^{def}$) *E. coli* grown to log phase in minimal medium then washed and transferred to minimal medium without arginine (-arg) or without leucine (-leu) for 60 min or -arg then -leu for 30 min each. Total mRNA was recovered and the level of *leuB* transcript determined by nuclease protection assay and densitometry.

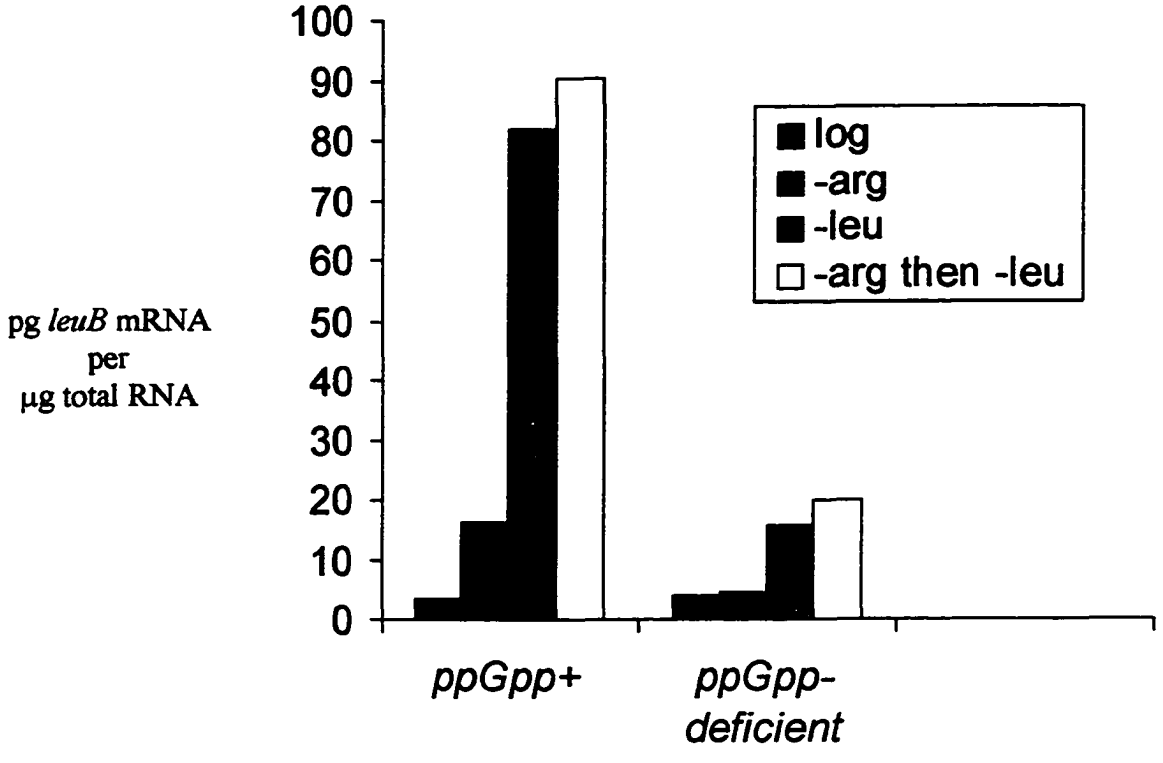

together, they derepress and activate the *leu* operon ~20-fold. In this way, ppGpp-dependent, full operon expression is specific to the operon derepressed by the particular starvation.

This enhancement of transcription due to ppGpp is important because there appears to be a link between transcription and mutation rates: genes are more susceptible to mutagenesis when they are transcribed. The first line of evidence for this is that deamination of cytosine residues occurs more frequently in ssDNA than in dsDNA (Lindahl and Nyberg, 1974). Frederico, et al. (1990) confirmed this observation by demonstrating that the rate of deamination in ssDNA is 140-fold higher than in dsDNA. In addition, Fix and Glickman (1987) found that 77 % of the G:C→A:T transitions they sequenced involved cytosines on the nontranscribed strand. Deamination of cytosine residues yields uracils which are normally removed by the product of the *ung* gene, UDP-glycosylase; absence of UDP-glycosylase leads to C→T transitions. Both Frederico, et al. (1990) and Fix and Glickman (1987) used *ung*$^-$ strains of *E. coli* so they could determine the total number of cytosine deaminations that occurred in the particular sequence under investigation.

During transcription, the nontranscribed strand is exposed as ssDNA while the transcribed strand is bound to the nascent mRNA in a DNA-RNA hybrid. Because ssDNA is more mutable than dsDNA, it follows that transcribed DNA and specifically the nontranscribed strand would be more susceptible to damage such as the deamination of cytosine residues. In order to prove this, several labs demonstrated that mutation rates increase when transcription is induced. Brock (1971) showed that mutagens which

directly damage nucleotides had increased mutagenic activity on a plasmid-carried *lacZ* gene when it was induced versus the same gene when non-induced. Brock inhibited replication during mutagen exposure by eliminating the carbon source, because replication also results in regions of periodically ssDNA that could interfere with the interpretation of the experiment. Herman and Dworkin (1971) tested the revertability of mutagen-induced mutations in the *lacZ* gene and found that 50 % of them exhibited at least 2-fold increased revertability when transcription was induced. In 1972, Savić and Kanazir compared the UV-induced reversion frequency of two chromosomal *his* operon mutants in a constitutive *his* operon to the same in a wild-type *his* operon and to the mutation frequency in an unlinked streptomycin allele. As expected, the transcriptionally active operons had a 5- to 8-fold higher reversion frequency and the mutability was specific to the derepressed operon because there was no increase in mutation frequency of the streptomycin allele.

To determine whether the nontranscribed strand is indeed more mutable than the transcribed (protected) strand, Beletskii and Bhagwat (1996) placed a kanamycin-resistance ($kan^r$) gene under transcriptional control of the inducible *tac* promoter ($tac^P$) in two orientations so that in one case the coding strand was transcribed and in the other case the noncoding strand was transcribed. The system was engineered so the deamination frequency of one specific cytosine residue could be studied and an $ung^-$ strain was used to ensure that all the deaminations would be detected. The result was a 4-fold higher mutation frequency in cytosines in the non-transcribed compared to the transcribed strand.

In the most direct evidence to date, Datta and Jinks-Robertson (1995) placed the yeast genomic *lys2* frameshift allele under the control of a highly inducible *gal80* promoter in two isogenic strains differing only in the presence of the *gal80* repressor (rep). Constitutive expression of the gene in the rep$^-$ strain resulted in a 50-fold increase in transcript level and a 35-fold increase in mutation rate over those in the rep$^+$ strain. This work is particularly relevant because the mutations were not caused by an added mutagen and because Datta and Jinks-Robertson also showed that the *lys*$^+$ to *lys*$^-$ forward mutation rate was 10-fold higher when the gene was derepressed.

So, if transcribed genes are more mutable than non-transcribed genes, then highly transcribed genes should have even higher mutation rates than non-transcribed genes; and, if the stringent response results in enhanced transcription of only those genes most likely to alleviate the starvation (in addition to the *rpoS* pathway), then only those genes should have increased mutation rates; therefore, the specific derepression of the operons by the stringent response should lead to specifically directed mutations. This is the working hypothesis of the work described here.

There are several predictions that would need to be satisfied in order to determine whether the stringent response results in specifically directed mutations. The first prediction is that mutations in an amino acid biosynthetic operon should increase in response to starvation for that amino acid, and this should not occur in a *relA* mutant strain that does not accumulate ppGpp upon amino acid starvation. This has been established for both the arginine and leucine operons (Wright, 1996). Reversion rates were determined for an *argH* and a *leuB* mutant allele in two isogenic *E. coli* K12 strains

differing only in *relA* ( CP78 is *relA*$^{wt}$ and CP79 is *relA2*). With arginine starvation the *argH*$^{-}$ reversion rate was 28-fold higher in the *relA*$^{wt}$ strain and with leucine starvation the *leuB*$^{-}$ reversion rate was about 7-fold higher in the *relA*$^{wt}$ strain.

The next prediction, which follows from establishment of the first prediction is that arginine starvation should only increase the *argH*$^{-}$ reversion rate and not affect the *leuB*$^{-}$ reversion rate and vice versa. This has not been determined because of the nature of the mutation rate experiment: for example if you want to determine the reversion rate of the *leuB*$^{-}$ allele in its repressed state, in response to arginine starvation, you could grow the cultures to stationary phase with limiting arginine and not derepress the *leu* operon, however, to measure the *leuB*$^{-}$ reversion rate the cultures must be plated on minimal medium devoid of leucine; thus, resulting in *leu* operon derepression. Until a method is devised for measuring the mutation rate without derepressing the operon, this prediction cannot be directly tested; however, the expected result can be inferred from several other lines of evidence.

Another way to look at the second prediction is that it implies specificity not only within amino acid biosynthetic operons but also between operons that are up-regulated and those that are down-regulated by ppGpp. It has already been established that up-regulated operons, *arg* and *leu*, have higher mutation rates when ppGpp accumulates. It follows that down-regulated operons should have decreased mutation rates when ppGpp accumulates. This was also established by Wright (1997; Figure 4): Wright predicted that since stable RNA and DNA synthesis is inhibited in *relA*$^{wt}$ strains during ppGpp accumulation, that the nucleotide biosynthetic operons might be down-regulated by

Fig 4. *leuB*⁻ reversion rates determined after leucine starvation in CP78 and CP79 and *pyrD*⁻ reversion rates determined after leucine starvation in *pyrD*⁻ transduced CP78 and CP79.

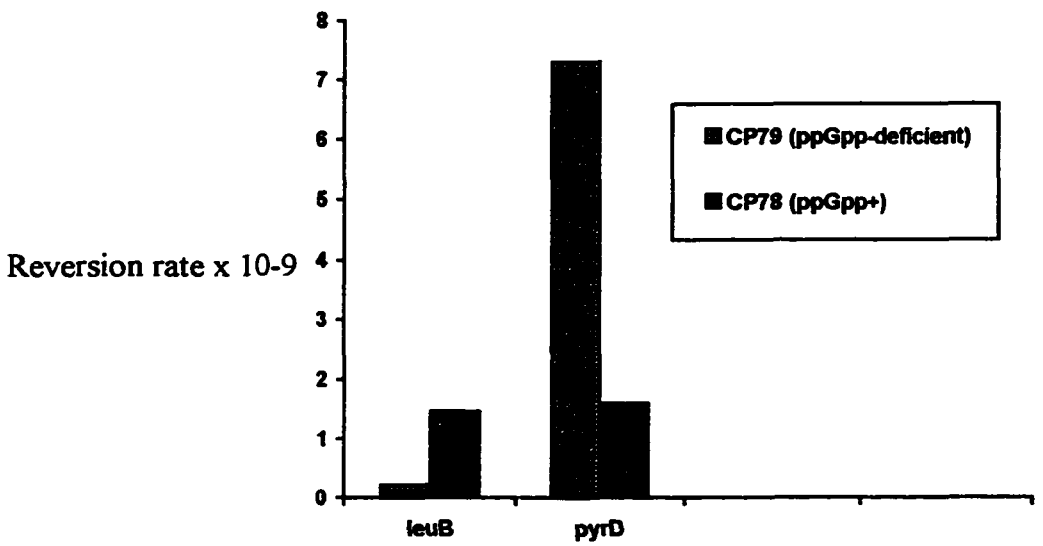

ppGpp - a look at the GC-rich discriminator sequences of both the purine and pyrimidine biosynthetic operons supported this hypothesis. A *pyrD*⁻ mutant allele was transduced into CP78 (*relA*$^{wt}$) and CP79 (*relA2*) and its reversion rate determined after amino acid starvation. With leucine starvation, the *pyrD*⁻ reversion was 4.5-fold lower in the ppGpp accumulating (*relA*$^{wt}$) strain (Fig. 4), just as predicted. Thus ppGpp-dependent mutations are specifically directed toward up-regulated operons.

The third prediction is that a positive correlation should exist between mutation rates, ppGpp concentration, and mRNA levels. This prediction was established in two parts, first a correlation was established between mutation rates and ppGpp concentration (Fig 5; Wright and Minnick, 1997). Since that report, a correlation between mutation rates and mRNA levels has been established (Wright et al., in preparation). Figure 6 is a picture of a scanned autoradiogram from a typical nuclease protection assay. The levels of *leuB* mRNA correlate with *leuB*⁻ reversion rates: *leuB* mRNA level and reversion rate are highest after leucine starvation in the *relA*$^{wt}$ strain. Also, the levels of *pyrD* mRNA correlate with *pyrD*⁻ reversion rates: *pyrD* mRNA level and reversion rate are highest in the *relA2* strain. Quantified *leuB* mRNA levels from several different nuclease protection assays are plotted against reversion rates in Figure 7 - there is a very good correlation between reversion rates and mRNA levels.

A fourth prediction, if confirmed, would establish enhanced transcription as the mutagenic culprit as opposed to some unrecognized mutagenic activity of ppGpp. The prediction is that by replacing the promoter in an amino acid biosynthetic operon with an inducible promoter, it should be possible to bypass the role of ppGpp and enhance

FIG 5. Adapted from Wright & Minnick, 1997; generation times and *leuB*$^-$ reversion rates were determined for four different *relA*$^{wt}$ and *relA2* strains under a total of nine different conditions that either induced or mimicked leucine starvation (minimal medium (MM) with limiting leucine, MM + serine hydroxamate, MM + γ-glutamyl leucine). Steady-state levels of ppGpp were determined during exponential growth in the same strains and under the same conditions.

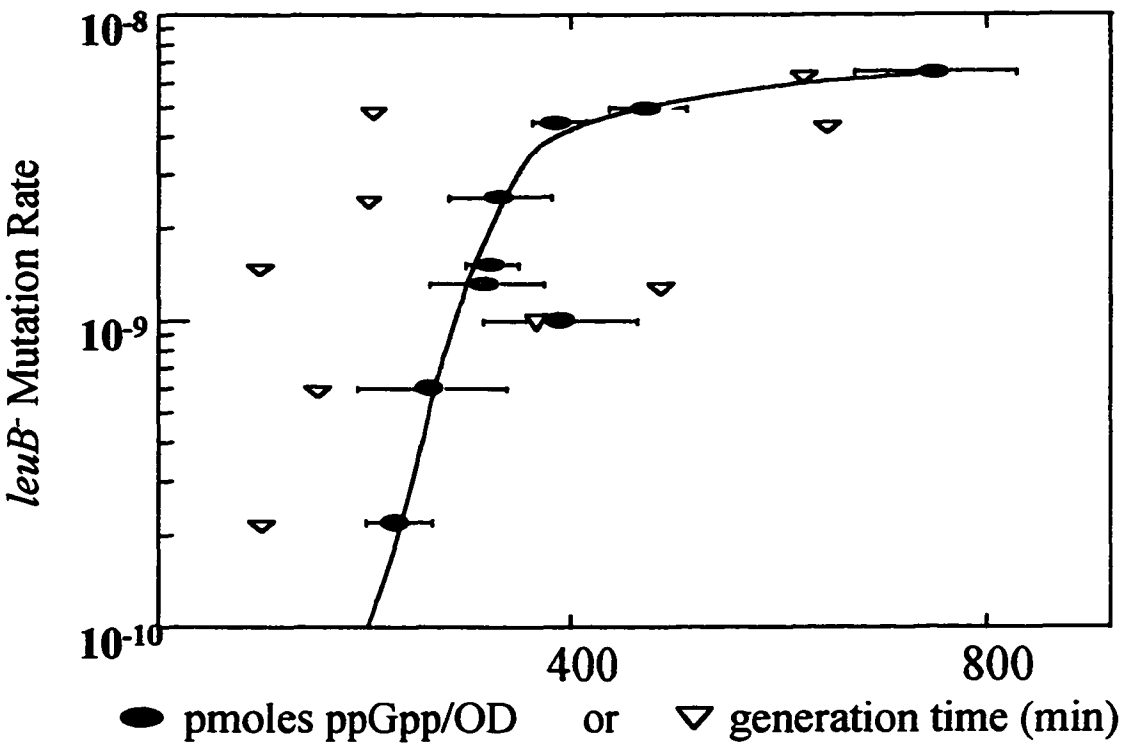

FIG 6. A typical nuclease protection assay of mRNA collected from ppGpp$^+$ (CP78) and ppGpp$^-$ (CP79) cells during log growth and after leucine starvation. With amino acid starvation, the *leuB*$^-$ reversion rate is higher in the *relA*$^+$ (ppGpp$^+$) strain and the *pyrD*$^-$ reversion rate is higher in the *relA*$^-$ (ppGpp$^-$) strain. The specific mRNA levels correlate with mutation rates.

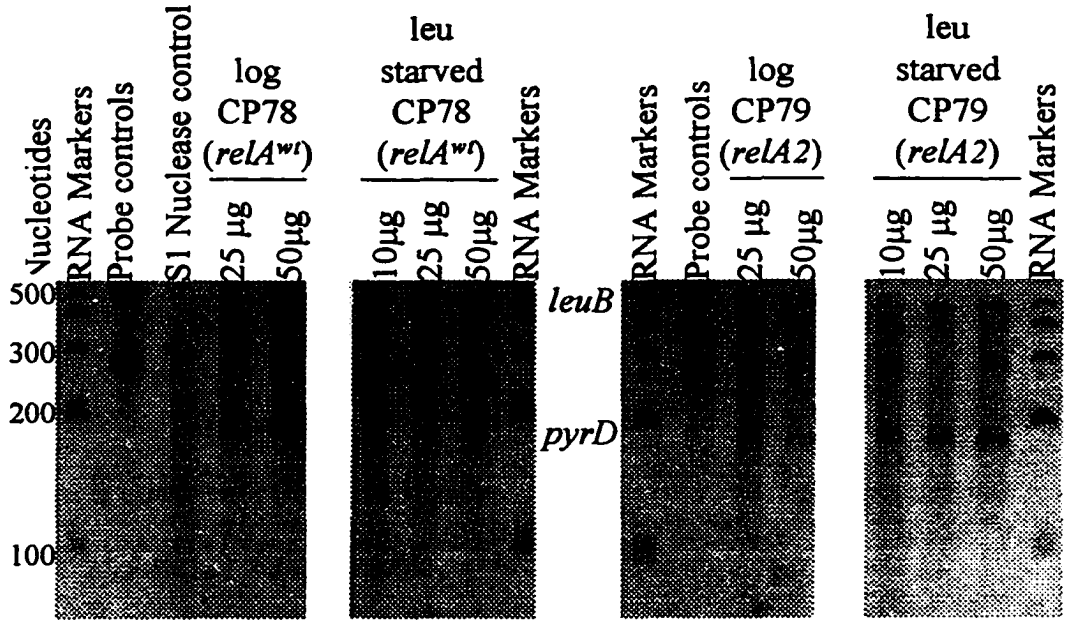

FIG 7. *leuB*$^-$ reversion rates and mRNA levels were determined in five different *relA*$^{wt}$ and *relA2* strains (CP78, CP79, CP78*pyrD*$^-$, CP79*pyrD*$^-$, and 78AL) under four different conditions (leucine starvation, arginine starvation followed by leucine starvation, or with and without IPTG induction for 78AL only). The boxed points are those for 78AL - the correlation is the same with or without these points.

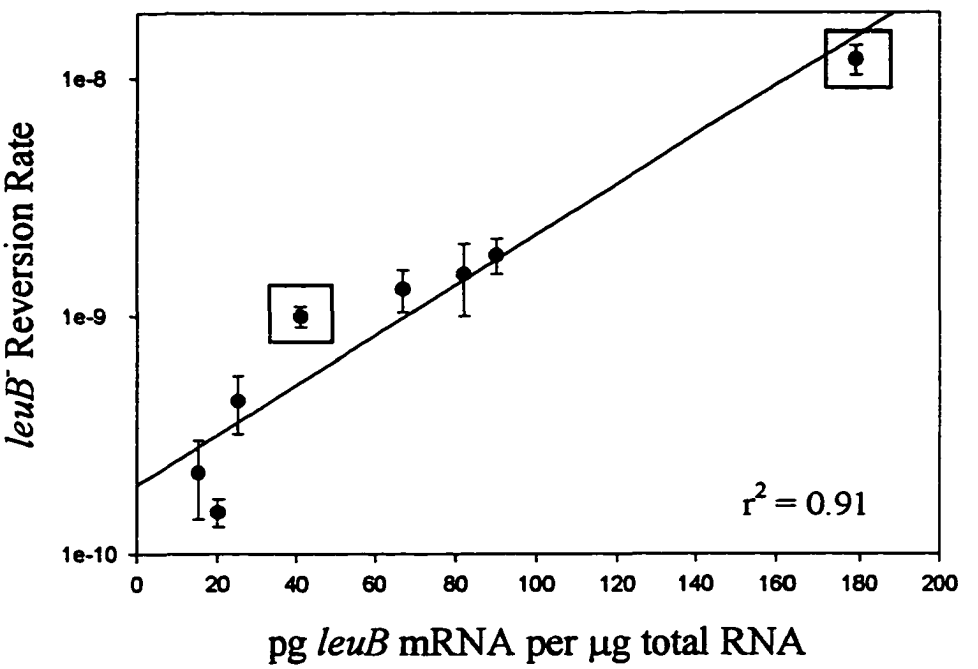

transcription and mutation rates directly, with the inducer. Establishment of this prediction is the subject of the work described here.

## RESEARCH DESIGN

The chromosomal *leu* promoter ($leu^P$) was replaced by the IPTG-inducible *tac* promoter ($tac^P$) in both CP78 ($relA^{wt}$) and CP79 (*relA2*). The *leu* promoter was replaced by double crossover homologous recombination of a 3.6 kb fragment of dsDNA containing a kanamycin resistance ($kan^r$) cassette and the *tac* promoter flanked by sequences homologous to regions of the *E. coli* chromosome both upstream and downstream of the *leu* promoter (Fig. 8).

Replacement of the promoter was confirmed by PCR band lengths and by sequencing. *leuB*⁻ reversion rates and transcript levels were determined in the recombinant $relA^{wt}$ strain (78AL) with and without IPTG induction and with varying IPTG concentrations. Results indicate a significant increase in *leuB* mRNA level and mutation rate when the operon is induced; thus confirming that enhanced transcription leads to increased mutation rates.

## MATERIALS AND METHODS

### Recombinant DNA Methods

*Preparation of chromosomal DNA*

Chromosomal DNA was prepared according to the well-established Miniprep procedure for Bacterial Genomic DNA in Current Protocols in Molecular Biology,

FIG 8. Research design: replacement of the *leu* promoter ($leu^P$) with the *tac* promoter ($tac^P$) by double crossover homologous recombination.

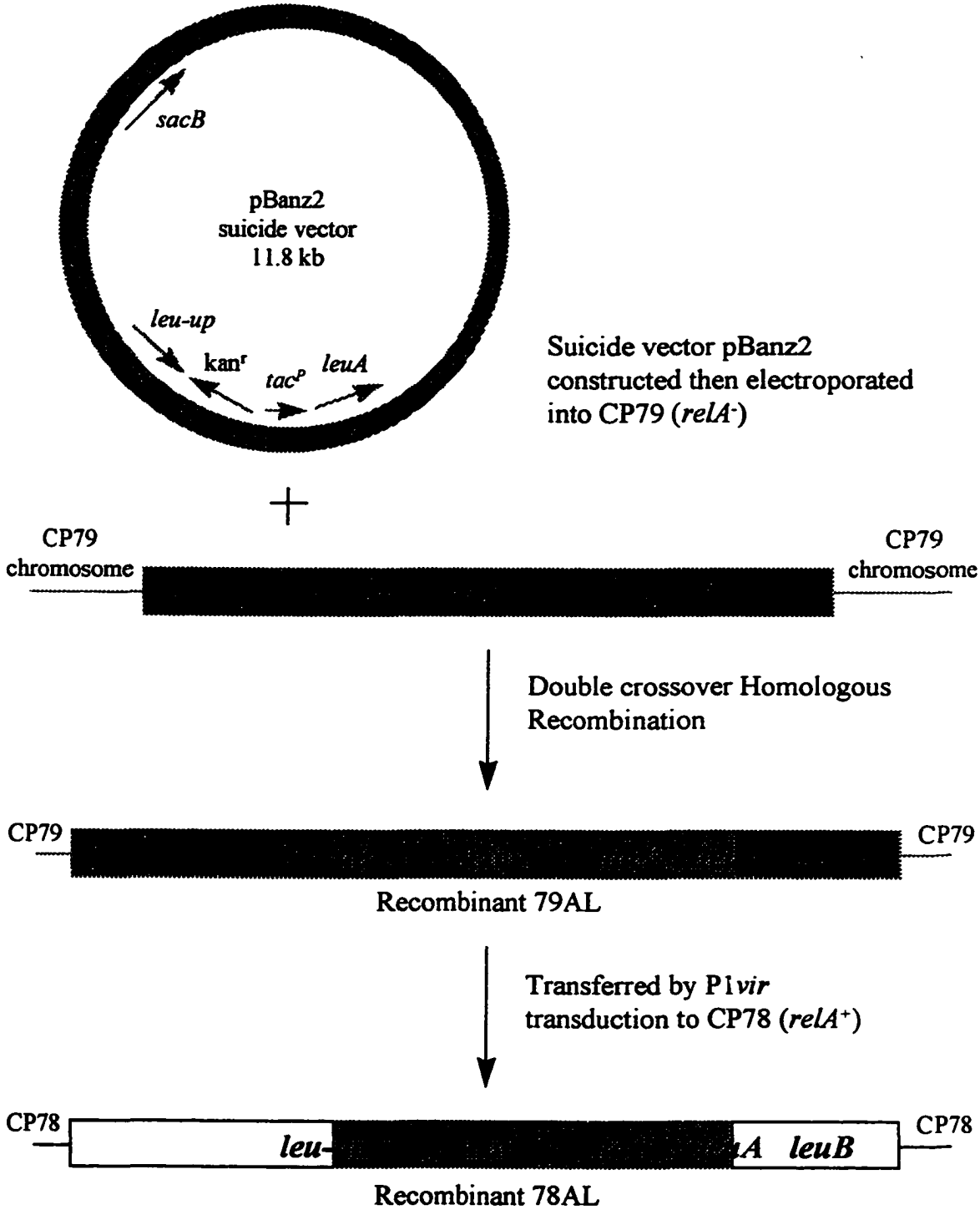

(Ausubel, et al., 1994-1997). The protocol utilizes sodium dodecyl sulfate (SDS) and proteinase K to destroy cell walls and denature proteins. Cell debris are precipitated with a CTAB/NaCL solution. The DNA is phenol/chloroform extracted, precipitated with isopropanol and resuspended in TE buffer.

*Polymerase Chain Reaction (PCR)*

Two different methods of PCR were utilized in this work; for PCR products of less than 2 kb, *Taq* DNA polymerase (Promega) was used and for PCR products longer than 2 kb, a high-fidelity mixture of *Taq* and *Pwo* DNA polymerases (Boehringer-Mannheim) was employed.

When *Taq* was used alone, a 100 µl reaction mixture consisted of 50 mM KCl, 10 mM Tris-HCl (pH 9.0), 0.1% Triton X-100, 2.0-3.0 mM $MgCl_2$ (optimized for individual primer sets), 20 µl chromosomal DNA, 50 pmol each primer, 0.2 mM dATP, 0.2 mM dCTP, 0.2 mM dGTP, 0.2 mM dTTP (Promega dNTPs), and 2.5 U Promega® *Taq* DNA polymerase. The reaction mix was overlayed with 30 µl mineral oil (Sigma) and placed in a TempCycler II, model 110S termalcycler (COY Corp.) at 94°C for 1 min, then 25 cycles of 92°C for 45 sec, 50°C for 30 sec, and 72°C for 2 min, followed by an elongation at 72°C for 15 min and 4°C hold temperature. The oil was removed from the reactions with Parafilm, the products were separated by agarose gel electrophoresis and the target products were recovered from the gel by GeneCleaning (Bio 101, inc.). The products were eluted into 20 µl $dH_2O$.

When long-PCR was required, the Expand™ High Fidelity PCR System of Boehringer Mannheim was utilized and the reaction mixture was generated as per their directions: a 50 µl reaction consisted of 0.2 mM each dNTP (Boehringer Mannheim PCR nucleotide mix), 50 pmol each primer, 01-0.75 µg template DNA, 5 µl of the Expand™ HF buffer (10x concentration of undisclosed elements), 1.5 mM $MgCl_2$, and 2.6 U Expand™ HF PCR System enzyme mix. The reaction mix was overlayed with 30 µl mineral oil (Sigma) and placed in a Perkin Elmer GeneAmp PCR System 2400 at 95°C for 3 min, 10 cycles of 94°C for 45 sec, 58°C for 30 sec, and 68°C for 2 min 20 sec, 20 cycles of 94°C for 45 sec, 58°C for 30 sec, and 68°C for 2 min 20 sec plus an elongation of 20 sec per cycle, followed by an elongation at 72°C for 15 min and 4°C hold temperature. The oil was removed with parafilm and a fraction of each reaction was observed for product size with agarose gel electrophoresis. The remainder of each reaction mix was cleaned with the Boehringer Mannheim High Pure PCR Product Purification Kit which utilizes the property of nucleic acids to bind to glass fibres in the presence of a chaotropic salt (guanidine-thiocyanate in this case). The products were eluted into 100 µl $dH_2O$.

*PCR primers*

The 1589 bp *leuA* gene was amplified with forward primer LeuA3 (5'-GCCGG AATTCATGAGCCAGC-3'; *leuA* start codon underlined) which includes an *EcoR*I site (5'-GAATTC-3'), and reverse primer LeuA2 (5'-ATCCTGCAGCACACGGTTTC-3') with a *Pst*I site (5'-CTGCAG-3').

The 572 bp *leu* upstream region was amplified with forward primer LeuA4 (5'-AAGGCGCATGCTCAGTAACGGGC-3') including an *Sph*I site (5'-GCATGC-3') and reverse primer LeuA5 (5'-CAACGGCTAGCACGCATGGTCGA-3') with a *Nhe*I site (5'-GCTAGC-3').

Primers used to amplify regions for sequencing were as follows: the forward primer, from upstream of the *leu* upstream region was SeqA (5'-cacgctaagtacgctcatc-3'), and the reverse primer, originating within the *leuB* gene downstream of the *leuA* gene was SeqZ (5'-ggcgatacgttcgatctca-3'). The size of the amplified fragment from this set of primers was designed to allow parents and recombinants to be distinguished: the parental product was 3683 bp and the recombinant product was 4254 bp.

*Plasmid Preparation*

Plasmid mini-preparations were done with the Quantum Prep Kit of BioRad and eluted into 100 µl $dH_20$ for restriction digestion and transformation or TE buffer for storage. Plasmid maxi-preparations were performed with alkaline lysis as described by Sambrook et al., 1989.

*Agarose gel electrophoresis and elution of DNA*

Agarose gel electrophoresis was performed according to standard protocol with a 1% agarose gel in 1x TAE buffer (0.04 M Tris-acetate, 0.001 M EDTA) with 0.06% ethidium bromide added to the gel. The loading dye, 7x concentration consisted of 31 mM EDTA, 40% glycerol, 0.05% bromophenol blue, and 0.05% xylene cyanol. Current was usually applied at 60 V for one hour.

DNA bands were excised from the gel and the DNA eluted with a GeneClean II kit according to manufacturer's suggestions (BIO 101, inc.).

*Ligation*

Ligations were performed via standard protocol with T4 DNA Ligase (Promega) and the supplied buffer. For all except T-vector ligations, the mixture of DNA was heated at 65°C for 2 min and then immediately placed on ice before the buffer and enzyme were added. The ligase was heat inactivated at 65°C for 10 min before each transformation.

*DNA Sequencing*

All DNA synthesis and sequencing was performed by Joan Strange in the Murdock Molecular Biology Facility at The University of Montana.

*T-Vector Cloning*

T-vector cloning takes advantage of the template-independent terminal transferase activity of *Taq* polymerase: during PCR amplification the *Taq* enzyme usually adds an adenine nucleotide to the 3' end of the amplified fragments. Commercial T-A cloning vectors have been developed which consist of a linear vector with 3' thymidine overhangs so that the complementary A and T overhangs will anneal, the PCR fragment will have been cloned and the plasmid can be utilized in transformation by standard protocols. In 1991 Marchuk et. al. published a protocol for developing T-vectors in the laboratory: the plasmid pBluescript is digested with *Eco*RV (blunt-end cutter) and Taq polymerase is used to add 3' thymidines. The Marchuk protocol is quick and cost-effective, however, it is less

efficient than commercially available kits and requires commercially prepared cells with very high transformation efficiency. In this laboratory, the Marchuk protocol is used often but if it is not effective after the first or second try, kits by Novagen or Invitrogen are utilized - thus, all PCR products are cloned into T-vectors.

*Suicide Vector and Sucrose Selection*

Plasmid pWM91 provided by Barry Wanner contains the R6K origin of replication which will only initiate replication in cells where the trans-acting lambda protein Pir is present. Therefore, the vectors are "suicide vectors" for non-Pir containing hosts such as CP78 and CP79 - the vector can transform CP78 and CP79 but cannot replicate. The only way a host will be transformed is if the plasmid genes are integrated into the host chromosome. This happens by a single-crossover homologous recombination event. A double-crossover recombination event will also yield a transformed organism but the rate at which this happens is so low as to not be practical to select for. Double-crossover homologous recombination is the ultimate goal, so organisms containing integrated plasmids (integrants) from a single-crossover event are selected after transformation, grown to high cell densities and a second selection is imposed to find double-crossover homologous recombinants. That second selection involves the *sacB* gene of *Bacillus subtilis* which when induced by sucrose codes for the enzyme levansucrase. The production of levansucrase is lethal in *E. coli* in the presence of ≥5% sucrose (Gay, et al., 1985). Plasmid pWM91 and its derivatives (e.g. pBanz2) contains the *sacB* gene and when integrants are grown in the presence of 10% sucrose only those cells which have

undergone double-crossover recombination and lost the *sacB* gene will survive. Survivors are screened for the loss of *sacB*-linked ampicillin resistance and the retention of $tac^P$-*leuA* linked kanamycin resistance - indicating the correct replacement of the *leu* promoter with the $kan^r$ cassette and *tac* promoter. PCR and sequencing are used to confirm replacement.

**DNA Transfer Protocols**

*Chemical Transformation*

Chemical transformations were performed according to a modified version of the protocol of Chung et al., 1989. To make competent cells for transformation, the appropriate strain was grown overnight in L-broth (LB; 10% (w/v) tryptone, 5% (w/v) yeast extract and 5% (w/v) NaCl) and diluted 1:20 in fresh LB then grown to early log (~2 h) at 37°C and 250 rpm. The cells were then centrifuged at 6000 rpm for 5 min and resuspended at one-tenth the original volume in ice-cold TSS (LB with 10% (w/v) PEG 8000, 5% (v/v) DMSO and 50 mM $MgSO_4$. The cells were aliquotted in 0.1 ml volumes to ice-cold polypropylene tubes and either frozen at -70°C in dry-ice and ethanol or used immediately for transformation.

Transformation was carried out on ice as per a modification by M. Minnick of the Chung, et al. procedure. A small aliquot of DNA (~100 pg) was mixed with an aliquot of competent cells and incubated on ice for 45 min. The cell-DNA mixture was then mixed with 0.9 ml room temperature TSS and transferred to a 15 ml round-bottom polypropylene culture tube. The transformed cells were incubated at 37°C with shaking at

250 rpm for 75 min to allow recovery and expression of antibiotic resistance. Appropriate dilutions were plated to selective media.

*Electroporation*

Cells for electroporation must be devoid of ions and were prepared as follows: cells from an overnight culture were diluted 1:100 in fresh LB for about 2 h to an $OD_{600}$ of 0.3-0.6. All subsequent procedures were carried out at 4°C. The culture was incubated on ice for 30 min, then centrifuged in 20 ml aliquots at 4500 rpm for 10 min at 4°C. The cells were washed twice with 20 ml ice-cold sterile Nanopure water and twice with 20 ml ice-cold sterile 15% glycerol. Centrifugation between washing steps was done for 10 min at 4°C at increasing speeds of 4500 rpm, 6000 rpm and 8000 rpm for the last two steps. The cell pellets became less compact with each wash so the centrifugation speed was increased to facilitate recovery and prevent loss of cells. After the last centrifugation, each cell pellet was resuspended in 0.2 ml sterile 15% glycerol, aliquotted into ice-cold polypropylene tubes and used immediately or frozen quickly in a dry ice/ethanol bath and stored at -80°C.

For electroporation the DNA also has to be relatively free of ions so all plasmids were resuspended in Nanopure water and all ligations were GeneCleaned (Bio 101, inc.) and then resuspended in Nanopure water. One to 10 µl of the DNA were mixed with 100 µl of cells thawed briefly on ice. The cells and DNA were mixed well, transferred to a chilled (-20°) cuvette (BioRad® GenePulser®/E. coli Pulser™ 0.1 cm cuvettes) and electroporated at 1.8 kV field strength, 25 µF capacitance and 200 Ohms resistance in a BioRad®

GenePulser® II electroporator with a Pulse Controller Plus. Efficient electroporations were those in which the pulse was maintained for at least 3.8 mSec. The maximum length of pulse observed was 4.9 mSec.

After electroporation cells were transferred to 0.9 ml SOC medium (2% tryptone, 0.5% yeast extract, 10 mM NaCl, 2.5 mM KCl, 10 mM $MgCl_2$, 10 mM $MgSO_4$, and 20 mM glucose) in a 15 ml round-bottom polypropylene culture tube and incubated at 37°C for 1 h to allow gene expression. Cells were then plated on selective media in 0.05 to 1.0 ml aliquots and observed for growth after 24 h at 37°C.

In some cases, especially when T-vector cloning was involved, very high efficiency ($10^9$ - $10^{10}$ transformants per μg DNA) electroporation competent cells were required. Because efficiency with cells prepared as described above was only about $10^6$ -$10^7$ transformants per μg DNA, Life Technologies™ (GIBCOBRL) MAX Efficiency DH5α™ competent cells were used and the protocol for electroporation was the same as described above except that the DNA was diluted 10-fold before use.

*P1vir Transduction*

This laboratory has employed P1*vir* transduction to transfer many genes among different bacterial strains (Wright and Minnick, 1997). The protocol was adapted from Ohman, 1988 and is based on the characteristic property of P1*vir* to transfer DNA from one bacterial host to another without integrating its own DNA into either host. P1*vir* is a mutant derivative of bacteriophage P1 that no longer can form lysogens; when it infects donor bacteria, it replicates and in the process of packaging its DNA picks up segments of

donor bacterial DNA. This phage can then transfer the newly packaged DNA to alternate host bacteria. The protocol for transduction involves infecting the donor strain with P1*vir*, collecting the lysate, killing any remaining host bacteria and using the lysate to infect the recipient strain. Transduced recipients carrying some selective marker in or near the desired gene are isolated on selective medium (usually containing an antibiotic).

**Promoter Replacement**

*Replacement of the leu with the tac promoter in CP78 and CP79*

A suicide vector containing the *tac* promoter, a kanamycin resistance cassette and ends which are homologous to the *E. coli* chromosome flanking the *leu* promoter was generated and then used to transform *E. coli* CP79 (*relA2, leuB*$^-$). Double crossover homologous recombination between the chromosome and the plasmid replaced the chromosomal *leu* promoter with the *tac* promoter and kanamycin resistance cassette. P1*vir* transduction was utilized to transfer the recombinant promoter to CP78 (*relA*$^{wt}$, *leuB*$^-$).

In order to replace the promoter in CP79 several things had to be accomplished: 1) *leuA* had to be PCR amplified and cloned into a vector just downstream of the *tac* promoter and the *tac* promoter had to direct expression of a functional *leuA* gene; 2) A kanamycin-resistance cassette had to be cloned into the *tac*$^P$-*leuA* vector; 3) about 600 bp upstream of the chromosomal *leu* promoter had to be amplified by PCR and cloned into the kan$^r$-*tac*$^P$-*leuA* vector; 4) because transformation with linear DNA resulted in no recombinants, the region from *leu-up* through kan$^r$ and *tac*$^P$-*leuA* had to be recovered and

cloned into a suicide vector; 5) the suicide vector had to become integrated into the *E. coli* chromosome under permissive conditions; and 6) double crossover homologous recombinants had to be selected under restrictive conditions. These things were accomplished through 13 cloning steps (steps I-XIII). The strains and plasmids used are indicated in Table 1.

The first goal was to clone the *leuA* gene into a $tac^P$ vector and confirm *leuA* expression from the *tac* promoter. In step I, a streptomycin- (Sm) spectinomycin- (Spc) resistance cassette ($Sm^r/Spc^r$) was cloned into pKK223-3 ($tac^P$) (Fig. 9) to provide strong selection of transformants. Several non-transformed ampicillin-resistant ($amp^r$) colonies developed during initial attempts to clone *leuA* so this first step became necessary. In step II, the *leuA* gene was PCR amplified with forward primer LeuA3 , containing an *Eco*RI site, and reverse primer LeuA2, containing a *Pst*I site. The gene was cloned into a Novagen T-vector (Fig. 10) to facilitate digestion with *Eco*RI and *Pst*I because cutting the linear PCR product was so inefficient as to prevent subsequent cloning. Recovery of *leuA* from the T-vector for subcloning was very efficient. In step III, *leuA* was recovered from the T-vector and cloned into the plasmid generated in step I to generate pAL1g (Fig. 11). At this stage it was very important to determine if the *leuA* gene was functionally expressed from the *tac* promoter; to do this pAL1g was transformed into a $leuA^-$ strain of *E. coli*, strain CV512. Growth of transformed CV512/pAL1g on amp, sm, spc and minimal medium without leucine confirmed that *leuA* is functionally expressed from the *tac* promoter.

Table 1. Bacterial strains and plasmids

| Bacterial Strain | Genotype | Source |
|---|---|---|
| CP78 | F⁻, *thr*-1, *leuB*6, *his*65, *argH*46, *thi*-1, *ara*13, *gal*3, *malA*1, (λ$^r$), *xyl*-7, *mtl*-2, *tonA*2, *supE*44 | M. Cashel |
| CP79 | CP78 but *relA*2 | M. Cashel |
| CV512 | F$^+$, *leuA*371 | CGSC |
| BW24551 | D*lac*169, *rpoS* (Am), *robA*1, *creC*510, *hsdR*514, *uidA* (pM*lu*I)::*pir* (wt), *recA*1, mini-Tn5Lac4 (Cm$^r$) | B. Wanner |
| DH5$_\alpha$ | F⁻, Φ80d*lacZ*ΔM15, Δ(*lacZYA-argF*)U169, *deoR*, *recA*1, *endA*1, *hsdR*17($r_K^-$, $m_K^+$), *phoA*, *supE*44, λ-, *thi*-1, *gyrA*96, *relA*1 | GIBCOBRL |
| **Plasmid** | **Genotype** | **Source** |
| pBSL15 | kan$^r$ | M. Alexeyev |
| pKK223-3 | amp$^r$, *tac*$^P$ | Pharmacia |
| pBluescript SK$^+$ | amp$^r$, *lacZα* | Stratagene |
| pHP45Ω | amp$^r$, Sm$^r$/Spc$^r$ | |
| Clonesure | amp$^r$, *lacI*$^q$, *tac*$^P$-δGATA-1 | CPG |
| pWM91 | amp$^r$, *lacZα*, ori$_{R6K}$, *sacB* | B. Wanner |

FIG 9. Cloning step I: the spectinomycin/streptomycin resistance gene ($Spc^r/Sm^r$) was recovered from pHP45Ω by restriction digestion with *Hin*dIII, gel purified, and cloned into the *Hin*dIII site of pKK223-3 to generate pAL0.5 which was selected for resistance to ampicillin (amp), Spc and Sm.

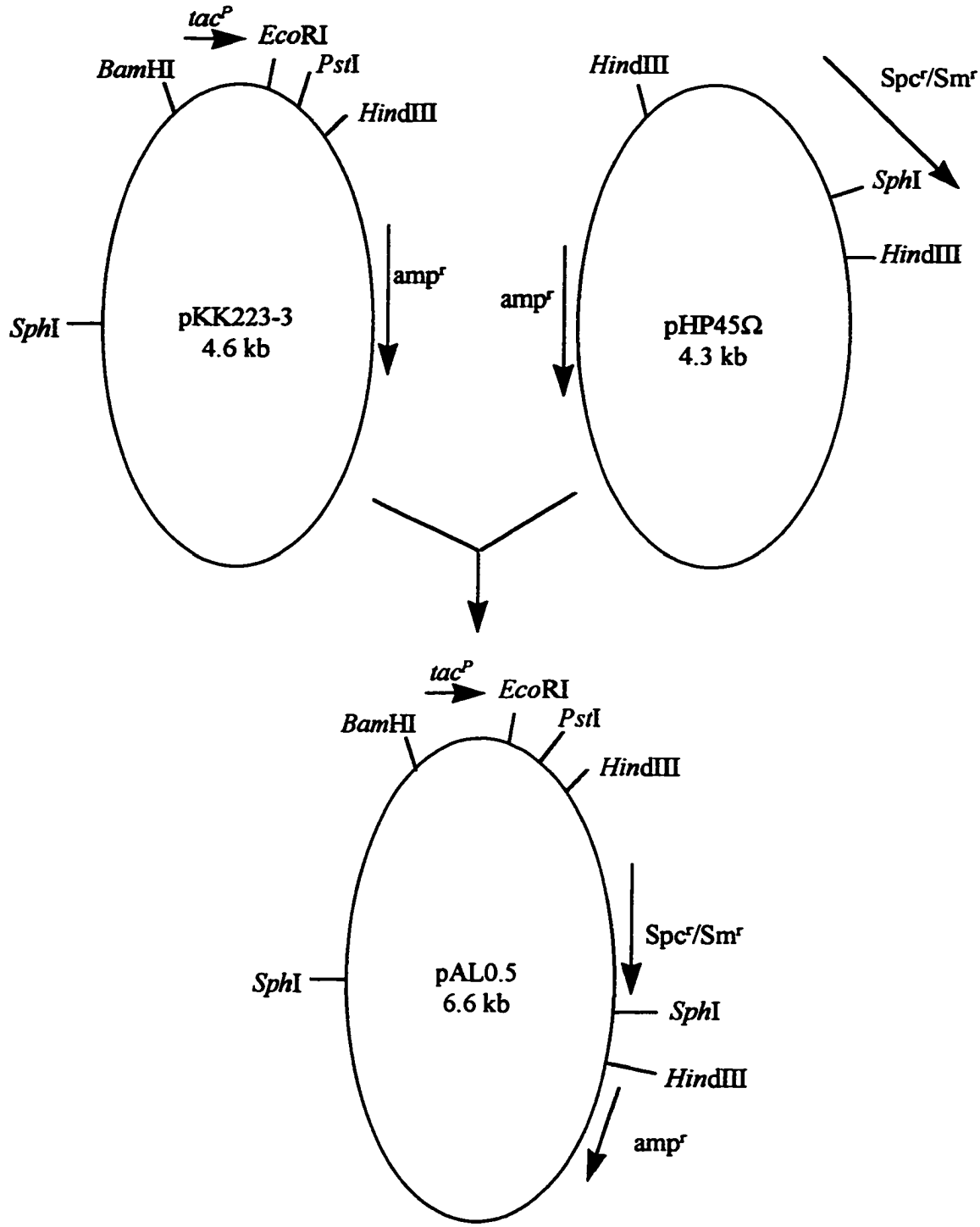

FIG 10. Cloning step II: the *leuA* gene was amplified by PCR, gel purified and cloned into a T-Vector (Novagen) to generate pTleuA which was selected for ampicillin (amp) resistance and screened for lack of blue color on X-gal.

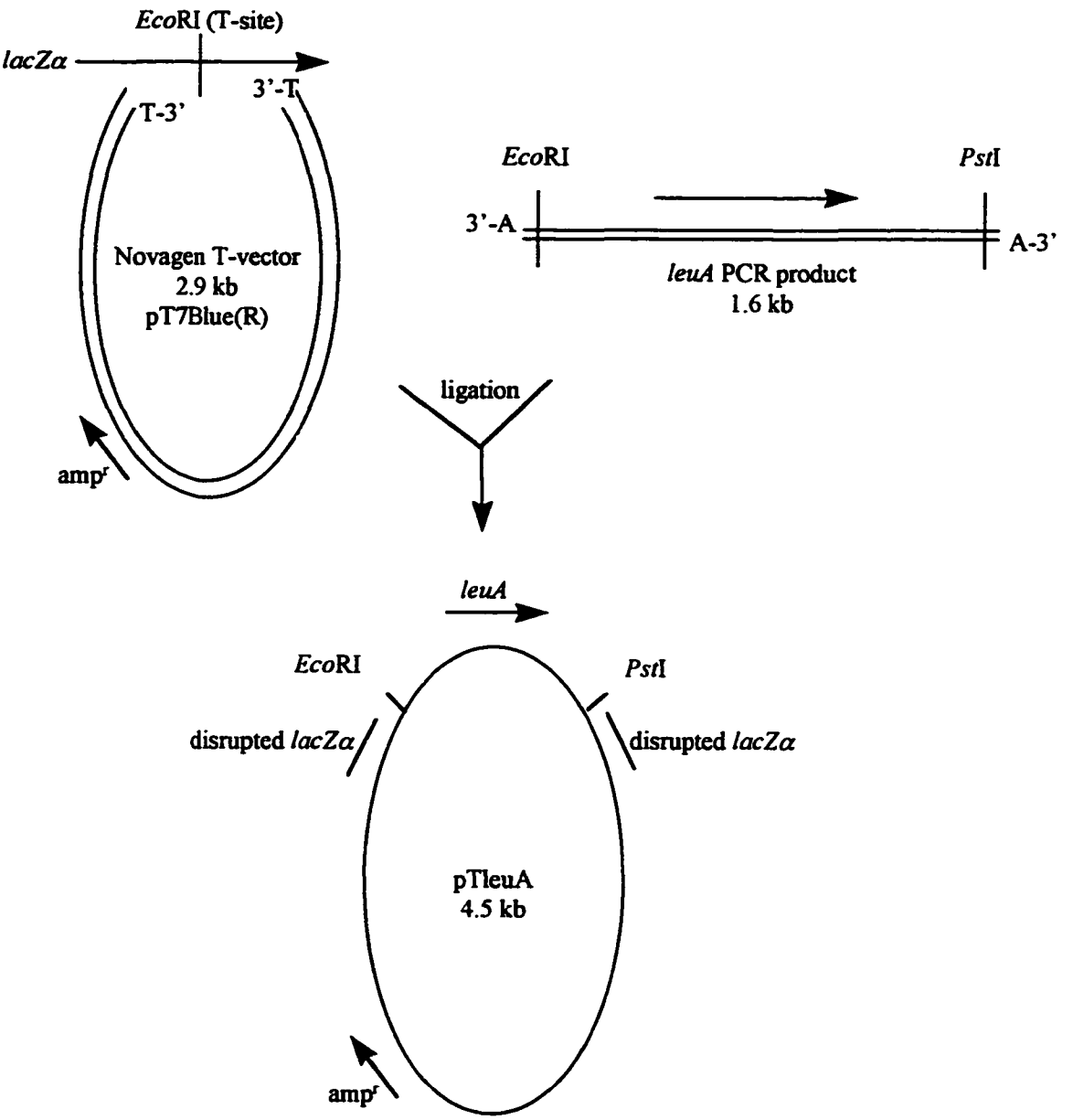

FIG 11. Cloning step III: the *leuA* gene was recovered from pTleuA by restriction digestion with *Eco*RI and *Pst*I, gel purified and cloned into *Eco*RI/*Pst*I digested and gel purified pAL0.5 to generate pAL1g which was selected for ampicillin (amp), spectinomycin (Spc) and streptomycin (Sm) resistance and screened for correct size by restriction digestion. The *leuA* gene was tested for expression in the *E. coli* strain CV512 (*leuA*$^-$) - the gene is functionally expressed from pAL1g.

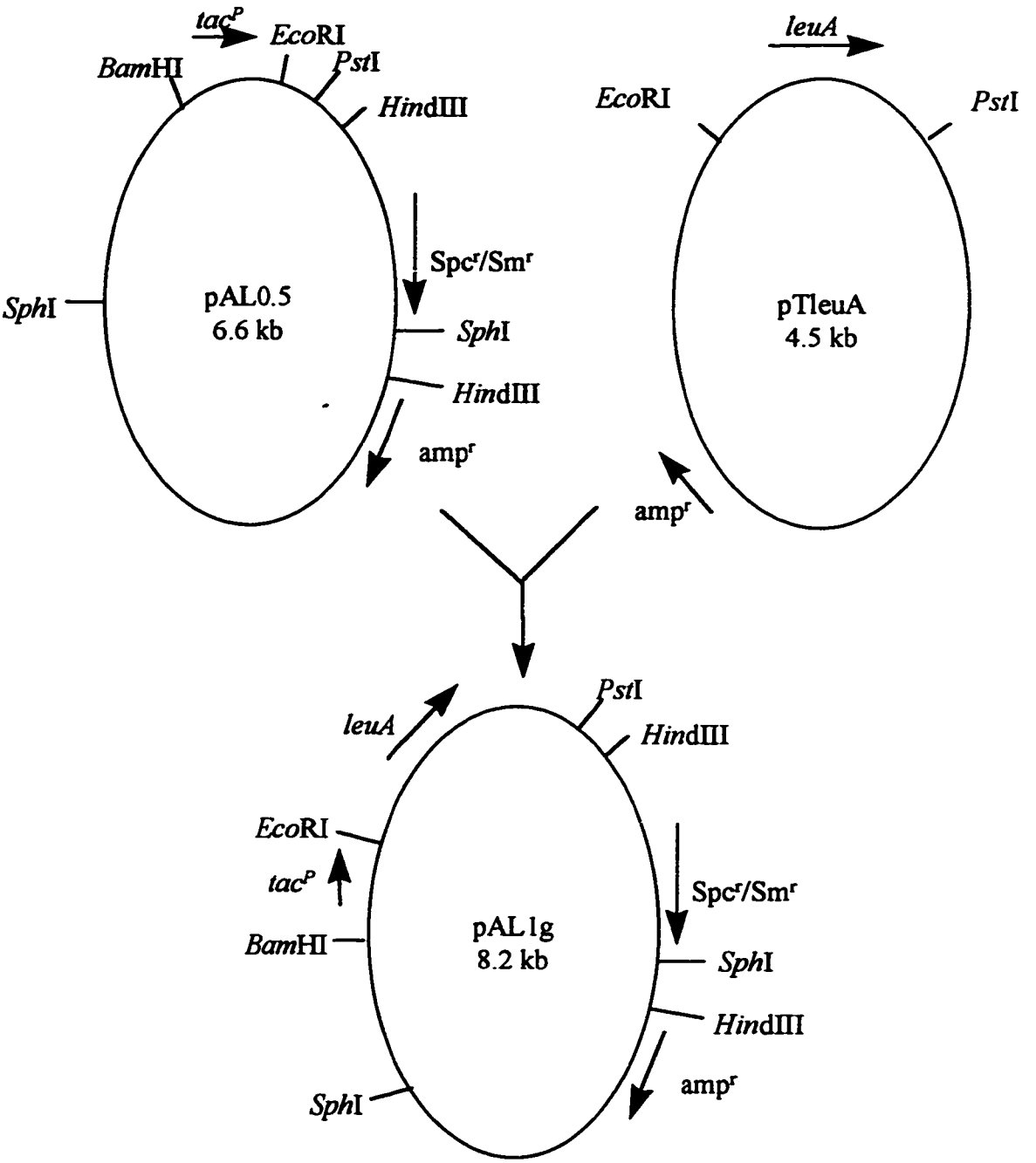

The second goal was to clone the kan$^r$ cassette into the *tac$^P$-leuA* plasmid. The path for this was complicated by the Sm$^r$/Spc$^r$ gene (step I) because it contained a *Sph*I site that would interfere with cloning the *leu-upstream* fragment into a *Sph*I/*Nhe*I site on the kan$^r$-*tac$^P$-leuA* vector. So, first the *leuA* gene had to be recovered and cloned into a *tac$^P$* vector that didn't contain the Smr/Spcr cassette. In step IV, another copy of the *leuA* gene was recovered from pTleuA and cloned into pKK223-3 to generate pAL1-2 (Fig. 12). As it turned out, the copy of *leuA* in pAL1-2 was not functionally expressed but the next step was accomplished before this was discovered - this was remedied in step VIII as described below. In step V, the kan$^r$ cassette was recovered from pBSL15 (M. Alexeyev) and cloned into pAL1-2 to generate pAL2-2 (Fig. 13).

The third goal was to PCR amplify a sequence of the chromosome upstream of the *leu* promoter and clone it into the kan$^r$-*tac$^P$-leuA* vector; this was accomplished in two steps. In step VI, the *leu-upstream* (*leu-up*) region was PCR amplified with forward primer LeuA4 , containing a *Sph*I site, and reverse primer LeuA5, containing a *Nhe*I site. The amplified fragment was cloned into a lab-generated T-vector to generate pT-up (Fig. 14). In step VII, *leu-up* was recovered from pT-up and cloned into pAL2-2 (kan$^r$-*tac$^P$-leuA*) (Fig. 15) to generate pAL3-2 (*leu-up*-kan$^r$-*tac$^P$-leuA*). However, as stated the *leuA* gene in this construct was not functionally expressed; therefore, in step VIII, the copy of *leuA* that was known to be functionally expressed (in pAL1g) was recovered and cloned into pKK223-3 to generate pBL1-4 (Fig. 16). This plasmid when transformed into CV512 (*leuA*$^-$) did express functional *leuA* from the *tac* promoter. After this it was just a matter of combining the functional *tac$^P$-leuA* region from pBL1-4 with the *leu-up*-kan$^r$

FIG 12. Cloning step IV: the *leuA* gene was recovered from pTleuA by restriction digestion with *Eco*RI and *Pst*I, gel purified and cloned into *Eco*RI/*Pst*I digested and gel purified pKK223-3 to generate pAL1-2 which was selected for ampicillin (amp) and screened for correct size by restriction digestion. The *leuA* gene was tested for expression in the *E. coli* strain CV512 (*leuA*-) - the gene is not functionally expressed from pAL1-2 however, the next step (Fig. 13) was completed before this was discovered.

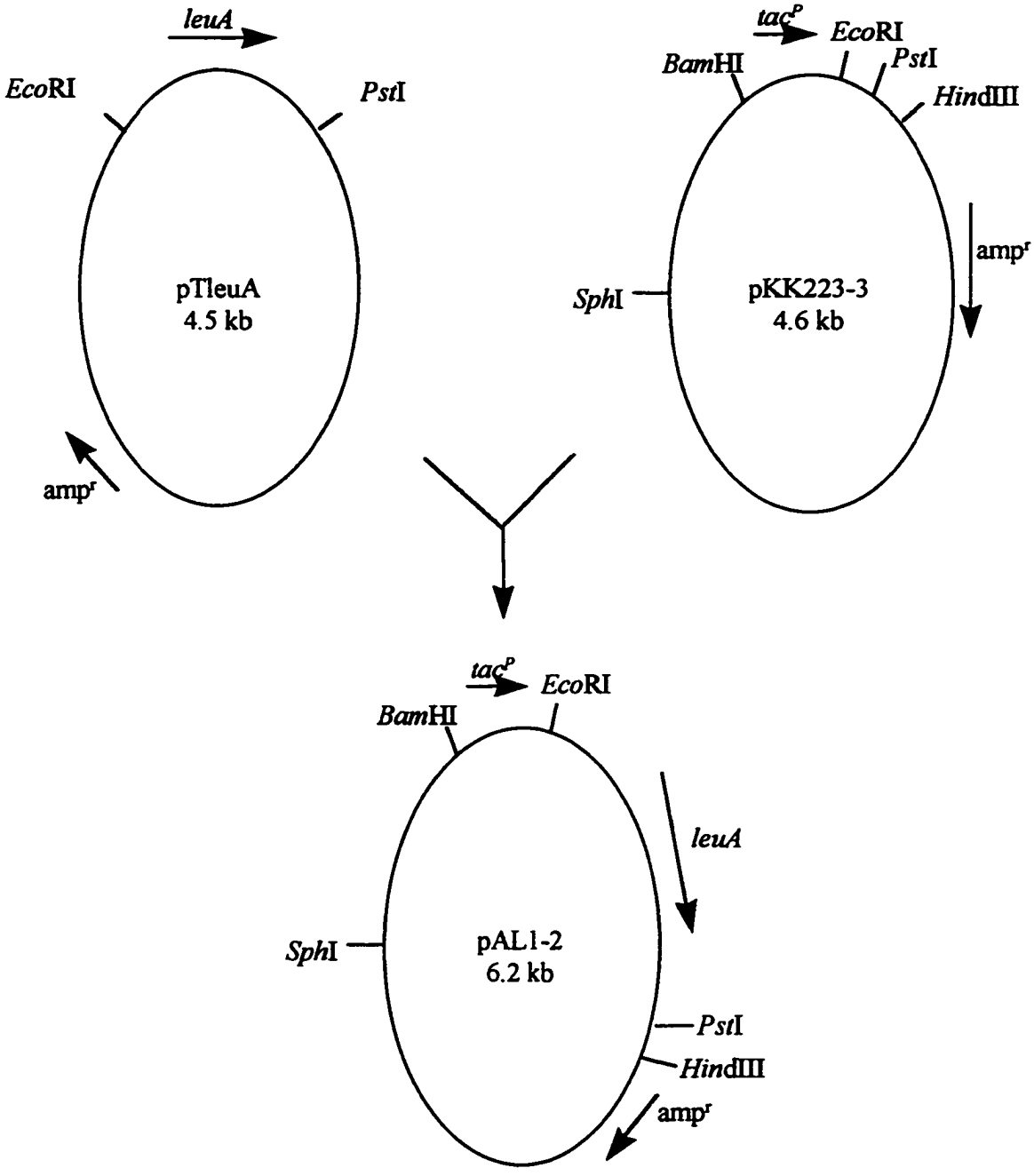

FIG 13. Cloning step V: the kanamycin resistance ($kan^r$) gene was recovered from pBSL15 (M. Alexeyev) by restriction digestion with *Bam*HI, gel purified and cloned into *BamHI* digested pAL1-2 to generate pAL2-2 which was selected for ampicillin (amp) and kanamycin resistance then screened for correct size by restriction digestion. The *leuA* gene was tested for expression in the *E. coli* strain CV512 (*leuA*-) - the gene is not functionally expressed from pAL2-2.

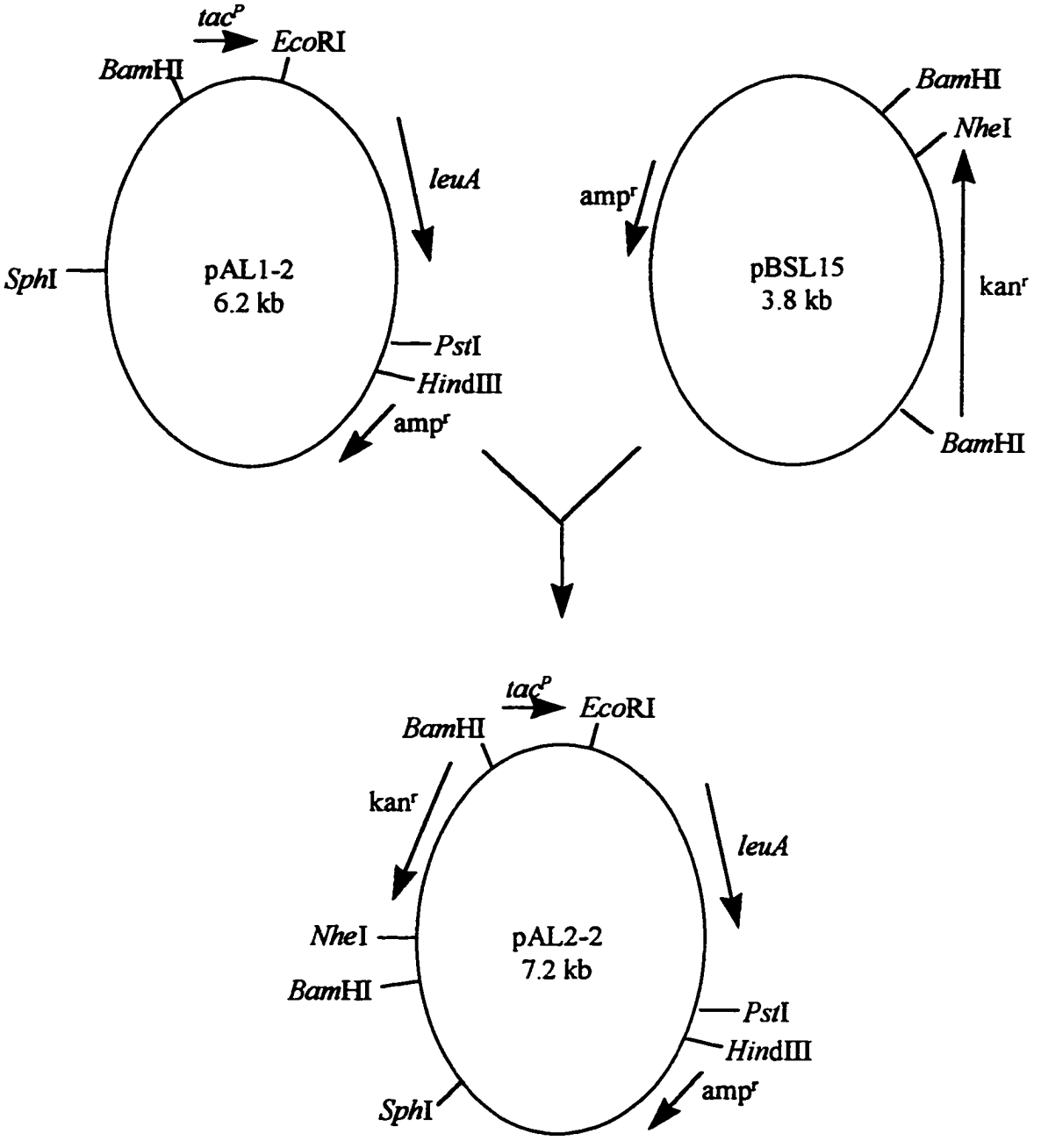

FIG 14. Cloning step VI: the *leu-upstream* region was amplified by PCR, gel purified and cloned into a T-vector to generate pT-up which was selected for ampicillin (amp) resistance then screened for correct size by restriction digestion.

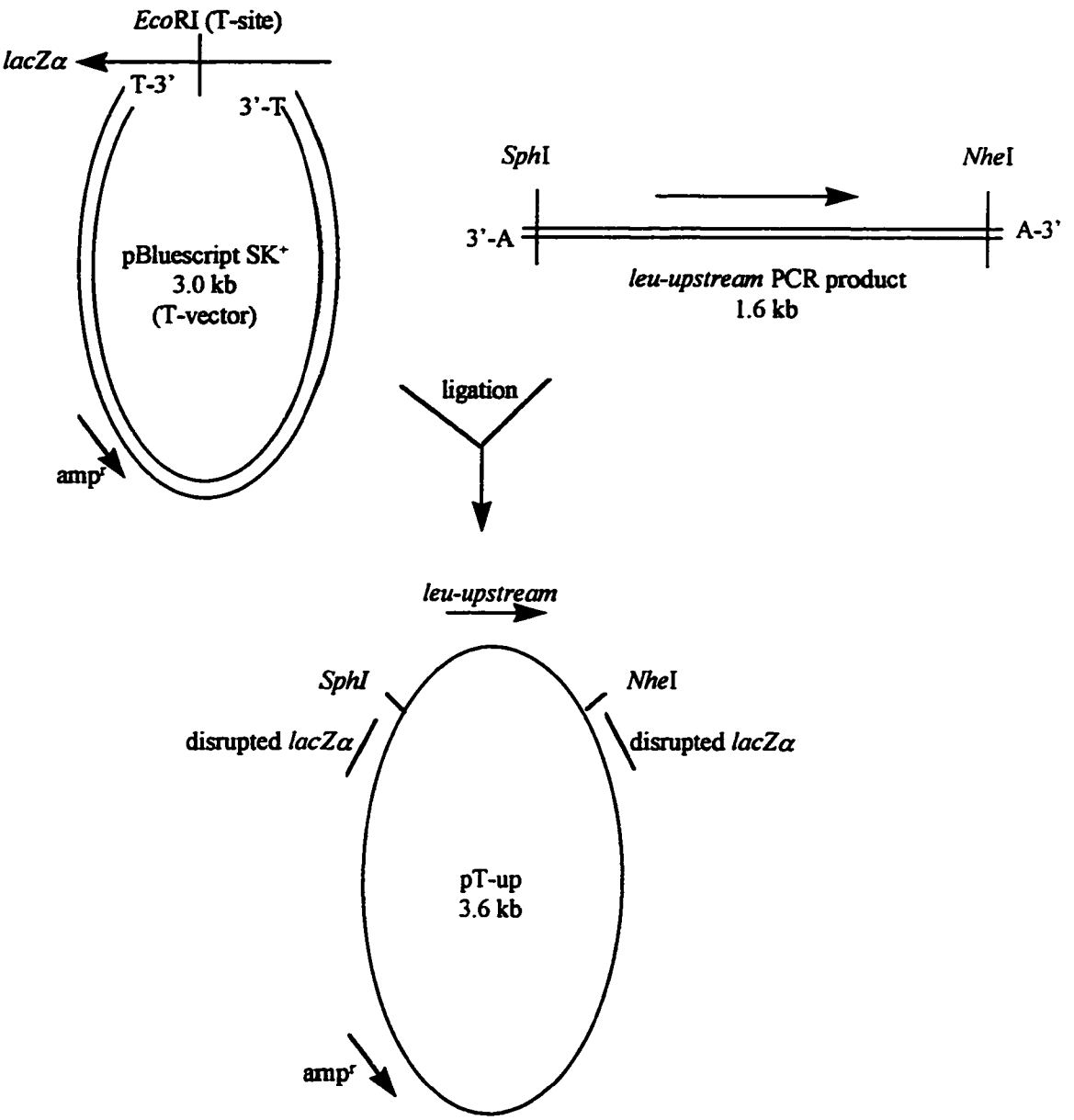

FIG 15. Cloning step VII: the *leu-upstream* region was recovered from pT-up by restriction digestion with *Sph*I and *Nhe*I, gel purified and cloned into *Sph*I/*Nhe*I digested and gel purified pAL2-2 to generate pAL3-2 which was selected for ampicillin (amp) and kanamycin (kan) resistance then screened for correct size by restriction digestion. The *leuA* gene in this construct is not functional.

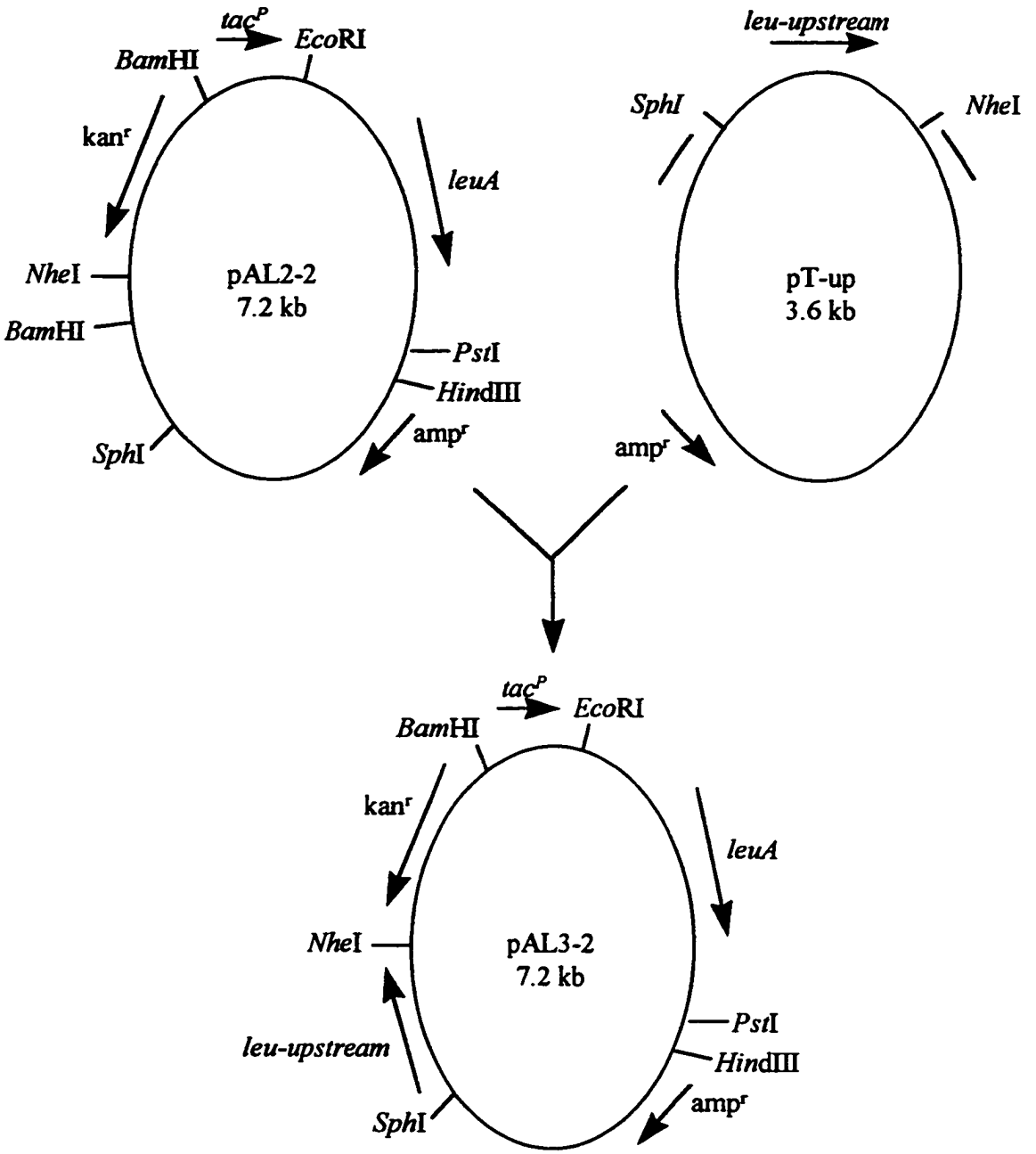

FIG 16. Cloning step VIII: the functional *leuA* gene was recovered from pAL1g by restriction digestion with *EcoR*I and *Pst*I, gel purified and cloned into EcoRI/*Pst*I digested and gel purified pKK223-3 to generate pBL1-4 which was selected for ampicillin (amp) resistance then screened for correct size by restriction digestion. The *leuA* gene was tested for expression in *E. coli* strain CV512 (*leuA*$^-$) - the gene is functionally expressed from pBL1-4.

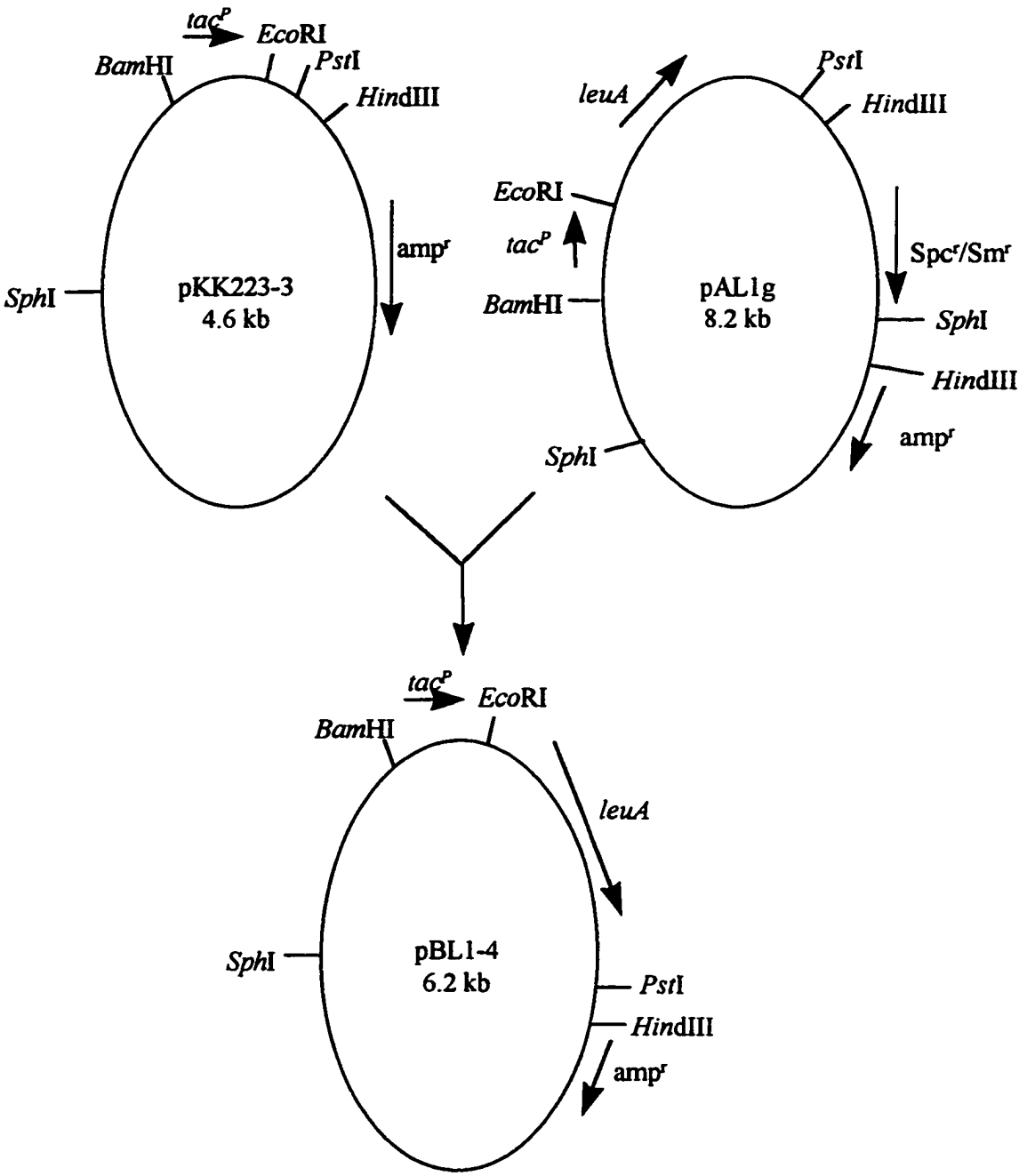

region from pAL3-2 to generate a complete and functional *leu-up*-kan$^r$-*tac*$^P$-*leuA* plasmid. To this end, in step IX, the *leu-up*-kan$^r$ region from pAL3-2 was recovered and cloned into pBL1-4 to generate pBL3 (Fig. 17) again, *tac*$^P$-*leuA* expression was tested and shown to be functional.

The fourth goal was to clone the *leu-up*-kan$^r$-*tac*$^P$-*leuA*, 3.6 kb fragment from pBL3 into a suicide vector. To accomplish this task it was necessary first to subclone the fragment into a vector with relevant restriction sites and from there subclone the fragment into the suicide vector. In step X, the 3.6 kb fragment (*leu-up*-kan$^r$-*tac*$^P$-*leuA*) of pBL3 was PCR amplified with the Expand™ High Fidelity PCR system (Boehringer Mannheim) using forward primer LeuA4 and reverse primer LeuA2. The PCR product was blunt-end ligated into CloneSure, a zero-background cloning vector (CPG inc.), to generate $pCS_{3.6\beta}$ (Fig. 18). In step XI, the 3.6 kb fragment (*leu-up*-kan$^r$-*tac*$^P$-*leuA*) was recovered from $pCS_{3.6\beta}$ and cloned into suicide vector pWM91 (B. Wanner) to generate pBanz2 (Fig. 19).

The fifth goal was to have the suicide vector integrate into the CP78 or CP79 chromosome; as it happens, the one integrant isolated was in CP79. Plasmid pBanz2 is a suicide vector because it contains an R6K origin of replication which makes it dependent upon the λ Pir protein for replication. A λ Pir strain was supplied with pWM91 so the plasmid could be propagated. When introduced into non-Pir *E. coli*, the only way plasmid carried genes will be expressed is if the genes (or whole plasmid) recombine with the *E. coli* DNA. Because double crossover homologous recombination is a rare event, integration of the whole plasmid at one of the homologous sites, either *leu-up* or *leuA*,

FIG 17. Cloning step IX: the region from *leu-upstream* through the kanamycin resistance (kan$^r$) gene was recovered from pAL3-2 by restriction digestion with *Sph*I and *Bam*HI, gel purified and cloned into *Sph*I/*Bam*HI digested and gel purified pBL1-4 to generate pBL3 which was selected for ampicillin (amp) and kan resistance then screened for correct size by restriction digestion. The *leuA* gene was tested for expression in *E. coli* strain CV512 (*leuA*$^-$) - the gene is functionally expressed from pBL3.

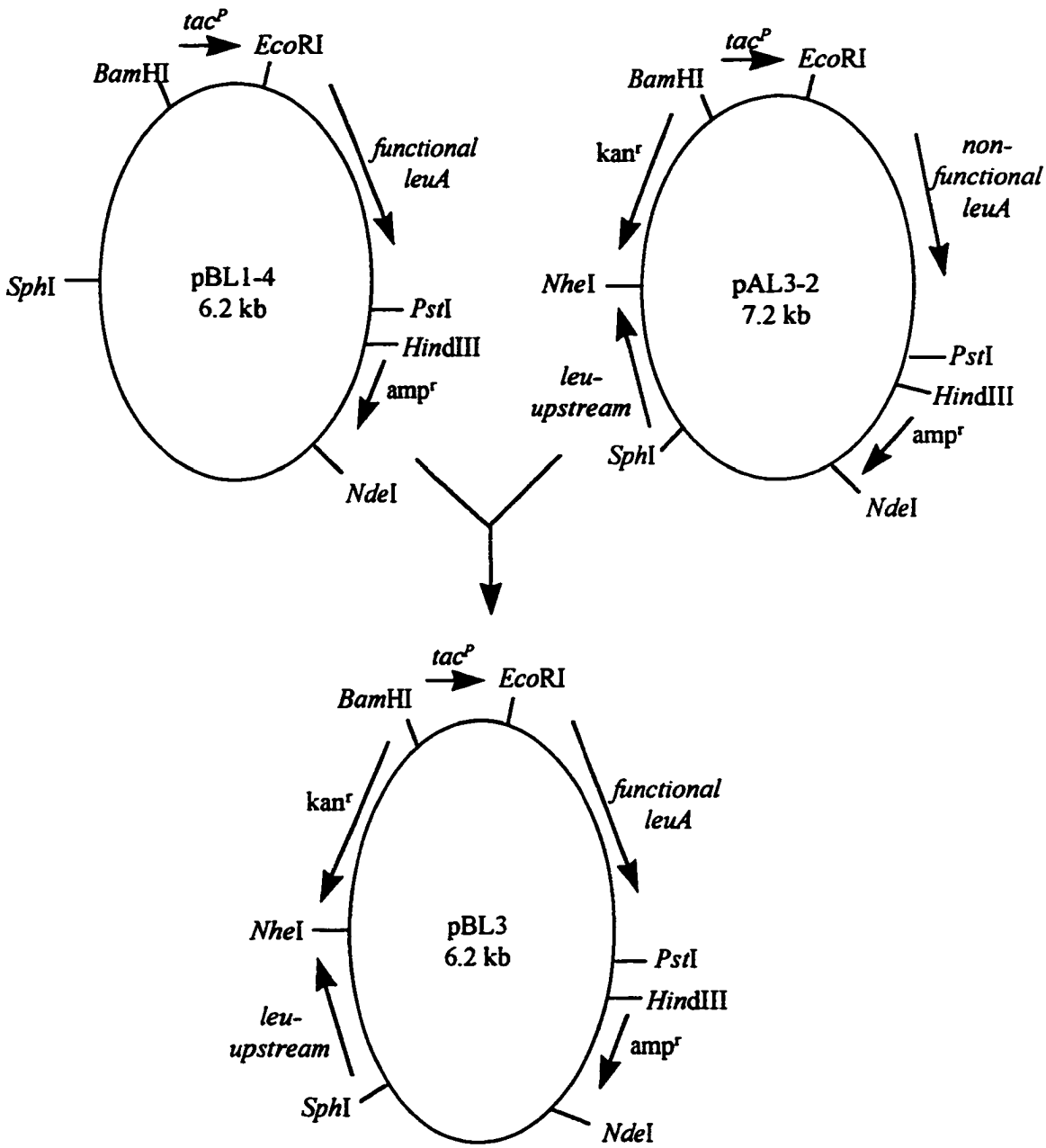

FIG 18. Cloning step X: *NdeI*/*PstI* digested pBL3 was used as template in a PCR reaction extending from the *SphI* site through *leuA* to the *PstI* site. The PCR product was blunt-end ligated into *SmaI* cut CloneSure (CPG) to generate $pCS_{3.6\beta}$.

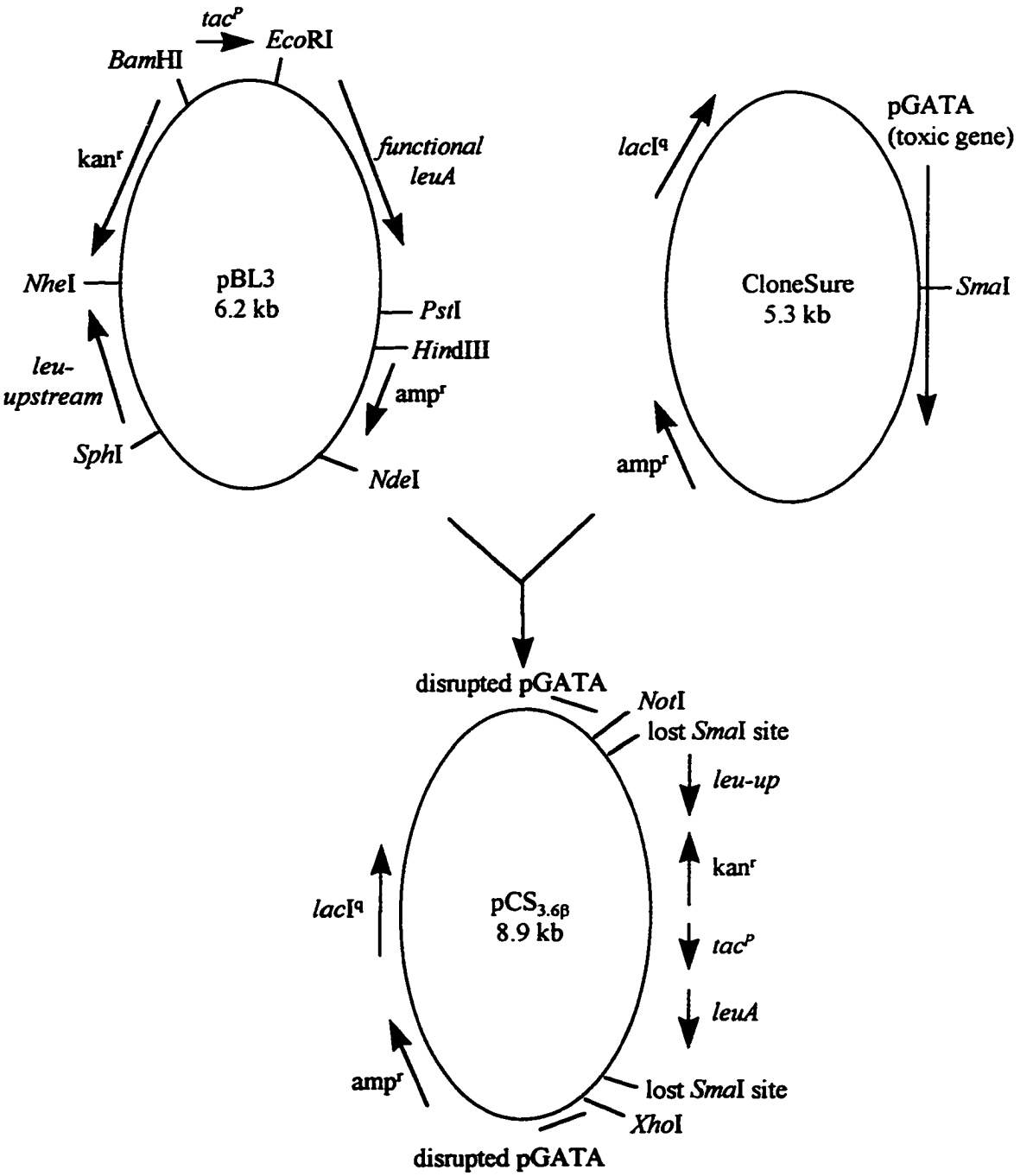

FIG 19. Cloning step XI: a 3.6 kb fragment containing the *leu-upstream* region through the *leuA* gene was recovered from $pCS_{3.6B}$ by restriction digestion with *Not*I and *Xho*I, gel purified and cloned into *Not*I/*Xho*I digested suicide vector pWM91 (B. Wanner) to generate pBanz2.

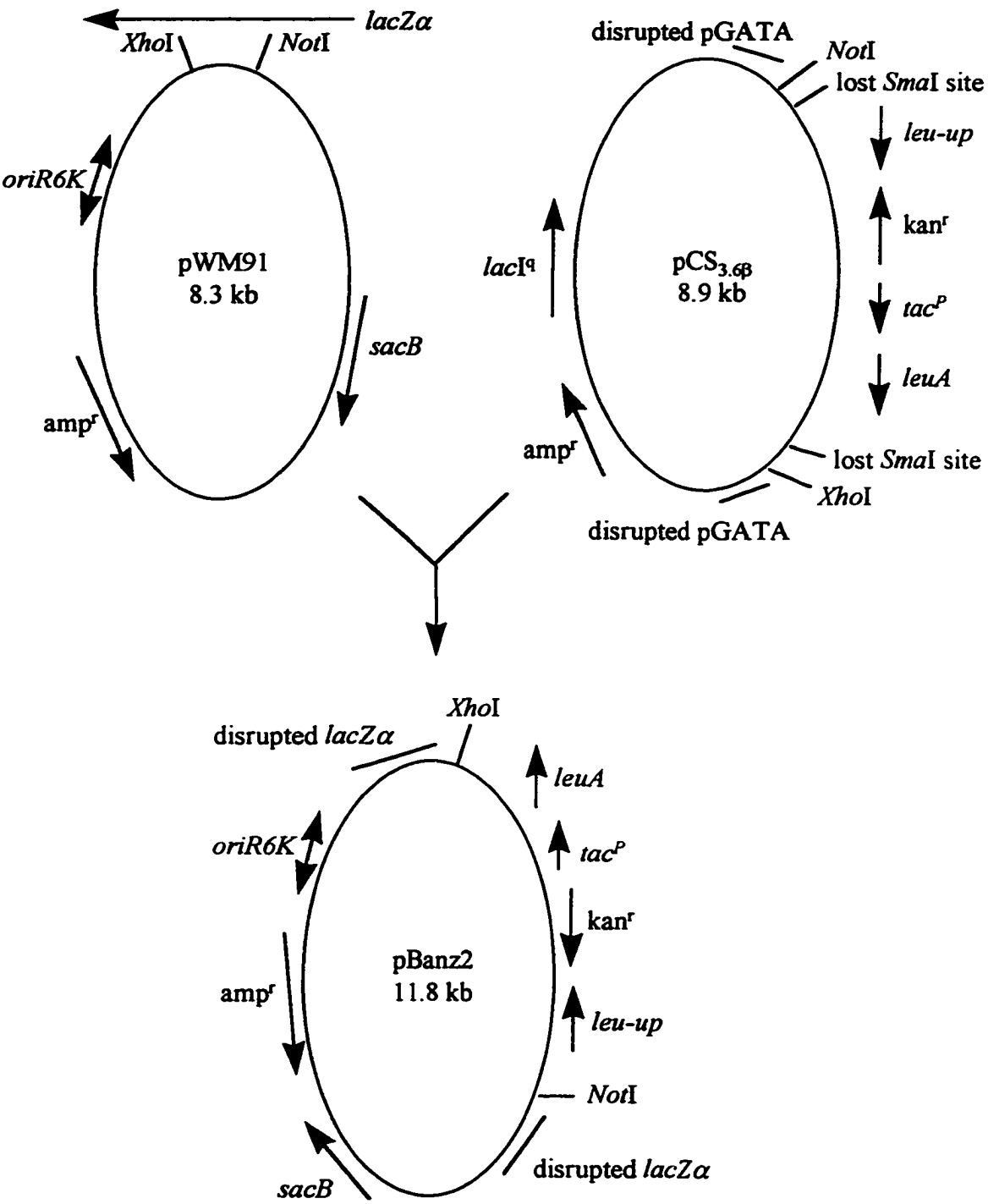

was anticipated. In step XII, suicide vector pBanz2 was electroporated into CP79 and an integrant selected by amp$^r$ (20 μg/ml) (Fig. 20) then screened for amp$^r$ at 50 μg/ml and kan$^r$ at 20 μg/ml.

The sixth goal was to select a recombinant in which the *leu* promoter had been successfully replaced by the *tac* promoter. The integrant (79-integrant) was sensitive to the presence of 10 % sucrose in the medium which indicated the whole plasmid had integrated, because the suicide vector contains a *Bacillus subtilis sacB* gene which when induced in *E. coli* by 5-10 % sucrose is lethal (Gay, et al., 1985). In step XIII, sucrose selection was used to allow the selection of recombinants that had a second homologous recombination event at the other site (*leu-up* or *leuA*). Double crossover homologous recombinants were selected by sucrose resistance (suc$^r$) and kan$^r$ and screened for ampicillin sensitivity (amp$^s$) (Fig. 21).

## Mutation Rate Determination

*Mutation rate determinations*

Cells were grown at 37°C for 42-48 hours in minimal medium consisting of 40 mM glycerol, 50 mM Na phosphate buffer, pH 6.5, 1.0 $gL^{-1}$ $(NH_4)SO_4$, 1.0 $gL^{-1}$ $MgSO_4$, 5.0 $mgL^{-1}$ thiamine, 1.0 mM threonine, 0.15 mM leucine, 0.3 mM arginine, and 0.3 mM histidine. When growth was limited by arginine, the amino acid was present at 0.03 mM. When growth was limited by leucine, leucine was present at 0.01-0.03 mM. The 'zero' method of Luria and Delbrück (1943) was used to determine mutation rates. In a typical experiment, a large culture inoculated with cells from a 7 h-old nutrient agar plate at a cell

FIG 20. Cloning step XII: integration of pBanz2 into CP79 chromosome via single crossover homologous recombination to yield strain 79-integrant. The integrant was selected by $amp^r$ and screened for $kan^r$ and sucrose sensitivity.

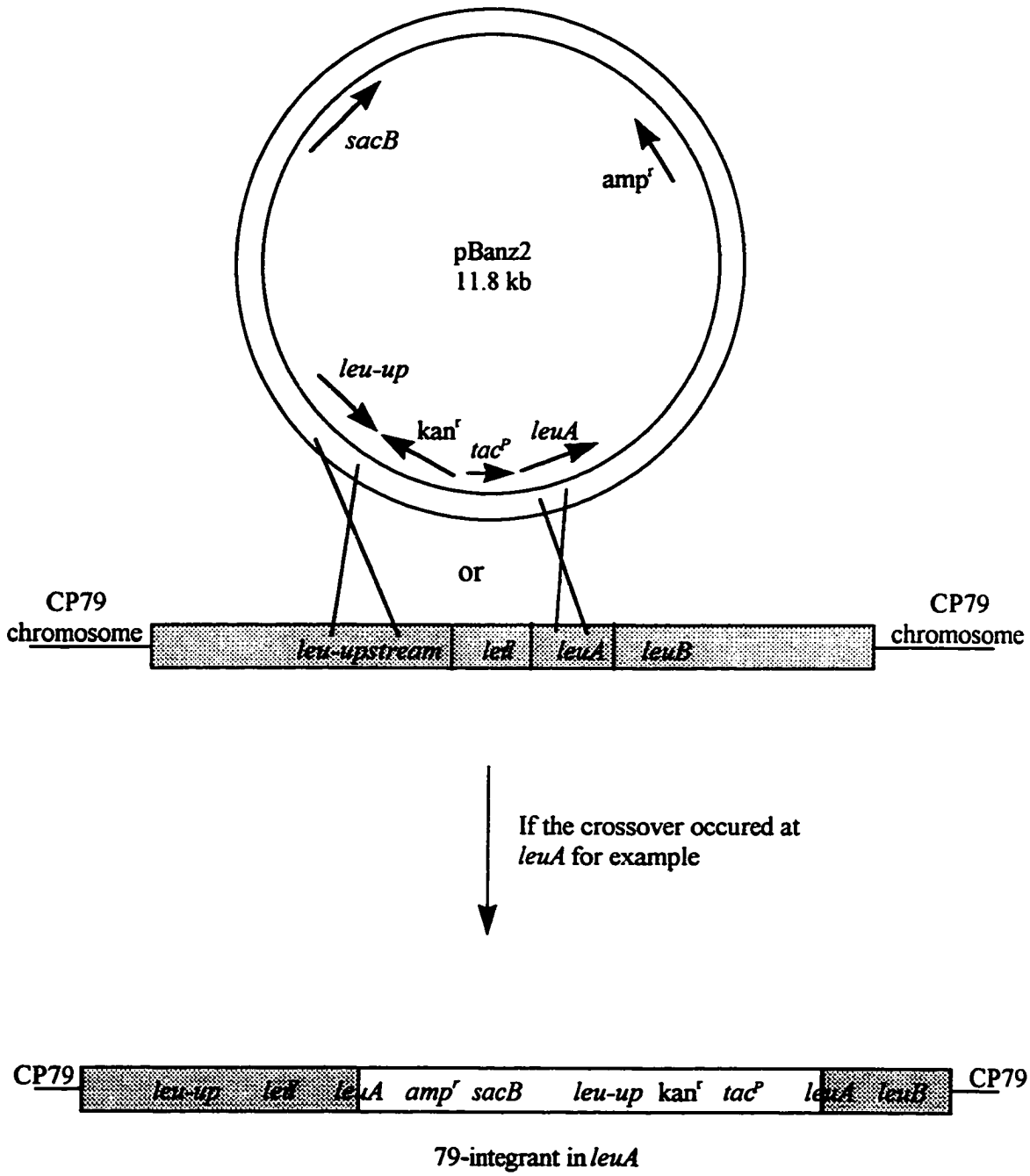


79-integrant in *leuA*

FIG 21. Cloning step XIII: double crossover homologous recombination facilitated by sucrose selection lead to replacement of the *leu* promoter ($leu^P$) with the *tac* promoter ($tac^P$) and kanamycin resistance ($kan^r$) cassette in CP79 resulting in strain 79AL. Double crossover homologous recombinants were selected by sucrose resistance ($suc^r$) and $kan^r$ and screened for ampicillin sensitivity ($amp^s$)

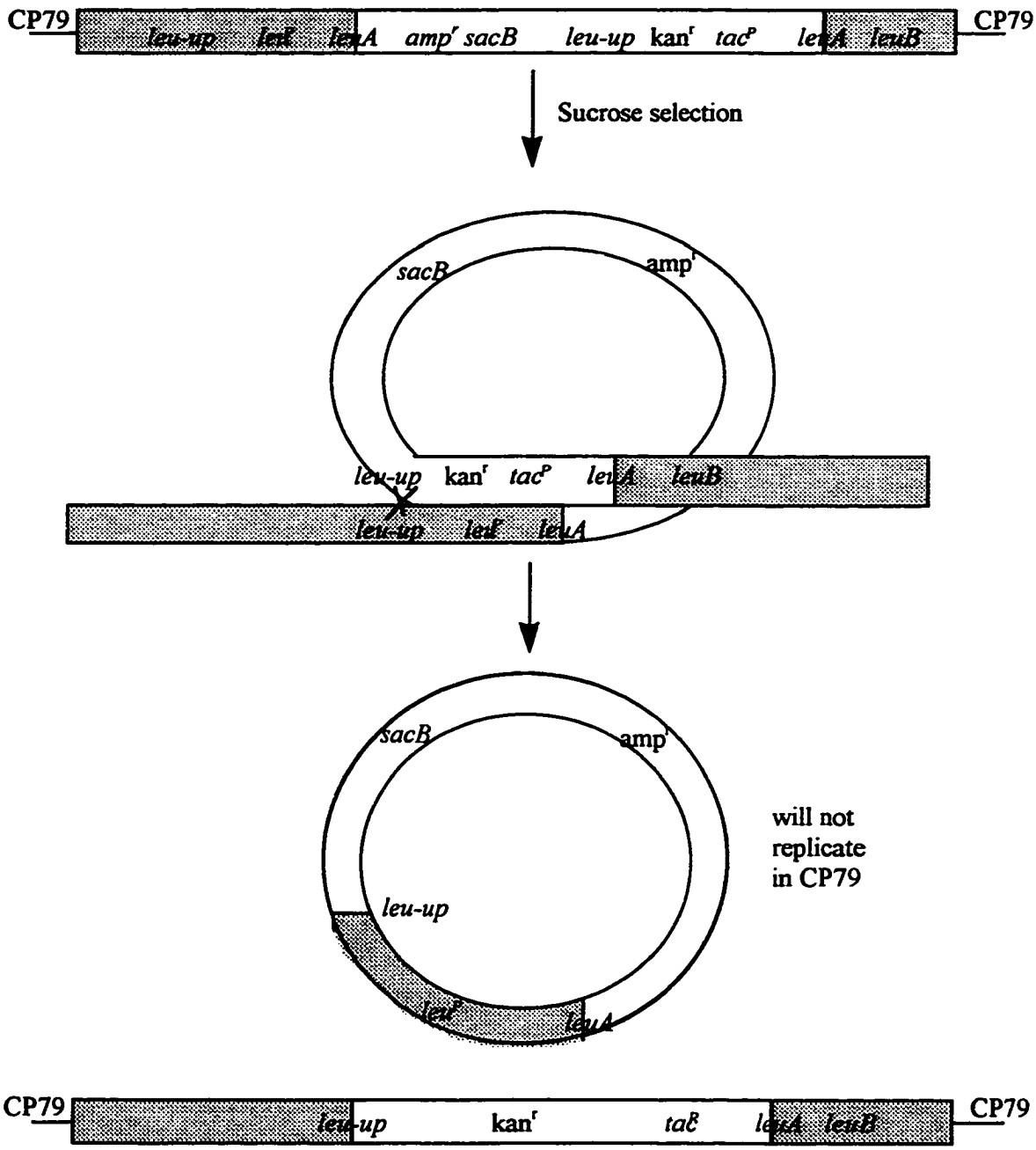


recombinant 79AL

density of about 5 x $10^4$ $ml^{-1}$ was prepared and 1.5 ml aliquots were distributed into 40 test tubes (2 cm-diameter) which were shaken at a 45° angle at 37°C for about 18 h until the end of log growth which was determined by following the $OD_{550}$. Each entire culture was then spread onto selective plates. Ten-fold dilutions in buffered saline were made of three cultures and the $OD_{550}$ values read to select the appropriate dilution for determining total viable cell numbers on yeast extract plates (0.1% yeast extract, 1% glucose, 1% peptone, 0.1% $MgSO_4 \cdot 7H_2O$, 0.098% $K_2HPO_4$, 0.146% $KH_2PO_4$, and 1.5% agar) and minimal medium plates containing all essential nutrients. Revertant colonies first appeared on selective plates about 40 h after plating and final counts were made at 65-70 h for CP78 and CP79 and 72-96 h for recombinant 78AL. Mutation rates were estimated by the 'zero' method (Luria and Delbrück, 1943) according to the expression MR=(-ln2)(ln $P_0$/N), where $P_0$=the proportion of cultures with no revertants, and N=the total number of cells per culture.

**mRNA Quantification**

*Preparation of RNA extracts*

Total RNA was isolated using Gentra Systems PureScript RNA kit. The RNA was further purified by treatment with RNase-free DNase followed by phenol-chloroform extraction and ethanol precipitation.

*DNA probe preparation*

The *E. coli leuB, pyrD* and *glpK* genes were cloned into a vector containing opposable T3 and T7 promoter sites. For each gene, plasmid DNA was isolated (QuantumPrep mini-prep kit, BioRad) and cut with a restriction enzyme to produce a 100-600 bp section of the gene with either the T3 or T7 promoter at one end. Antisense RNA probes were produced by *in vitro* transcription (Ampliscribe T3 & T7 *in vitro* transcription kit, Epicenter). The probes were purified on a denaturing polyacrylamide gel and then labeled with Psoralen-biotin (BrightStar Psoralen-Biotin nonisotopic labeling kit, Ambion) using long-wave UV irradiation. After labeling, the single-stranded antisense biotin probes were gel-purified and used to hybridize to *leuB, pyrD* or *glpK* mRNA. Positive-sense standard mRNA was generated for each gene, from the same plasmid but utilizing the other promoter. It is desirable for the probe to contain some vector sequence at the 5' end that is nonhomologous to the target mRNA and will be degraded by the nucleases. This produces protected hybrids that are shorter than the full length probe and can be differentiated by gel electrophoresis. A difference in protected hybrid vs. full length probe is evidence of a working assay.

*Nuclease protection assay and densitometry*

The Multi-NPA kit (Ambion) has been improved and optimized for detecting and quantifying specific mRNA species. The biotinylated antisense RNA probe of defined length is hybridized to the target mRNA. S1 nuclease and RNases A and T1 degrade any single strand nucleic acids while leaving the hybrids intact. The hybrids are precipitated, separated by denaturing polyacrylamide gel electrophoresis and then transferred to

positively charged nylon membrane by semi-dry electroblotting. The biotinylated probe is conjugated to streptavidin-alkaline phosphatase and CDP-Star using Ambion's BrightStar BioDetect kit. Chemiluminescent probes are detected with x-ray film. A set of standards is run with each sample and relative intensities of different mRNA species within a single RNA extract are compared by densitometry using an Astra 1200S document scanner with transparency adapter and Scanalytics ONE-Dscan software. The probe molecules are present in 4- to 10-fold molar excess of the target mRNA so that linearity between the amount of RNA present and the amount of binding to probe is demonstrated.

## RESULTS

*Replacement of the leu with the tac promoter in CP78 and CP79*

The chromosomal *leu* promoter was replaced with the *tac* promoter by double-crossover homologous recombination of a 3.6 kb fragment of dsDNA containing a kanamycin cassette and the *tac* promoter flanked by sequences homologous to regions of the *E. coli* chromosome both upstream and downstream of the *leu* promoter. The 3.6 kb fragment was generated as follows, in brief: (1) homologous regions were PCR amplified, with specific restriction sites in the primers, from the CP78 chromosome and cloned into T-Vectors (Marchuk et al., 1991), (2) the *leu* upstream and the *leuA* fragments were recovered from the T-Vectors by restriction digestion, (3) the kanamycin cassette was acquired by restriction digest of plasmid pBSL15 (Alexeyev, 1995), (4) the fragments were sequentially cloned into plasmid pKK223-3 ($tac^P$, $amp^r$; Pharmacia Biotech), (5) the

3.6 kb fragment was recovered by PCR amplification using the Expand High Fidelity PCR System of Boehringer-Mannheim and a primer set (called "internal" which includes only the 3.6 kb fragment) and cloned into suicide vector pWM91 (*oriR6K*, *amp*$^r$, sucrose$^s$ due to *sacB;* Metcalf et al., 1996) to generate plasmid pBanz2 which was introduced into CP79 by electroporation.

Plasmid pBanz2 replicates only in *E. coli* strains that produce the lambda (λ) Pir protein and will not replicate in CP78 or CP79; therefore rendering pBanz2 a suicide vector for these strains. When introduced into CP79 by electroporation, single-crossover homologous recombination resulted in integration of the suicide vector into the *leu* operon. An integrant (CP79-integrant) was selected by resistance to kanamycin and ampicillin. Double-crossover homologous recombinants that maintained the 3.6 kb fragment (kan$^r$) but which lost the remainder of the suicide vector containing the toxic *sacB* gene were selected by sucrose and kanamycin resistance and screened for ampicillin sensitivity. Recombinant CP79 (called 79AL) was used as the donor in P1*vir* transduction to transfer the recombinant allele to CP78.

It was possible to predict the size of PCR products that would be obtained, using two different primer sets, from the parents (CP78 and CP79), an integrant (79-integrant) and the desired recombinants (78AL and 79AL). Figure 22 is a diagram of the expected outcomes using an "internal" primer set which amplified the whole of the constructed region from *leu-upstream* through the kan$^r$ cassette and *tac*$^P$*-leuA* gene. The internal primer set would be expected to produce a 3.0 kb product from the parents because the region from *leu-up* through *leu*$^P$*-leuA* is about 0.6 kb shorter than the constructed region

**Fig 22. Design of PCR primers to determine if the *leu* promoter was replaced by the *tac* promoter.**

**Parent (CP79 & CP78)**

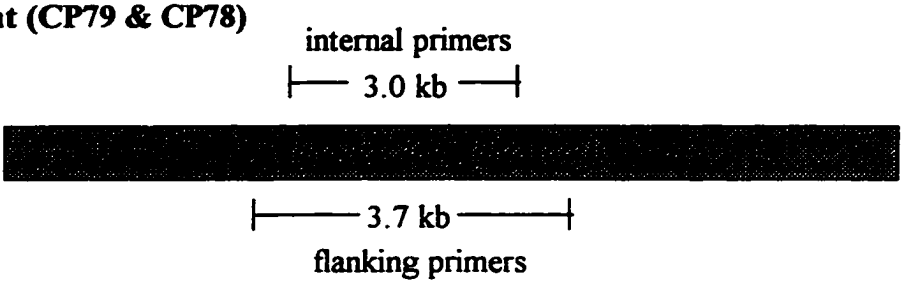


**Integrant in *leuA***

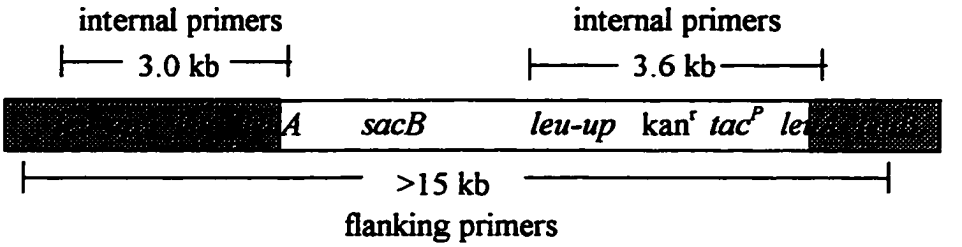


**Integrant in *leu-up***

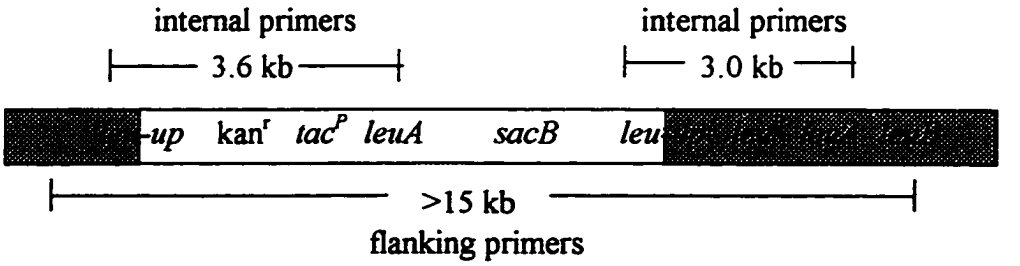


**Recombinant (79AL & 78AL)**

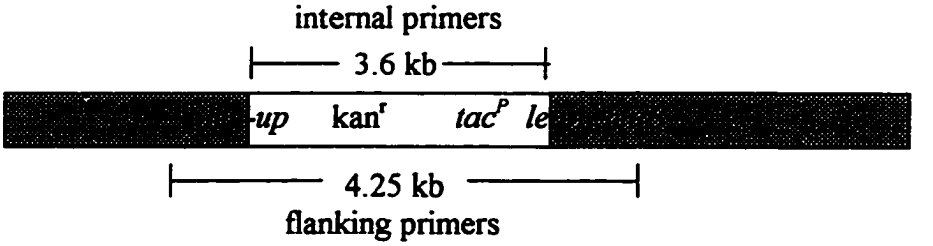

containing the $kan^r$ gene. Integrants were predicted to yield both a 3.0 kb fragment and a 3.6 kb fragment as bacteria with an integrated plasmid would carry both the chromosomal *leu* operon and the constructed sequences.

Figure 22 also depicts the expected sizes of PCR products from a set of "flanking" primers. The flanking primers were constructed to flank the whole of the constructed region. Sequencing of the PCR product produced by the flanking primers in the desired recombinant would provide definitive proof that the *leu* promoter had been replaced, because only a double crossover homologous recombinant would be flanked by chromosomal upstream and downstream (*leuB*) sequences. The flanking primer set was predicted to yield a 3.7 kb product from the parents and a 4.25 kb product from the recombinants. Integrants were theoretically expected to yield a product greater than 15 kb, but as this was too big for the amplification protocol used, it was not expected to be recovered.

PCR amplification with both sets of primers was performed and the products separated by agarose gel electrophoresis: the results are presented in Figure 23. Both parents (CP78 and CP79) gave the expected results and attest to the accuracy in test design. The one integrant isolated, 79-integrant gave the expected result with the internal primers providing evidence that the integrant contains both promoter regions. However an unexpected result was obtained with the flanking primer set: a 3.7 kb product was observed and theoretically should not have been. It is possible that some of the 79-integrant bacteria used for chromosomal DNA isolation had recombined to lose the integrated plasmid and only one copy of the parental-type chromosomal DNA would have

FIG 23. A PCR fragment, using primers SeqA and SeqZ (called the "flanking" primer set - flanking the 3.6 kb fragment), beginning upstream of the 3.6 kb fragment and ending inside the *leuB* gene (on the chromosome, downstream of the *leuA* gene), was amplified from each recombinant and confirmed replacement of the *leu* promoter. In addition, an "internal" primer set (leuA2 and leuA4) was used to amplify a 3.0 kb region. Presented here are the agarose gels after electrophoresis of the PCR products. Lanes 1, 10, 11, & 20 contain HiLo DNA markers (of sizes 10, 8, 6 , 4, 3, 2, 1.55, 1.4, 1, 0.75, 0.5, 0.4, 0.3, 0.2, and 0.1kb). Contents of the remaining lanes with expected and observed PCR product lengths are presented in a short table below the gels.

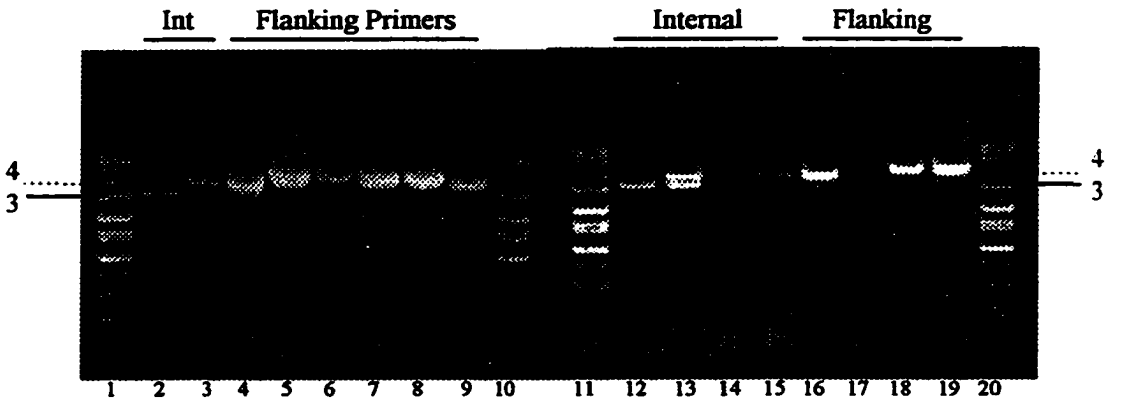


| Lane # | Primer Set | Strain | Band(s) expected | Band(s) observed |
|---|---|---|---|---|
| 2 | internal | CP78 (parent) | 3.0 | 3.0 |
| 3,4 | flanking | CP78 (parent) | 3.7 | 3.7 |
| 5 | flanking | 78AL (recombinant) | 4.25 | 4.25 |
| 6,7,8 | flanking | 79AL (recombinant) | 4.25 | 4.25 |
| 9 | flanking | CP79 (parent) | 3.7 | 3.7 |
| 12 | internal | CP79 (parent) | 3.0 | 3.0 |
| 13 | internal | CP79-integrant | 3.0 & 3.6 | 3.0 & 3.6 |
| 14,15 | internal | 79AL (recombinant) | 3.6 | 3.6 |
| 16 | flanking | CP79 (parent) | 3.7 | 3.7 |
| 17 | flanking | CP79-integrant | none | 3.7 |
| 18,19 | flanking | 79AL (recombinant) | 4.25 | 4.25 |

to be present to yield a 3.7 kb PCR product. This is the most likely explanation because when the same cells were forced to grow on sucrose plates, the majority of survivors lost not only the *sacB* gene but also the kan$^r$ cassette and *tac* promoter - these cells would yield a 3.7 kb PCR product from the flanking primers.

The 4.25 kb flanking PCR product of recombinant 78AL was sequenced by Joan Strange in the Murdock Molecular Biology Facility at The University of Montana and confirmed that the *leu* promoter was replaced by the *tac* promoter and kan$^r$ cassette. The sequence comparison between parent, expected recombinant and observed 78AL is presented in Figure 24.

*78AL and CP78 Growth Rates*

Growth rates of the recombinant (78AL) and parent (CP78) were compared in the absence and in the presence of 1 mM IPTG. Cells were grown to stationary phase in limiting leucine (0.03 mM), then 1/7 the volume of medium containing 0.03 mM leucine with or without 1 mM IPTG was added to each culture and the $OD_{550}$ monitored over time. In both strains the rate of growth was slowed (or the lag time increased) by the presence of IPTG (Table 2). Beletskii and Bhagwat (1996) also found IPTG to slightly inhibit growth rate.

Inhibition of growth rate by IPTG was observed in mutation rate experiments in which 78AL *leuB*$^+$ revertants that developed in cultures without IPTG were always bigger than those that appeared in IPTG-exposed cultures on the same day (Tables 3 and 4). Suspected suppressor colonies were always small and remained so over several days.

Fig 24. Sequence comparison of the expected recombinant sequence (exp78AL) with observed 78AL (78AL) and with parent (CP78) sequence. The sequences were aligned with PCGene cluster alignment function. The *tac* promoter is underlined with a dashed line in the exp78AL sequence. The *leuA* gene is underlined in the CP78 sequence but is the same for all, the *leu* promoter is in lower case letters in the CP78 sequence as it differs from the recombinant $kan^r$ and *tac* promoter sequence (- indicates no base), sections of the recombinant were not sequenced because the sequence obtained was enough to indicate that the *leu* promoter had been replaced (x indicates not sequenced), the *leu-upstream* region is boxed in grey in the CP78 sequence.

```
exp78AL  GGCGATACGTTCGATCTCAAAACGGTGATACACCTCGGTATCAAAGGCTT  50
CP78     GGCGATACGTTCGATCTCAAAACGGTGATACACCTCGGTATCAAAGGCTT  50
78AL                               GATACACCTCGGTATCAAAGGCTT  24

exp78AL  TTTCATATTGTCCGCTACCTTCGCGGCCTTTTGGCTGACCGAAATAGATG  100
CP78     TTTCATATTGTCCGCTACCTTCGCGGCCTTTTGGCTGACCGAAATAGATG  100
78AL     TTTCATATTGTCCGCTACCTTCGCGGCCTTTTGGCTGACCGAAATAGATG   74

exp78AL  CCGCCGGTCAGTTCGCGCACACACAGGATGTCGAAGCCGTTTGCGGCAAT  150
CP78     CCGCCGGTCAGTTCGCGCACACACAGGATGTCGAAGCCGTTTGCGGCAAT  150
78AL     CCGCCGGTCAGTTCGCGCACACACAGGATGTCGAAGCCGTTTGCGGCAAT  124

exp78AL  GTCTGCACGCAGCGGACAGAATGCTTCCAGCCCCTGATACAGTTTTGCCG  200
CP78     GTCTGCACGCAGCGGACAGAATGCTTCCAGCCCCTGATACAGTTTTGCCG  200
78AL     GTCTGCACGCAGCGGACAGAATGCTTCCAGCCCCTGATACAGTTTTGCCG  174

exp78AL  GGCGCAGGTTGCTGAATAATTTGAAGTGCTTACGCAGAGGCAGCAGCGCG  250
CP78     GGCGCAGGTTGCTGAATAATTTGAAGTGCTTACGCAGAGGCAGCAGCGCG  250
78AL     GGCGCAGGTTGCTGAATAATTTGAAGTGCTTACGCAGAGGCAGCAGCGCG  224

exp78AL  CCGCGTTCTGGTTGCTGGTCTGGTGGTAAATGTTCCCACTTCGGGCCGCC  300
CP78     CCGCGTTCTGGTTGCTGGTCTGGTGGTAAATGTTCCCACTTCGGGCCGCC  300
78AL     CCGCGTTCTGGTTGCTGGTCTGGTGGTAAATGTTCCCACTTCGGGCCGCC  274

exp78AL  TACCGAGCCAAACAGCACGGCATCGGCTTGCTCACAACCTTCAACCGTCG  350
CP78     TACCGAGCCAAACAGCACGGCATCGGCTTGCTCACAACCTTCAACCGTCG  350
78AL     TACCGAGCCAAACAGCACGGCATCGGCTTGCTCACAACCTTCAACCGTCG  324

exp78AL  CAGGCGGCAGTGGTTGCCCGTGGTTATCAATGGCTGCGCCGCCTACATCG  400
CP78     CAGGCGGCAGTGGTTGCCCGTGGTTATCAATGGCTGCGCCGCCTACATCG  400
78AL     CAGGCGGCAGTGGTTGCCCGTGGTTATCAATGGCTGCGCCGCCTACATCG  374

exp78AL  TAATGGCTGGTGGTGATGCGCATCGCAAAGCGGTTGCGCACGGCATCCAG  450
CP78     TAATGGCTGGTGGTGATGCGCATCGCAAAGCGGTTGCGCACGGCATCCAG  450
78AL     TAATGGCTGGTGGTGATGCGCATCGCAAAGCGGTTGCGCACGGCATCCAG  424

exp78AL  CACTTTCAGCGCCTGGGTCATCACTTCCGGACCAATACCGTCCCCCGGCA  500
CP78     CACTTTCAGCGCCTGGGTCATCACTTCCGGACCAATACCGTCCCCCGGCA  500
78AL     CACTTTCAGCGCCTGGGTCATCACTTCCGGACCAATACCGTCCCCCGGCA  474

exp78AL  ATACGGCAATATGGTAATTCTTCGACATCACACGGTTTCCTTGTTGTTTT  550
CP78     ATACGGCAATATGGTAATTCTTCGACATCACACGGTTTCCTTGTTGTTTT  550
78AL     ATACGGCAATATGGTAATTCTTCGACATCACACGGTTTCCTTGTTGTTTT  524

exp78AL  CGTTGTGTTGAGCTTTGCGTTGCAACTCTTTTTCGACTTCTGCGGCACGC  600
CP78     CGTTGTGTTGAGCTTTGCGTTGCAACTCTTTTTCGACTTCTGCGGCACGC  600
78AL     CGTTGTGTTGAGCTTTGCGTTGCAACTCTTTTTCGACTTCTGCGGCACGC  574

exp78AL  CAGATATTGTTCAGAACGTGCACCATGGCTTTGGCAGATGACTCGACAAT  650
CP78     CAGATATTGTTCAGAACGTGCACCATGGCTTTGGCAGATGACTCGACAAT  650
78AL     CAGATATTGTTCAGAACGTGCACCATGGCTTTGGCAGATGACTCGACAAT  624
```

```
exp78AL  ATCGGTAGCCAGGCCGACGCCGTGGAAGCGGCGACCGTTGTAGTTAGCGA  700
CP78     ATCGGTAGCCAGGCCGACGCCGTGGAAGCGGCGACCGTTGTAGTTAGCGA  700
78AL     ATCGGTAGCCAGGCCGACGCCGTGGAAGCGGCGACCGTTGTAGTTAGCGA  674

exp78AL  CGATATCCACCTGACCCAGCGCATCTTTACCGTGGCCTTTGGCGGTCAGG  750
CP78     CGATATCCACCTGACCCAGCGCATCTTTACCGTGGCCTTTGGCGGTCAGG  750
78AL     CGATATCCACCTGACCCAGCGCATCTTTACCGTGGCCTTTGGCGGTCAGG  724

exp78AL  CTGTATTTCACCAGTTCGACGTTATATTCAGTGATGCGGTTAATTGCCTG  800
CP78     CTGTATTTCACCAGTTCGACGTTATATTCAGTGATGCGGTTAATTGCCTG  800
78AL     CTGTATTTCACCAGTTCGACGTTATATTCAGTGATGCGGTTAATTGCCTG  774

exp78AL  ATAGACGGCATCGACCGGACCGTTACCGTTGGCGGCTTCTGCTTTGACTT  850
CP78     ATAGACGGCATCGACCGGACCGTTACCGTTGGCGGCTTCTGCTTTGACTT  850
78AL     ATAGACGGCATCGACCGGACCGTTACCGTTGGCGGCTTCTGCTTTGACTT  824

exp78AL  CTTCGCCACAGGCCAGTTTGACGGCGGCGGTGGCGATATCGTTAGAGCCA  900
CP78     CTTCGCCACAGGCCAGTTTGACGGCGGCGGTGGCGATATCGTTAGAGCCA  900
78AL     CTTCGCCACAGGCCAGTTTGACGGCGGCGGTGGCGATATCGTTAGAGCCA  874

exp78AL  GACTGCACGCTGAAGTAATCCAGACGGAAATGCTCCGGCTCTTCTTGCTG  950
CP78     GACTGCACGCTGAAGTAATCCAGACGGAAATGCTCCGGCTCTTCTTGCTG  950
78AL     GACTGCACGCTGAAGTAATCCAGACGGAAATGCTCCGGCTCTTCTTGCTG  924

exp78AL  CTTACCGATGAAGGCCAGCGCCTCCAGATCGTAATCAAACACCTGACCT   999
CP78     CTTACCGATGAAGGCCAGCGCCTCCAGATCGTAATCAAACACCTGACCT   999
78AL     CTTACCGATGAAGGCCAGCGCCTCCAGATCGTAATCAAACACCTGACCTA  974

exp78AL  TTTTTGTCCGCCAGCTTCAGGAAAGCATCGTACAAATTGTCTAAATTATA  1049
CP78     TTTTTGTCCGCCAGCTTCAGGAAAGCATCGTACAAATTGTCTAAATTATA  1049
78AL     TTTTTGTCCGCCAGCTTCAGGAAAGCATCGTACAAATTGTCTAAATTATA  1024

exp78AL  TTCACTTTCTTTATACCCCATCTCATCCATGCGATGTTTCACCGCCGCAC  1099
CP78     TTCACTTTCTTTATACCCCATCTCATCCATGCGATGTTTCACCGCCGCAC  1099
78AL     TTCACTTTCTTTATACCCCATCTCATCCATGCGATGTTTCACCGCCGCAC  1074

exp78AL  GCCCCGAACGAGAGGTCAGATTCAGCTGGATTTGGTTCAGACCAATAGAT  1149
CP78     GCCCCGAACGAGAGGTCAGATTCAGCTGGATTTGGTTCAGACCAATAGAT  1149
78AL     GCCCCGAACGAGAGGTCAGATTCAGCTGGATTTGGTTCAGACCAATAGAT  1124

exp78AL  TCTGGTGTCATGATTTCGTAGTTTTCGCGGTTTTTCAGCACGCCATCCTGG  1200
CP78     TCTGGTGTCATGATTTCGTAGTTTTCGCGGTTTTTCAGCACGCCATCCTGG  1200
78AL     TCTGGTGTCATGATTTCGTAGTTTTCGCGGTTTTTCAGCACGCCATCCTGG  1175

exp78AL  TGTATACCGGAGGAGTGTGCGAATGCGCCGCTGCCAACAATGGCTTTGTT  1250
CP78     TGTATACCGGAGGAGTGTGCGAATGCGCCGCTGCCAACAATGGCTTTGTT  1250
78AL     TGTATACCGGAGGAGTGTGCGAATGCGCCGCTGCCAACAATGGCTTTGTT  1225

exp78AL  TGCCGGGATCGGCATATTACAAATCTGGCTAACTAACTGGCTGGTG CGC  1299
CP78     TGCCGGGATCGGCATATTACAAATCTGGCTAACTAACTGGCTGGTG CGC  1299
78AL     TGCCGGGATCGGCATATTACAAATCTGGCTAACTAACTGGCTGGTGGCGC  1275
```

```
exp78AL  CATATCTCCTGGTGATTAATGGCGGTGTGGACGTTGAGAATATCCTT AC  1348
CP78     CATATCTCCTGGTGATTAATGGCGGTGTGGACGTTGAGAATATCCTT AC  1348
78AL     CATATCTCCTGGTGATTAATGGCGGTGTGGACGTTGAGAATATCCTTT AC  1325

exp78AL  GAACTTTGATCGCCATGATGACTTCTTCCAGGGAACAGTTTCCGGCACGC  1398
CP78     GAACTTTGATCGCCATGATGACTTCTTCCAGGGAACAGTTTCCGGCACGC  1398
78AL     GAACTTTGATCGCCATGATGACTTCTTCCAGGGAACAGTTTCCGGCACGC  1375

exp78AL  TCGCCGATCCCGTTCATTGCGCCTTCCACCTGGCGTGCACCGGCATGTAC  1448
CP78     TCGCCGATCCCGTTCATTGCGCCTTCCACCTGGCGTGCACCGGCATGTAC  1448
78AL     TCGCCGATCCCGTTCATTGCGCCTTCCACCTGGCGTGCACCGGCATGTAC  1425

exp78AL  CGCCGCCAGTGAGTTTCCGACCGCCAGGCCCAAATCGTCGTGGGTATGTA  1498
CP78     CGCCGCCAGTGAGTTTCCGACCGCCAGGCCCAAATCGTCGTGGGTATGTA  1498
78AL     CGCCGCCAGTGAGTTTCCGACCGCCAGGCCCAAATCGTCGTGGGTATGTA  1475

exp78AL  CGGAGATAATGGCTTTGCCGATGCTAGGCACGCGTTCATACAGGCCGCTG  1548
CP78     CGGAGATAATGGCTTTGCCGATGCTAGGCACGCGTTCATACAGGCCGCTG  1548
78AL     CGGAGATAATGGCTTTGTCGATGTTAGGCACGCGTTCATACAGGCCGCTG  1525

exp78AL  ATGATTCCGGCGAACTCAAACGGCATGGTGTAGCCCACGGTGTCCGGAAT  1598
CP78     ATGATTCCGGCGAACTCAAACGGCATGGTGTAGCCCACGGTGTCCGGAAT  1598
78AL     ATGATTCCGGCGAACTCAAACGGCATGGTGTAGCCCACGGTGTCCGGAAT  1575

exp78AL  GTTGATGGTGGTGGCACCGGCATTAATCGCCGCTTCGACCACTCGCGCCA  1648
CP78     GTTGATGGTGGTGGCACCGGCATTAATCGCCGCTTCGACCACTCGCGCCA  1648
78AL     GTTGATGGTGGTGGCACCGGCATTAATCGCCGCTTCGACCACTCGCGCCA  1625

exp78AL  GATCGGCAATGGGTGTACGCCCGGCATCTTCGCAAGAAAA TTCAACATC  1697
CP78     GATCGGCAATGGGTGTACGCCCGGCATCTTCGCAAGAAAA TTCAACATC  1697
78AL     GATCGGCAATGGGTGTACGCCCGGCATCTTCGCAAGAAAAATTCAACATC  1675

exp78AL  ATCGGTGTAATTACGGGCGCGTTTCACCATATAGATAGCGCGTTCGATCA  1747
CP78     ATCGGTGTAATTACGGGCGCGTTTCACCATATAGATAGCGCGTTCGATCA  1747
78AL     ATCGGTGTAATTACGGGCGCGTTTCACCATATAGATAGCGCGTTCGATCA  1725

exp78AL  CCTCGTCCAGCGTGCTGCGCAGCTTGGTGGCGATGTGCATTGGCGAAGTG  1797
CP78     CCTCGTCCAGCGTGCTGCGCAGCTTGGTGGCGATGTGCATTGGCGAAGTG  1797
78AL     CCTCGTCCAGCGTGCTGCGCAGCTTGGTGGCGATGTGCATTGGCGAAGTG  1775

exp78AL  GCAATAAAGGTATGAATACGGAAGGCTTCGGCGACTTTCAGGGATTCGGC  1847
CP78     GCAATAAAGGTATGAATACGGAAGGCTTCGGCGACTTTCAGGGATTCGGC  1847
78AL     GCAATAAAGGTATGAATACGGAAGGCTTCGGCGACTTTCAGGGATTCGGC  1825

exp78AL  CGCCACGTCGATATCTTTTTCCACGCAGCGAGCTAACGCACATACGCGGC  1897
CP78     CGCCACGTCGATATCTTTTTCCACGCAGCGAGCTAACGCACATACGCGGC  1897
78AL     CGCCACGTCGATATCTTTTTCCACGCAGCGAGCTAACGCACATACGCGGC  1875

exp78AL  TGTTTTT AACCTGGCGGGCGATGGTTTGCACCGATTCAAAA TCGCCCG  1945
CP78     TGTTTTT AACCTGGCGGGCGATGGTTTGCACCGATTCAAAA TCGCCCG  1945
78AL     TGTTTTTTAACCTGGCGGGCGATGGTTTGCACCGATTCAAAAATCCCCCG  1925
```

```
exp78AL  GCGAAGAGACGGGGAAACCGACTTCCATCACGTCAACACCCATACGCTC  1994
CP78     GCGAAGAGACGGGGAAACCGACTTCCATCACGTCAACACCCATACGCTC  1994
78AL     GCCAAGAGACGGGGAAACCGACTTCCATCACGTCAACACCCATACGCTC

exp78AL  AAGGGCCAGCGCAATTTGCAGTTTTTCTTTCACACTCAAGCTTGCCTGTA  2044
CP78     AAGGGCCAGCGCAATTTGCAGTTTTTCTTTCACACTCAAGCTTGCCTGTA  2044
78AL     AAGGGCCAGCGCAATTTGCAGTTTTTCTTTCACACTCAAGCTTGCCTGTA

exp78AL  ACGCCTGTTCACCGTCGCGCAATGTGGTATCGAAAATAATGACTTGCTGG  2094
CP78     ACGCCTGTTCACCGTCGCGCAATGTGGTATCGAAAATAATGACTTGCTGG  2094
78AL     ACGCCTGTTCACCGTCGCGCAATGTGGTATCGAAAATAATGACTTGCTGG

exp78AL  CTCAT GAATTCTGTTTCCTGTGTGAAATTGTTATCCGCTCACAATTCCAC  2144
CP78     CTCAT ggtttgggtccttgtctcttttagagcgcctcgcttcgggcataaaaaaacccgcgcaatg  2169
78AL     CTCAT GAATTCTGTTTCCTGTGTGAAATTGTTATCCGCTCACAATTCCAC

exp78AL  ACATTATACGAGCCGATGATTAATTGTCAACAGCTCATTTCAGAATATTT  2194
CP78     gcgcgggttttttgtttgactgcgtgctggcttaatgctggatgccgctcactcgtctaccgcgcaaa  2239
78AL     ACATTATACGAGCCGATGATTAATTGTCAACAGCTCATTTCAGAATATTT

exp78AL  GCCAGAACCGTTATGATGTCGGCGCAAAAAACATTATCCAGAACGGGAGT  2244
CP78     gaagatgcgtttagtagtagtagaccgataaagcgaacgatgtgagtcattaaatcagctccagatgaa  2308
78AL     GCCAGAACCGTTATGATGTCGGCGCAAAAAACATTATCCAGAACGGGAGT

exp78AL  GCGCCTTGAGCGACACGAATTATGCAGTGATTTACGACCTGCACAGCCAT  2294
CP78     tgcgatatgcttttagagttactggatacaaaaacggatgtcaaccctgacgcaataaaaacgtcccgc  2378
78AL     GCGCCTTGAGCGACACGAATTATGCAGTGATTTACGACCTGCACAGCCAT

exp78AL  ACCACAGCTTCCGATGGCTGCCTGACGCCAGAAGCATTGGTGCACCGTGC  2344
CP78     cagcgtgagttctgcatccgtaaaattagctaattgtgctgcggtggttaaagtaagcgatattaatttc  2442
78AL     ACCACAGCTTCCGATGGCTGCCTGACGCCAGAAGCATxxxxxxxxxxxxxxxxxx

exp78AL  AGTCGATAAGCTCCGGATCCCCGGGTACCGAGCTC  2379
CP78     tgcttaactaccgacgcttttcatcggttgacatatttcagcataaatttttgcatctaatcaacgaggaa  2513
78AL     xxxxxxxxxxxxxxxxxxxxxxxxxxxxxxxxxxxxxxxxxxxxxxxxxxxxxxxxxxxxxxxxxxxxxx

exp78AL  GAATTCNNNNNTTCGAACCCCAGAGTCCCGCTCAGAAGAA  2409
CP78     aaaggggacaaaatgcacgcgttgcaaaacctatcctgatgatttgtattgaattatatgttttgcgatt  2585
78AL     xxxxxxxxxxxxxxxxxxxxxxxxxxxxxxxxxxxxxxxxxxxxxxxxxxxxxxxxxxxxxxxxxxxxx

exp78AL  CTCGTCAAGAAGGCGATAGAAGGCGATGCGCTG-CGAATCGGGAGCGGCG  2468
CP78     ttttttgatattgatttggtgaatattattgatcaattaatgttaagaattaatgcattaaatatataaattaat  2660
78AL     xxxxxxxxxxxxxxxxxxxxxxxxxxxxxxxxxxxxxxxxxxxxxxxxxxxxxxxxxxxxxxxxxxxxx

exp78AL  ATACCGTAAAGCA-CGAGGAAGCGGTCAGCCCATTCGCCGCCAAGCTCTT  2518
CP78     tattaaataagcacatttaatccattttgtagatgattgagtattcgcggtagttatgattagattgttttc  2732
78AL     xxxxxxxxxxxxxxxxxxxxxxxxxxxxxxxxxxxxxxxxxxxxxxxxxxxxxxxxxxxxxxxxxxxxx
```

```
exp78AL  CAGCAATATCACGGGTAGCCAACGCTATGTCCTGATAGCGGTCCGCCACA  2568
CP78     gcaacaaaaacattatggattattatgctgtggtaaatgactcattccacggcaatggattctgtttttat  2803
78AL     xxxxxxxxxxxxxxxxxxxxxxxxxxxxxxxxxxxxxxxxxxxxxxxxxxxxxxxxxxxxxxxxxxxxxxx

exp78AL  CCCAGCCGGCCACAGTCGATGAATCCAGAAAAGCGGCCATTTTCCACCAT  2618
CP78     cagaacccgtatcttttaaatcatattcttcaggattatttctctgcattccaataagggaaagggagtta  2874
78AL     xxxxxxxxxxxxxxxxxxxxxxxxxxxxxxxxxxxxxxxxxxxxxxxxxxxxxxxxxxxxxxxxxxxxxxx

exp78AL  GATATTCGGCAAGCAGGCATCGCCATGGGTCACGACGAGATCCTCGCCGT  2668
CP78     agtgtgacagtggagttaagtatgccagaggtacaaacagatcatccagagacggcggagttaagc  2940
78AL     xxxxxxxxxxxxxxxxxxxxxxxxxxxxxxxxxxxxxxxxxxxxxxxxxxxxxxxxxxxxxxxxxxxxxxx

exp78AL  CGGGCATCCGCGCCTTGAGCCTGGCGAACAGTTCGGCTGGCGCGAGC  2715
CP78     aaaccacagct----------  2951
78AL     xxxxxxxxxxxxxxxxxxxxxxxxxxxxxxxxxxxxxxxxxxxxxxxxxxxxxxxxxxxxxxxxxxxxxxx

exp78AL  CCCTGATGCTCTTCGTCCAGATCATCCTGATCGACAAGACCGGCTTCCAT  2765
CP78     ----------
78AL     xxxxxxxxxxxxxxxxxxxxxxxxxxxxxxxxxxxxxxxxxxxxxxxxxxxxxxxxxxxxxxxxxxxxxxx

exp78AL  CCGAGTACGTGCTCGCTCGATGCGATGTTTCGCTTGGTGGTCGAATGGGC  2815
CP78     ----------
78AL     xxxxxxxxxxxxxxxxxxxxxxxxxxxxxxxxxxxxxxxxxxxxxxxxxxxxxxxxxxxxxxxxxxxxxxx

exp78AL  AGGTAGCCGGATCAAGCGTATGCAGCCGCCGCATTGCATCAGCCAT  2861
CP78     ----------
78AL     xxxxxxxxxxxxxxxxxxxxxxxxxxxxxxxxxxxxxxxxxxxxxxxxxxxxxxxxxxxxxxxxxxxxxxx

exp78AL  GATGGATACTTTCTCGGCAGGAGCAAGGTGAGATGACAGGAGA  2904
CP78     ----------
78AL     xxxxxxxxxxxxxxxxxxxxxxxxxxxxxxxxxxxxxxxxxxxxxxxxxxxxxxxxxxxxxxxxxxxxxxx

exp78AL  TCCTGCCCCGGCACTTCGCCCAATAGCAGCCAGTCCCTTCCCGCT  2949
CP78     ----------
78AL     xxxxxxxxxxxxxxxxxxxxxxxxxxxxxxxxxxxxxxxxxxxxxxxxxxxxxxxxxxxxxxxxxxxxxxx

exp78AL  TCAGTGACAACGTCGAGCACAGCTGCGCAAGGAACGCCCGT  2990
CP78     ----------
78AL     xxxxxxxxxxxxxxxxxxxxxxxxxxxxxxxxxxxxxxxxxxxxxxxxxxxxxxxxxxxxxxxxxxxxxxx

exp78AL  CGTGGCCAGCCACGATAGCCGCGCTGCCTCGTCTTGGAGT  3030
CP78     ----------
78AL     xxxxxxxxxxxxxxxxxxxxxxxxxxxxxxxxxxxxxxxxxxxxxxxxxxxxxxxxxxxxxxxxxxxxxxx

exp78AL  TCATTCAGGGCACCGGACAGGTCGGTCTTGACAAAAAGAACCGGGCG  3077
CP78     ----------
78AL     xxxxxxxxxxxxxxxxxxxxxxxxxxxxxxxxxxxxxxxxxxxxxxxxxxxxxxxxxxxxxxxxxxxxxxx
```

```
exp78AL  CCCCTGCGCTGACAGCCGGAACACGGCGGCATCAGAGCAGCCGAT  3122
CP78     ----------------------------------------------
78AL     xxxxxxxxxxxxxxxxxxxxxxxxxxxxxxxxxxxxxxxxxxxxxx

exp78AL  TGTCTGTTGTGCCCAGTCATAGCCGAATAGCCTCTCCACCC      3163
CP78     ---------------------------------------
78AL     xxxxxxxxxxxxxxxxxxxxxxxxxxxxxxxxxxxxxxxxxxxxx

exp78AL  AAGCGGCCGGAGAACCTGCGTGCAATCCATCTTGTTCAATCATGCG  3209
CP78     -----------------------------------------------
78AL     xxxxxxxxxxxxxxxxxxxxxxxxxxxxxxxxxxxxxxxxxxxxxx

exp78AL  AAACGATCCTCATCCTGTCTCTTGATCAGATCTTGATCCCCTGCGCCATC  3259
CP78     -------------------------------------------------
78AL     xxxxxxxxxxxxxxxxxxxxxxxxxxxxxxxxxxxxxxxxxxxxxxxx

exp78AL  AGATCCTTGGCGGCAAGAAAGCCATCCAGTTTACTTTGCAGGGCTTCCCA  3309
CP78     ---------------------------------------------------
78AL     xxxxxxxxxxxxxxxxxxxxxxxxxxxxxxxxxxxxxxxxxxxxxxxxxxx

exp78AL  ACCTTACCAGAGGGCGCCCCAGCTGGCAATTCCGGTTCGCT-TGCTG  3355
CP78     ----------------------------------------------
78AL     xxxxxxxxxxxxxxxxxxxxxxxxxxxxxxxxxxxxxxxxxxxxxx

exp78AL  TCCATAAAACCGCCCAGTCTAGCTATCGCCATGTAAGCCCAC      3397
CP78     ---------------------------------------
78AL     xxxxxxxxxxxxxxxxxxxxxxxxxxxxxxxxxxxxxxxxxxxxx

exp78AL  TGCAAGCTACCTGCTTTCTCTTTGCGCTTGCGTTTT            3433
CP78     ----------------------------------
78AL     xxxxxxxxxxxxxxxxxxxxxxxxxxxxxxxxxxxxxxxx


exp78AL  CCC-TTGTCCAGATAGC-CCAGTAGCTGACATTCATCCGGGGTCAGCA  3479
CP78     -----------------------------------------------
78AL     xxxxxxxxxxxxxxxxxxxxxxxxxxxxxxxxxxxxxxxxxxxxxx

exp78AL  CCGTTTCTGCGGACTGGCTTTCTACGTGTTCCGCTTCC           3517
CP78     -------------------------------------
78AL     xxxxxxxxxxxxxxxxxxxxxxxxxxxxxxxxxxxxxxxxx

exp78AL  TTTAGCAGCCCTTGCGCCCTGAGTGCTTGCGGCAGCGTGAAGCTAGC  3564
CP78     -----------------------------------------------
78AL     xxxxxxxxxxxxxxxxxxxxxxxxxxxxxxxxxxxxxxxxxxxxxx

exp78AL  ACGCATGGTCGATCTCAACTTATTAACCGTTTTCGATGCCGTGATGCAGGA  3614
CP78     ACGCATGGTCGATCTCAACTTATTAACCGTTTTCGATGCCGTGATGCAGGA  3001
78AL     xxxxxxxxxxxxxxxxxxxxxxxxxxxxxxxxxxxxxxxxxxxxxxxxxx
```

```
exp78AL  GCAAAACATTACTCGTGCCGCTCATGTTC                                  3643
CP78     GCAAAACATTACTCGTGCCGCTCATGTTC                                  3030
78AL     xxxxxxxxxxxxxxxxxxxxxxxxxxxxxxxxxxxx

exp78AL  TGGGAATGTCGCAACCTGCGGTCAGTAACGCTGTTGCACGCCTGAAGGTG            3693
CP78     TGGGAATGTCGCAACCTGCGGTCAGTAACGCTGTTGCACGCCTGAAGGTG            3080
78AL     xxxxxxxxxxxxxxxxxxxxxxxxxxxxxxxxxxxxxxxxxxxxxxxxxxxxxxxxxxxx

exp78AL  ATGTTTAATGACGAGCTTTTTGTTCGTTATGGCCGTGGTATTCAACCGAC            3743
CP78     ATGTTTAATGACGAGCTTTTTGTTCGTTATGGCCGTGGTATTCAACCGAC            3130
78AL     xxxxxxxxxxxxxxxxxxxxxxxxxxxxxxxxxxxxxxxxxxxxxxxxxxxxxxxxxxxx

exp78AL  TGCTCGCGCATTTCAACTTTTTGGTTCAGTTCGTCAGGCATTGCAACTAG            3793
CP78     TGCTCGCGCATTTCAACTTTTTGGTTCAGTTCGTCAGGCATTGCAACTAG            3180
78AL     xxxxxxxxxxxxxxxxxxxxxxxxxxxxxxxxxxxxxxxxxxxxxxxxxxxxxxxxxxxx

exp78AL  TACAAAATGAATTGCCTGGTTCAGGTTTTGAACCCGCGAGCAGTGAACGT            3843
CP78     TACAAAATGAATTGCCTGGTTCAGGTTTTGAACCCGCGAGCAGTGAACGT            3230
78AL     xxxxxxxxxxxxxxxxxxxxxxxxxxxxxxxxxxxxxxxxxxxxxxxxxxxxxxxxxxxx

exp78AL  GTATTTCATCTTTGTGTTTGCAGCCCGTTAGACAGCATTCTGACCTCGCA            3893
CP78     GTATTTCATCTTTGTGTTTGCAGCCCGTTAGACAGCATTCTGACCTCGCA            3280
78AL     GTATT CATCTTTGTGTTTGCAGCCCGTTAGACAGCATTCTGACCTCGCA

exp78AL  GATTTATAATCACATTGAGCAGATTGCGCCAAATATACATGTTATGTTCA            3943
CP78     GATTTATAATCACATTGAGCAGATTGCGCCAAATATACATGTTATGTTCA            3330
78AL     GATTTATAATCACATTGAGCAGATTGCGCCANATATACATGTTATGTTCA

exp78AL  AGTCTTCATTAAATCAGAACACTGAACATCAGCTGCGTTATCAGGAAACG            3993
CP78     AGTCTTCATTAAATCAGAACACTGAACATCAGCTGCGTTATCAGGAAACG            3380
78AL     AGTCTTCATTAAATCAGGACACTGGACATCAGCTGCGTTATCAGGAAACG

exp78AL  GAGTTTGTGATTAGTTATGAAGACTTCCATCGTCCTGAATTTACCAGCGT            4043
CP78     GAGTTTGTGATTAGTTATGAAGACTTCCATCGTCCTGAATTTACCAGCGT            3430
78AL     GAGTTTGTGATTAGTTATGAAGACTTCCATCGTCCTGAATTTACCAGCGT

exp78AL  ACCATTATTTAAAGATGAAATGGTGCTGGTAGCCAGCAAAAATCATCCAA            4093
CP78     ACCATTATTTAAAGATGAAATGGTGCTGGTAGCCAGCAAAAATCATCCAA            3480
78AL     ACCATTATTTAAAGATGAAATGGTGCTGGTAGCCAGCAAAAATCATCCAA

exp78AL  CAATTAAGGGCCCGTTACTGAAACATGATGTTTATAACGAACAACATGCG            4143
CP78     CAATTAAGGGCCCGTTACTGAAACATGATGTTTATAACGAACAACATGCG            3530
78AL     CAATTAAGGGCCCGTTACTGAAACATGATGTTTATAACGAACAACATGCG

exp78AL  GCGGTTTCGCTCGATCGTTTCGCGTCATTTAGTCAACCTTGGTATGACAC            4193
CP78     GCGGTTTCGCTCGATCGTTTCGCGTCATTTAGTCAACCTTGGTATGACAC            3580
78AL     GCGGTTTCGCTCGATCGTTTCGCGTCATTTAGTCAACCTTGGTATGACAC

exp78AL  GGTAGATAAGCAAGCCAGTATCGCGTATCAGGGCATGGCAATGATGAGCG            4243
CP78     GGTAGATAAGCAAGCCAGTATCGCGTATCAGGGCATGGCAATGATGAGCG            3630
78AL     GGTAGATAAGCAAGCCAGTATCGCGTATCAGGCAT
```

Table 2. Growth rates of CP78 and 78AL with and without IPTG during the end of log-growth.

| | ΔOD | Δt (h) | growth rate (gr) (OD units per h) |
|---|---|---|---|
| CP78 no IPTG | 0.095 | 5.42 | 0.018 |
| CP78 1 mM IPTG | 0.067 | 5.42 | 0.012 |
| 78AL no IPTG | 0.098 | 5.42 | 0.018 |
| 78Al 1 mM IPTG | 0.075 | 5.42 | 0.014 |

Table 3. Size (mm) of *leuB* revertant colonies from a typical mutation rate experiment of 78AL with 1 mM IPTG during growth. Results from the comparable experiment with no IPTG are presented in Table 4. Presumed suppressers are indicated by an asterisk. Those that did not change in size are indicated NC.

| colony | 43h | 51h | 68h | 92h | 121h |
|---|---|---|---|---|---|
| 1 | 0.80 | | 1.35 | 1.55 | NC |
| 2 | 0.55 | | 1.00 | 1.10 | NC |
| 3 | 0.60 | | 1.25 | NC | 1.40 |
| 4 | 1.10 | 1.35 | 1.70 | NC | NC |
| 5 | 0.55 | 0.70 | 1.15 | 1.30 | NC |
| 6 | 0.70 | | 1.50 | 1.55 | 1.60 |
| 7 | 0.75 | | 1.60 | NC | NC |
| 8 | 0.60 | | 1.85 | 2.20 | NC |
| 9 | 0.75 | | 1.90 | NC | NC |
| 10 | 0.80 | | 1.70 | NC | 1.80 |
| 11 | 0.80 | | 1.40 | 1.55 | NC |
| 12 | 1.10 | | 1.35 | 1.55 | NC |
| 13 | 0.85 | | 1.30 | 1.60 | NC |
| 14 | 0.80 | | 1.55 | 1.75 | NC |
| 15 | 0.75 | | 1.25 | 1.65 | NC |
| 16 | 0.85 | | 1.35 | 1.45 | NC |
| 17 | 0.70 | | 1.55 | 1.85 | NC |
| 18 | 0.50 | | 1.60 | 1.90 | NC |
| 19 | | 0.40 | 1.00 | 1.30 | NC |
| 20 | | | 0.40 | 0.95 | NC |
| 21 | | | 0.80 | 1.00 | NC |
| 22 | | | 0.50 | 1.15 | NC |
| 23 | | | 0.50 | 0.90 | NC |
| 24 | | | 0.60 | 1.00 | NC |
| 25 | | | 0.75 | 1.15 | NC |
| 26 | | | 0.50 | 0.90 | NC |
| 27 | | | 0.75 | 1.40 | NC |
| 28 | | | 0.80 | 1.50 | NC |
| 29 | | | 0.40 | 1.00 | NC |
| 30 | | | 0.75 | 1.50 | NC |
| 31 | | | 1.00 | 1.70 | NC |
| 32 | | | 1.00 | 1.40 | NC |
| 33 | | | 0.85 | NC | 1.20 |
| 34 | | | 0.55 | 1.15 | NC |
| 35 | | | 1.15 | 2.00 | NC |
| 36 | | | 0.50 | 1.10 | 1.20 |
| 37 | | | 1.10 | 1.60 | NC |
| 38* | | | | 0.55 | NC |
| 39* | | | | 0.60 | NC |
| 40* | | | | 0.70 | NC |
| 41* | | | | 0.55 | NC |
| 42* | | | | 0.60 | 0.70 |
| 43* | | | | 0.25 | 0.50 |
| 44 | | | | 1.10 | NC |
| 45 | | | | 1.50 | NC |

Table 4. Size (mm) of *leuB* revertant colonies from a typical mutation rate experiment of 78AL with no IPTG. Results from the comparable experiment with 1 mM IPTG are presented in Table 3. Presumed suppressers are indicated by an asterisk. Those that did not change in size are indicated NC.

| colony | 43h | 51h | 68h | 92h | 121h |
|---|---|---|---|---|---|
| 1 | 1.90 | | 3.60 | 4.45 | NC |
| 2 | 1.60 | | 2.70 | 3.55 | 3.80 |
| 3 | 1.55 | | 2.80 | 3.60 | NC |
| 4 | 2.05 | 2.50 | 3.50 | 4.05 | 4.20 |
| 5 | 1.25 | 1.80 | 2.70 | 3.55 | NC |
| 6 | 0.90 | | 1.60 | 2.00 | 2.30 |
| 7 | 1.40 | | 2.40 | 3.25 | NC |
| 8 | 1.20 | | 2.25 | 2.45 | NC |
| 9 | 1.35 | | 2.40 | 2.40 | NC |
| 10 | | 0.50 | 1.60 | 2.00 | 2.85 |
| 11 | | | | 1.70 | 3.60 |
| 12* | | | | 0.35 | NC |
| 13* | | | | | ~0.40 |
| 14* | | | | | ~0.40 |
| 15* | | | | | ~0.40 |
| 16* | | | | | ~0.40 |
| 17* | | | | | ~0.40 |

In previous experiments, Wright (1996) observed two types of *leuB*$^+$ revertant colonies in CP78 and CP79 and subsequent sequencing of the *leuB* gene revealed that the bigger colonies were true revertants and the smaller colonies that appeared later and remained small were suppressers. In later experiments, (Card and Wright, unpublished) these suppressers were shown to most likely be intra-operonic because they could be transduced with a *leu* operon-linked marker to other *leuB*$^-$ bacteria.

Revertant colonies of 78AL of the same and different ages from IPTG-exposed cultures and from non-IPTG cultures were plated to fresh minimal medium without leucine and without IPTG. All the colonies grew at the same rate to the same size; indicating that the IPTG-exposed revertants (Table 3) were smaller because of growth inhibition by IPTG not because they were suppressers - every indication is that they are true revertants.

*78AL and CP78 Growth Curves*

In order to compare CP78 mutation rates as a control for *leuB*$^-$ reversion in the presence and absence of IPTG, growth curves of CP78 with and without 10 mM IPTG included during growth were conducted (Figure 25).

After refining reversion experiments in 78AL, it was necessary to compare the numbers of viable cells on each plate over the entire length of a mutation rate experiment (Figures 26 and 27).

FIG 25. Growth curves for CP78 with 10 mM IPTG added at the time of inoculation versus the same cells with no IPTG. Growth was limited with leucine (0.03 mM) and the experiments were performed as for mutation rate determination; each culture was inoculated then divided into 40 tubes. At 5 timepoints near the end of log-growth three tubes were randomly selected, $OD_{550}$ of a $10^{-1}$ dilution recorded and serial dilutions made for viable count determinations. The remaining 25 tubes were plated to minimal medium without leucine. At 3 additional timepoints 5 plates were selected with no visible revertants and the cells harvested as described in Materials and Methods; $OD_{550}$ recorded and serial dilutions made for viable count determinations.

CP78 without IPTG

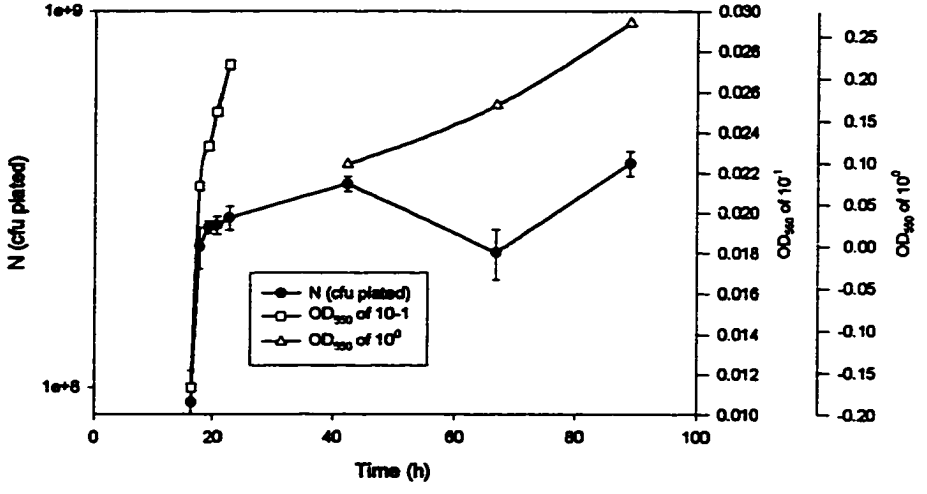


CP78 with 10mM IPTG

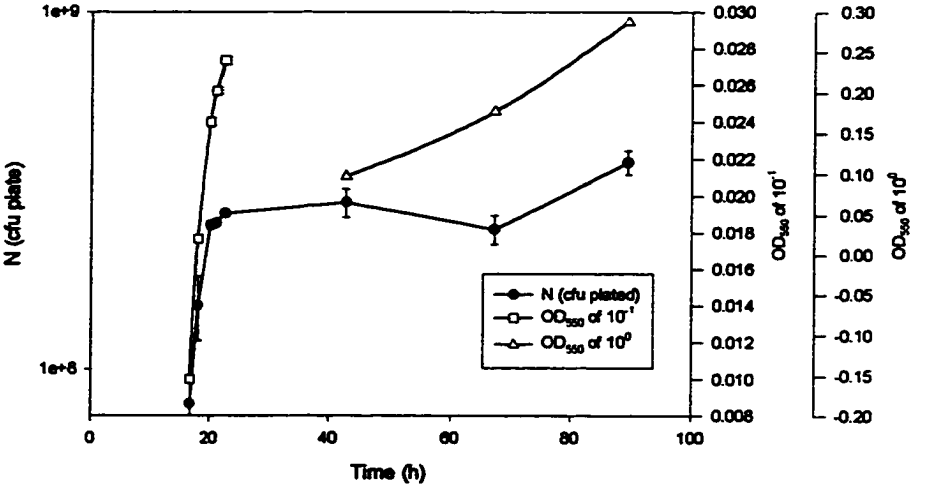

FIG 26. Viable counts for 78AL with 1 mM IPTG added at the end of log-growth versus the same cells with no IPTG. Growth was limited with leucine (0.03 mM) and the experiments were performed as for mutation rate determination; each culture was inoculated then divided into 40 tubes. After 3 h exposure to IPTG or no IPTG, each tube was plated to minimal medium without leucine. At 4 timepoints 10 plates were randomly selected, without regard to the presence of revertants, and the cells harvested as described in Materials and Methods; $OD_{550}$ recorded and serial dilutions made for viable count determinations.

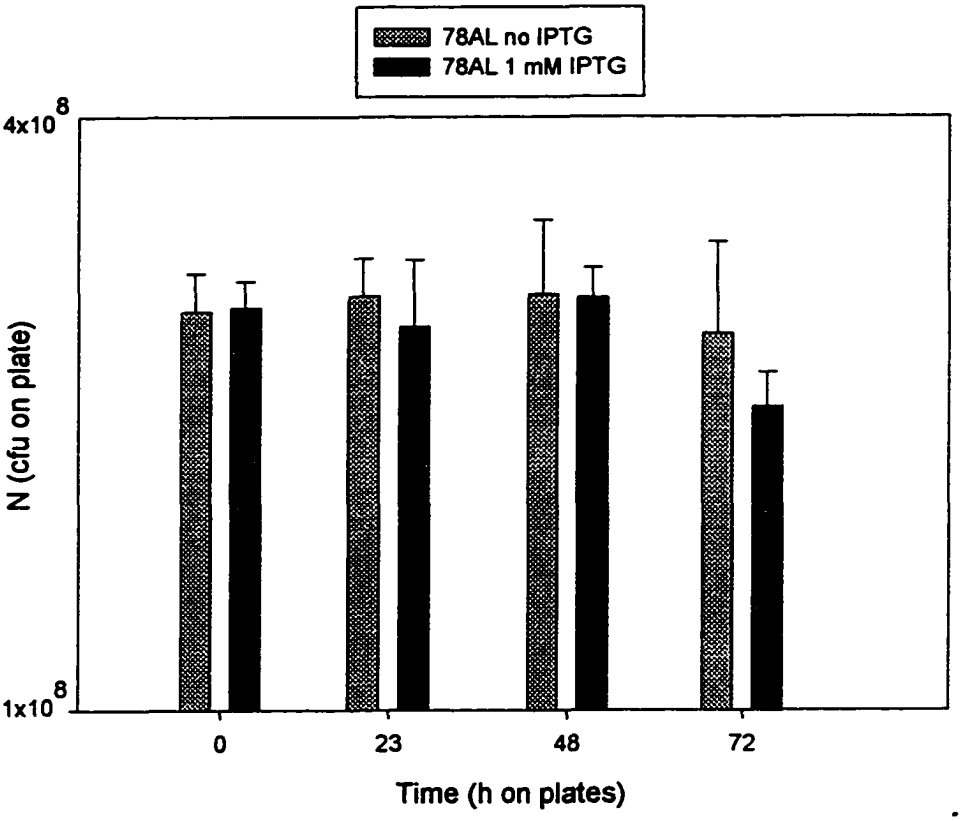

FIG 27. Viable counts for 78AL with 1 mM IPTG added 2 h after the end of log-growth versus the same cells with no IPTG. Growth was limited with leucine (0.015 mM) and the experiments were performed as for mutation rate determination; each culture was inoculated then divided into 40 tubes. After 3 h exposure to IPTG or no IPTG, each tube was plated to minimal medium without leucine. At 4 timepoints 10 plates were randomly selected, without regard to the presence of revertants, and the cells harvested as described in Materials and Methods; $OD_{550}$ recorded and serial dilutions made for viable count determinations.

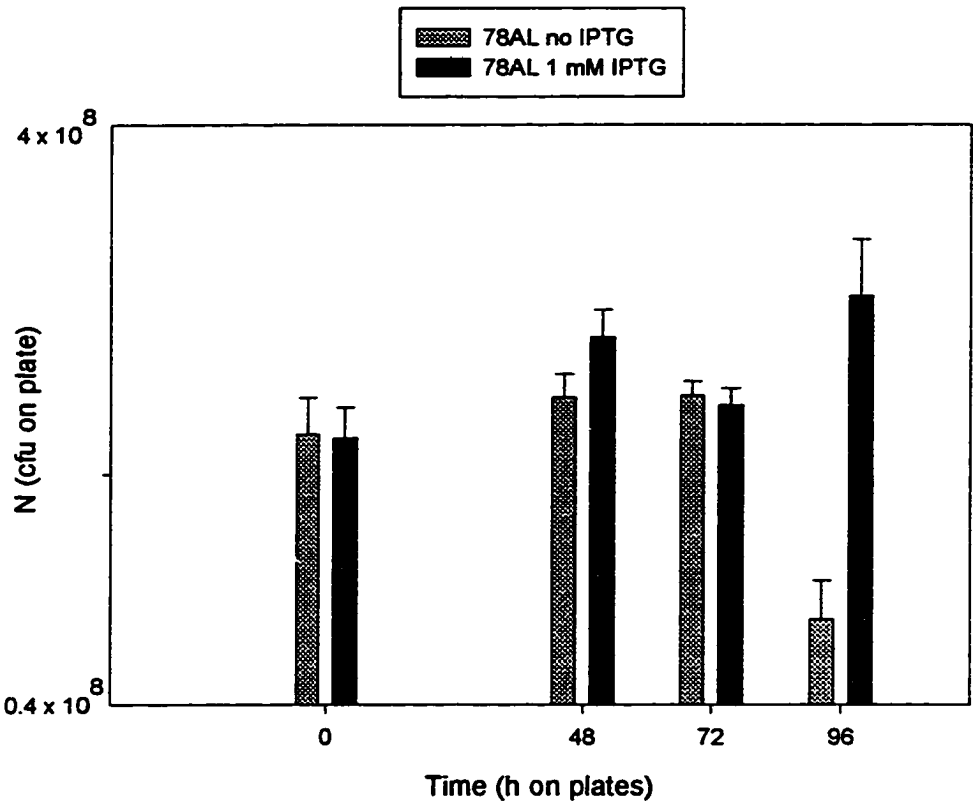

*Mutation Rates*

Mutation rate experiments were conducted on 78AL to compare *leuB*$^{-}$ reversion rates in the presence and absence of IPTG and with different concentrations of IPTG in order to determine if induction of transcription of the leu operon alone could account for the difference in *leuB*$^{-}$ reversion rate observed between CP78 (ppGpp$^{+}$) and CP79 (ppGpp$^{def}$). Table 5 is a summary of the data generated by the experiments.

IPTG induction should be specific to the recombinant *leu* operon and have no effect on the *arg* operon; therefore, *argH*$^{-}$ reversion rates were studied: *argH*$^{-}$ reversion rates for (1) parent CP78, (2) recombinant 78AL without IPTG, and (3) recombinant with 1 mM IPTG were indistinguishable: $6.2 \pm 1.1 \times 10^{-9}$, $5.96 \pm 1.59 \times 10^{-9}$, and $6.06 \pm 1.53 \times 10^{-9}$, respectively.

*mRNA levels*

Nuclease protection assays were employed to measure the levels of *leuB* transcript in 78AL cultures under various conditions. Figure 28 is a scanned image of the exposed film of a nuclease protection assay, the areas of greatest optical density show up as black bands. A densitometry program was utilized to analyze the optical density and relate that to a standard curve of known *leuB* mRNA concentration run with each experiment. When 78AL is exposed to ITPG for 1 h, there is a greater than four-fold increase in *leuB* mRNA level - confirming that the *leu* promoter was replaced by a functional *tac* promoter. When these transcript levels are related to

Table 5. 78AL *leuB*⁻ reversion rates.

| | MR x $10^{-9}$ 72 h | MR x $10^{-9}$ 96 h |
|---|---|---|
| 78AL no IPTG | 0.82 ± 0.10 | 1.12 ± 0.24 |
| 78AL 1 mM IPTG at the end of growth | 1.58 ± 0.57 | 4.84 ± 0.70 |
| 78AL 1 mM IPTG 2 h after end of growth | 1.77 ± 0.22 | 8.10 ± 1.23 |
| 78AL 0.1 mM IPTG after end (unspecified time >2 h) | 2.33 ± 0.59 | 9.92 ± 0.74 |
| 78AL 0.5 mM IPTG after end (unspecified time >2 h) | 3.17 ± 1.72 | 11.0 ± 1.74 |
| 78AL 1.0 mM IPTG after end (unspecified time >2 h) | 2.99 ± 1.08 | 13.6 ± 4.74 |
| 78AL 0.1 mM IPTG during growth | 1.82 ± 0.46 | >9* |
| 78AL 0.5 mM IPTG during growth | 2.81 ± 0.66 | >9* |
| 78AL 1.0 mM IPTG during growth | 3.96 ± 1.03 | >9* |

*These values could not be determined with the Zero method because no negative plates remained at this timepoint.

FIG 28. Nuclease protection assay of 78AL cultures treated just as for a mutation rate experiment. The cultures were exposed to either no IPTG or to 1 mM IPTG for 1 h after the end of log-growth. (A) a set of standards with known *leuB* mRNA concentration were run with the experiment, a standard curve established and pg *leuB* mRNA per μg total RNA determined from the optical density of each band as calculated by ONE-Dscan software (Scanalytics). (B) Messenger RNA levels are indicated below the 78AL blot.

A. Standards

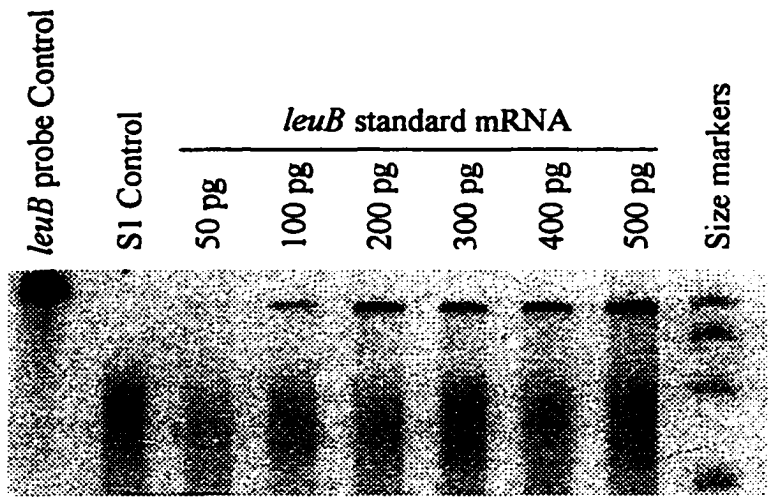


B. 78AL

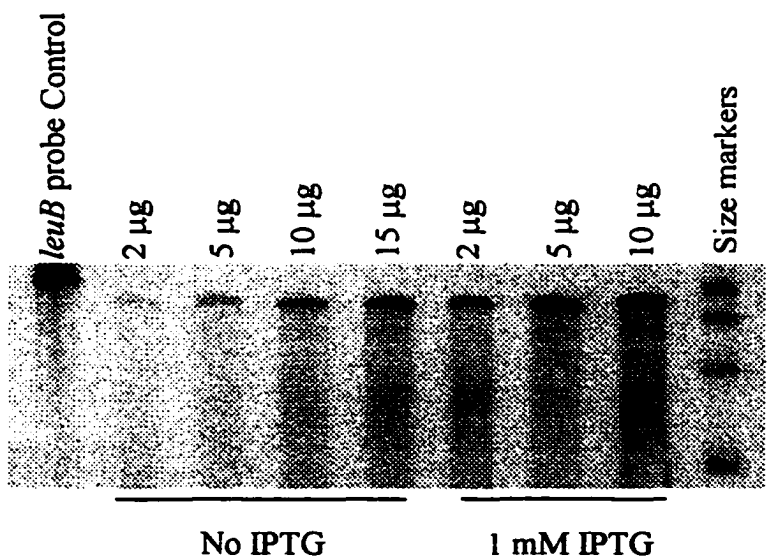


| | | |
|---|---|---|
| Average pg *leuB* mRNA per µg total RNA | 30 ± 5 | 131 ± 25 |

mutation rates measured under the same conditions, the points fit on the curve established for CP78 and CP79 (see Figure 7).

A similar nuclease protection assay was performed to determine if increased time of exposure to IPTG, for 3 h (Figure 29) as opposed to 1 h (Figure28), would yield higher levels of *leuB* transcription: it does (see Figure 29).

78AL *leuB* mRNA levels after leucine starvation are no different than *leuB* mRNA levels after arginine starvation (Figure 30) further confirming that the *leu* promoter was replaced by a functional *tac* promoter and that the leucine starvation necessarily imposed in order to measure *leuB*$^-$ reversion rates did not contribute to the amount of transcription initiated from the *tac* promoter. This result was expected because the attenuator region of the *leu* operon was removed when the *leu* promoter was replaced.

Because more revertants continue to appear for many days in 78AL cultures exposed to IPTG than in 78AL cultures not exposed to IPTG, it was hypothesized that IPTG stimulation of *leuB* transcription might continue for several days after the initial IPTG exposure. To determine if this could be the case, mRNA from the cells on plates of four different experiments, half exposed to IPTG for 3 h before plating and the other half not exposed, was collected and assayed for *leuB* mRNA concentration. A typical experiment is depicted in Figure 31. The levels in IPTG-exposed cultures do remain higher over 96 h, the length of typical mutation rate experiments.

FIG 29. Nuclease protection assay of 78AL cultures treated just as for a mutation rate experiment. The cultures were exposed to either no IPTG or to 1 mM IPTG for 3 h after the end of log-growth. (A) a set of standards with known *leuB* mRNA concentration were run with the experiment, a standard curve established and pg *leuB* mRNA per μg total RNA determined from the optical density of each band as calculated by ONE-Dscan software (Scanalytics). (B) Messenger RNA levels are indicated below the 78AL blot.

A. Standards

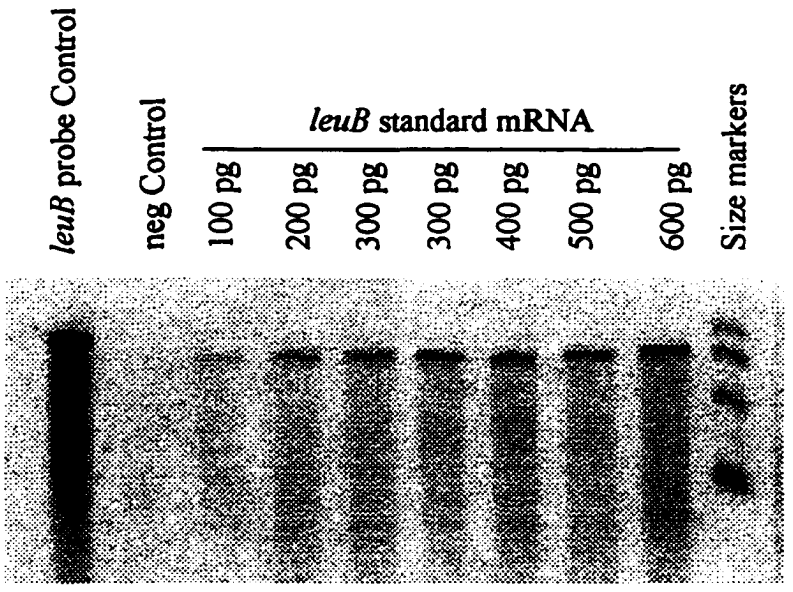


B. 78AL

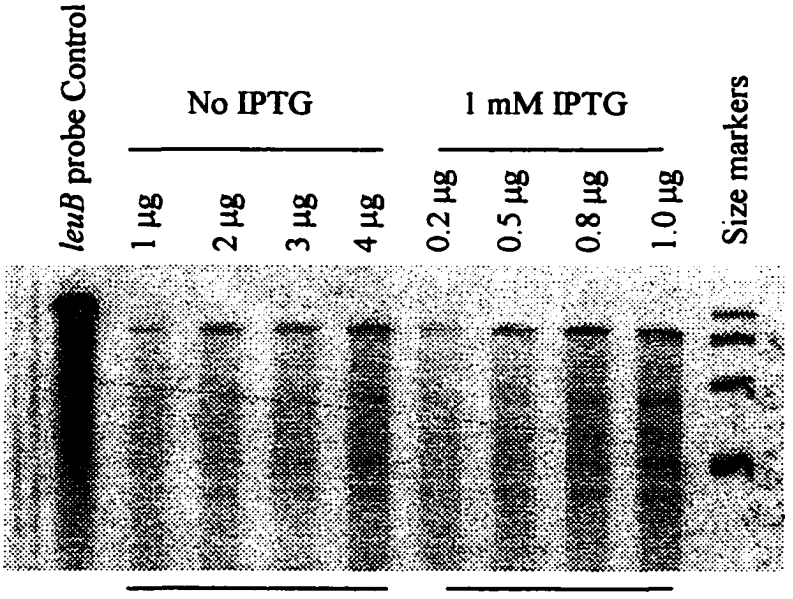


| | | |
|---|---|---|
| Average pg *leuB* mRNA per µg total RNA | 77 ± 18 | 406 ± 52 |

FIG 30. Nuclease protection assay of 78AL cultures treated just as for a mutation rate experiment. The cultures were limited for growth by either leucine or arginine starvation and neither set of cultures was exposed to IPTG. (A) a set of standards with known *leuB* mRNA concentration were run with the experiment, a standard curve established and pg *leuB* mRNA per μg total RNA determined from the optical density of each band as calculated by ONE-Dscan software (Scanalytics). (B) Messenger RNA levels are indicated below the 78AL blot; the small x under 8 μg leucine starved 78AL RNA indicates that the level of optical density exceeded the range of readability for the program and therefore was not included in the calculation of concentration.

A. Standards

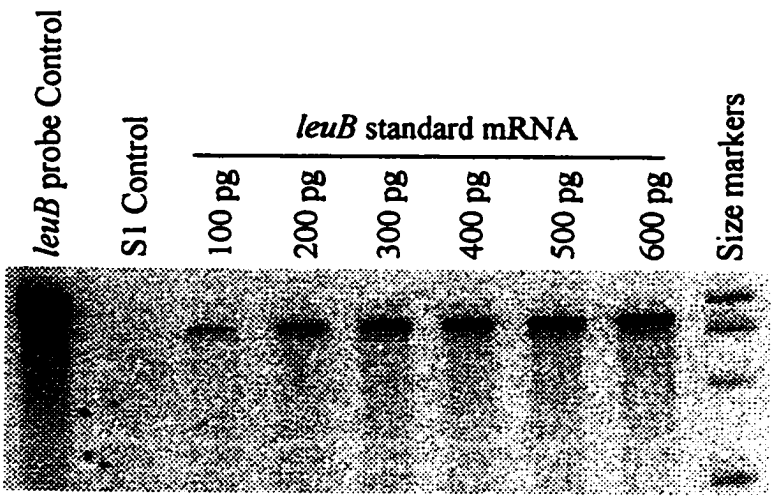


B. 78AL

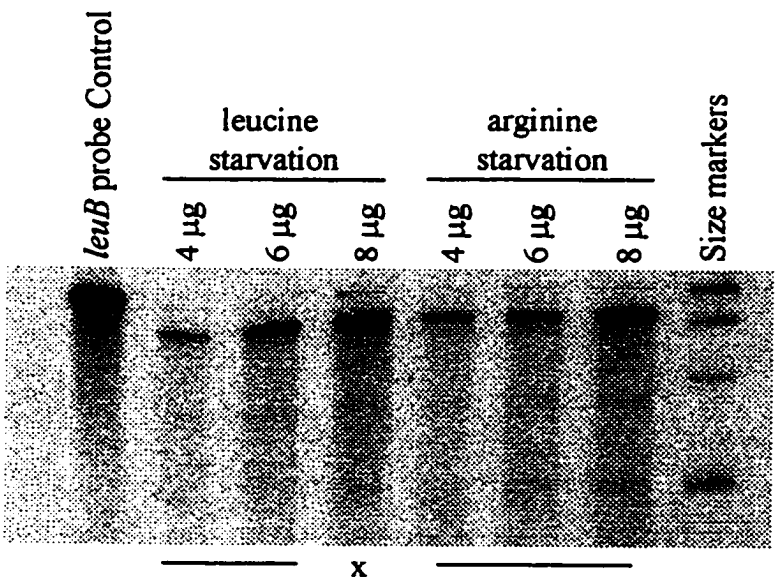


| | | |
|---|---|---|
| Average pg *leuB* mRNA per µg total RNA | 59 ± 16 | 60 ± 7 |

FIG. 31. Nuclease protection assay of 78AL cultures treated as for mutation rate experiments. The cultures were grown to stationary phase with limiting leucine, left for 3 h in stationary phase, then exposed to 1 mM IPTG (or no IPTG) for 3 h before being plated to minimal medium without leucine. Total RNA was collected from cells harvested from plates at 24, 48, 72 and 96 h after plating. (A) a set of standards with known *leuB* mRNA concentration were run with the experiment, a standard curve established and pg *leuB* mRNA per μg total RNA determined from the optical density of each band as calculated by ONE-Dscan software (Scanalytics). (B) 2 μg of each RNA were probed with the *leuB* specific probe.

A. Standards

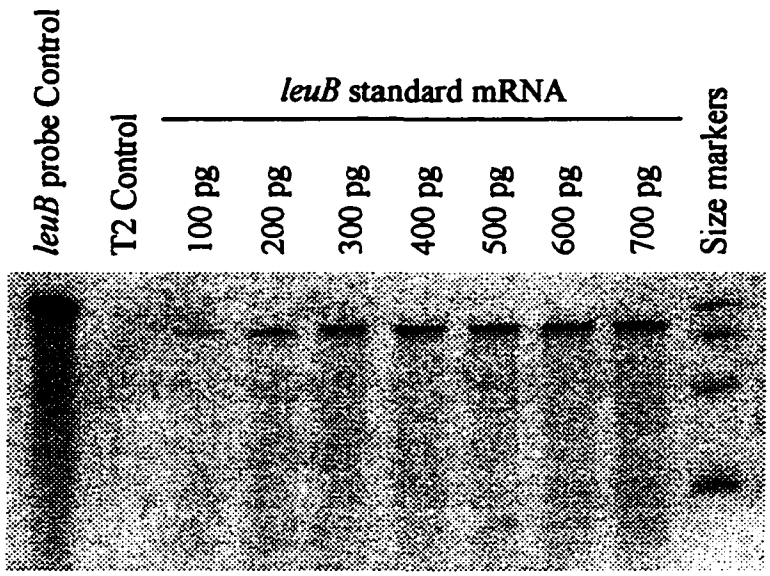


B. 78AL

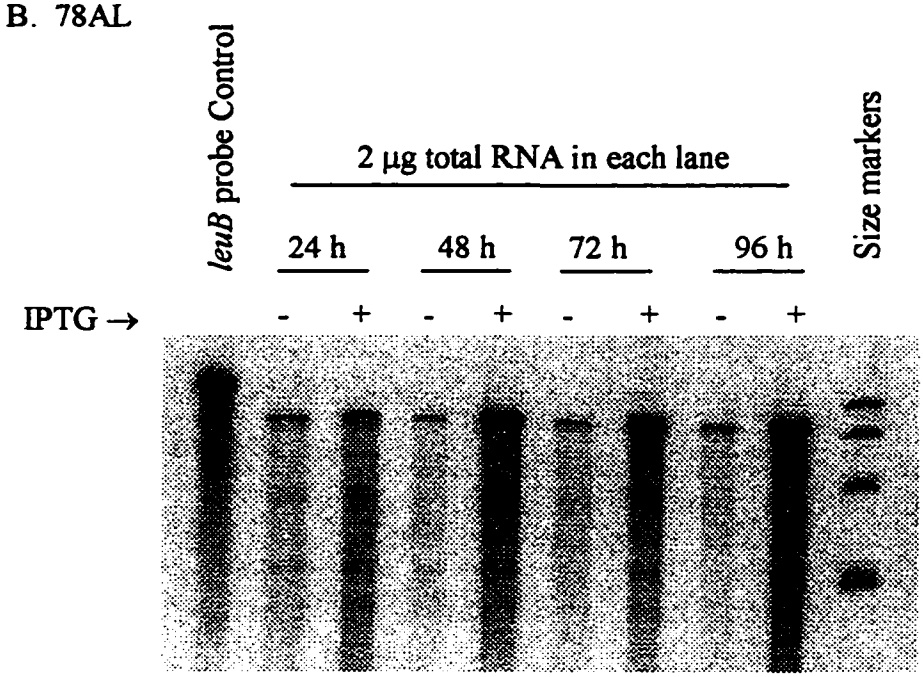

# DISCUSSION

It is well known that mutations occur in DNA because of nucleotide mis-incorporation during replication and because of damage incurred during normal metabolism. It is also known that the environment can "cause" mutations by providing chemicals that damage DNA. However, it is thought that all of these mutations occurs at characteristic frequencies throughout the genome without regard to any fitness advantage that might be obtained by a mutation happening in a particular gene. So, it is thought that the environment can not specifically influence the mutagenesis of a particular gene or set of genes.

Many researchers have looked for evidence of environmentally-directed mutations and have found none, but none of the experiments has been able to directly test whether an environmental influence could increase the mutation rate of a gene(s) above the mutation rate in the alternative (theoretical) situation without the environmental influence. This is because the control experiments, without the environmental influence, are difficult to design. For instance, if one studies reversion rates to prototrophy in bacterial amino acid biosynthetic operons, the ideal experiment would be to test the reversion rate with and without starvation for that amino acid (without and with environmental stress). However, this experiment is impossible because, for example, if you want to determine the reversion rate of a *leuB*$^-$ allele in the presence (no environmental stress) and absence (environmental stress) of leucine, you must plate all the cultures on minimal medium devoid of leucine – thus exposing them equally to the environmental stress. Even replica plating must involve

differentiation of revertant from non-revertant colonies on medium without leucine. Until a method is devised for measuring the mutation rate without exposing cultures to the stress at any time during experimentation, this question cannot be directly tested.

Because of the limitations just described, we have chosen to approach the question from a different angle and propose a hypothesis that can be directly tested. We ask the questions, "If the environment could influence the mutagenesis of a particular gene(s), how would it do so? Specifically, what is the connection between the environment and specific genes and what is the further connection to mutation rates?"

*What is the connection between the environment and specific genes?* The answer to this question is: the regulation of gene expression. The environment, by providing nutrients or the lack of nutrients and by exposing cells to harsh conditions, influences the level of transcription of specific microbial genes depending upon the particular set of circumstances. For instance, extremes in temperature result in the induction of the heat shock or cold shock responses. Likewise, the lack of particular nutrients results in the induction of the stringent response. The major effector of the stringent response, produced by the *relA* gene product, is ppGpp, which serves to further enhance transcription of only those operons already derepressed by the specific starvation.

*What is the connection between transcription and mutation rates?* It is possible that increases in transcription can lead to increased mutation rates. During transcription, the nontranscribed strand is exposed as ssDNA while the transcribed strand is bound to the nascent mRNA in a DNA-RNA hybrid. Because ssDNA is more mutable than dsDNA, it follows that transcribed DNA and specifically the nontranscribed strand would be more

susceptible to damage such as the deamination of cytosine residues. In order to prove this, several labs demonstrated that mutation rates increase when transcription is induced (Brock,1971; Herman and Dworkin, 1971; Datta and Jinks-Robertson,1995).

*If the environment could influence the mutagenesis of a particular gene or set of genes, how would it do so?* A testable hypothesis is that the environment, by altering transcription in specific genes, can influence the mutagenesis of those specific genes. To test this hypothesis the following predictions were made and substantiated experimentally: (1) reversion rates to amino acid prototrophy should be highest in *relA*$^{wt}$ strains that accumulate ppGpp and in which the specific biosynthetic operon is maximally derepressed, compared to *relA2* strains that don't accumulate ppGpp in response to amino acid starvation; (2) down-regulated operons should have decreased mutation rates when ppGpp accumulates; and (3) a positive correlation should exist between mutation rates, ppGpp concentration, and mRNA levels.

To determine if increased transcription alone (without amino acid starvation) could account for the increased mutation rate in amino acid biosynthetic genes observed in ppGpp$^{+}$ strains versus ppGpp$^{def}$ strains, the *E. coli* chromosomal *leu* promoter was replaced by the IPTG-inducible *tac* promoter (Figure 23 and 24).

Reversion rates of the *tac*$^{P}$*-leuB* gene were measured in the recombinant 78AL, with and without IPTG. It became apparent after several experiments that the Luria-Delbrück zero method for mutation rate calculation was limited by the requirement for a reasonable number of negative plates out of the total number of plates per experiment. Forty cultures are plated for each condition in each experiment and a valid experiment should have at

least 5 positive or 5 negative plates. When 0.03 mM leucine was used to limit growth in the 78AL cultures the cell numbers reached at stationary phase were ~3 x $10^8$ cfu per culture. This number of bacteria if exposed to no IPTG usually resulted in 25-30 negative plates at 72 h and 20-30 negative plates at 96 h – both within the calculable range for the zero method. The same experiments conducted with 0.015 mM leucine resulted in ~1.5 x $10^8$ cfu per culture and ~30 negative plates at both 72 and 96 h – also reasonable for the zero method calculation of mutation rate. The overall *leuB*$^-$ reversion rate of 78AL without IPTG was ~1 x $10^{-9}$ reversions per genome per generation (Table 5).

When 1 mM IPTG was added to the cultures along with the inoculum in 0.03 mM leucine, ~10 negative plates were present at 72 h but none at 96 h; therefore, only the 72 h *leuB*$^-$ reversion rate could be calculated (~4 x $10^{-9}$; Table 5) and the 96 h reversion rate was estimated to be at least 9 x $10^{-9}$ but could not be calculated.

An interesting phenomenon was observed when the same cultures (0.03 mM leucine or 0.015 mM leucine) were exposed to IPTG at various times during growth, at the end of log-growth, or at various times after the end of log-growth, the number of negative plates at 96 h went up, allowing calculation of the 96 h *leuB*$^-$ reversion rate. Therefore, the effect of adding IPTG later was to reduce the overall mutation rate. Moreover, adding the IPTG after the end of growth allows one to distinguish growth mutations from those that occur in stationary phase, non-dividing cells. The interesting observed result was that the later the 1 mM IPTG was added, up to at least 24 h, the higher the 96 h reversion rate: ~5 x $10^{-9}$ if added at the end of growth, ~8 x $10^{-9}$ if added 2 h after the end of growth, and ~14 x $10^{-9}$ if added later than 2 h after the end of growth (Table 5).

In the parent strains, stringent response mutations occur immediately when the cells run out of leucine and ppGpp accumulates and transcription increases. These mutations are visualized as revertant colonies that appear on minimal medium plates devoid of leucine about 48 h after plating. It takes 30-40 h of growth from a single cell for a colony to become visible on minimal medium so at 48 h we observe reversions that occurred during growth as well as those that occurred within the first 10 h or so of leucine starvation. Any new reversions that occurred between 10 and 40 h after plating would be visualized at 72 h. In the parent strains there are usually no new revertants at 72 h indicating that the mutations occurred during growth or just after the end of growth. Statistical analysis revealed that the mutations occurred just after the end of grwoth (Wright, 1996).

The situation is very different in the recombinant strains with IPTG- induced reversions. In 78AL without IPTG the *leuB*$^{-}$ reversion rate appeared to remain constant during growth, and for the first 18 h after growth (visualized on plates at 48 h), as well as for the period between 18-42 h after the end of growth (visualized on plates at 72 h), and for the period between 42-66 h after the end of growth (visualized on plates at 96 h). Periodic mutation rates were calculated by counting only new positive plates at each subsequent time point and using $P_0' =$ (# negative plates)/(total # plates left negative after the previous time point). The growth reversion rate was estimated by dividing the 48 h cumulative reversion rate by 2 because one half of the cells present at the end of growth were present cumulatively for the entire period of growth. The effect of a constant 0.3 x

$10^{-9}$ reversion rate over the four time periods was an observed *leuB*$^-$ reversion rate at 96 h of $1.12 \pm 0.24 \times 10^{-9}$ (see Table 5).

When 78AL cells were exposed to IPTG after the end of growth, the *leuB*$^-$ reversion rate increased over the 96 h: the reversion rate during growth, assumed to be the same as in 78AL cells not exposed to IPTG (as the IPTG isn't added until after growth stops) went up to $0.9 \times 10^{-9}$ for 0-18 h after the end of growth and climbed to $1.8 \times 10^{-9}$ for 18-42 h after the end of growth, then went up even further to $9.9 \times 10^{-9}$ for 42-66 h after the end of growth, for a cumulative reversion at 96 h of $13.6 \pm 4.7 \times 10^{-9}$. This indicates that the majority of reversions occurred between 42-66 h after growth ended. In order to determine if the IPTG-induced reversions correlated with IPTG-induced transcription, *leuB*$^-$ transcript levels in 78AL stationary phase cultures at 24 h intervals for 96 h were determined in cells exposed to 1 mM IPTG for 3 h before plating and cells not exposed to IPTG. Without IPTG there was a low level of *leu* operon transcription that appeared to remain constant even in starving cultures (see Figure 31) and this correlated with a constant *leuB*$^-$ reversion rate. With IPTG, the level of *leuB* transcript increases immediately with IPTG addition (see Figure 28) and increased further over a 3 h period (see Figure 29), then increased slowly or remained constant until about 48 h at which time there was a significant increase in *leuB* transcript (see Figure 31). This increase in transcript level at 48 h correlated with the increase in mutagenesis between 42-66 h and the increase in revertants visualized on the plates at 96 h.

The conclusion that increasing transcription correlates with increasing mutation rates suggests that a range of increasing IPTG concentrations should yield an increasing range

of *leuB*⁻ reversion rates in 78AL. The expected result was achieved; however, the reversion rates overlap in some cases so further experiments with greater variation in IPTG concentration will be conducted. When the IPTG (0.1, 0.5 and 1.0 mM) was added during growth only the 72 h reversion rate could be calculated: the range was respectively ~2 x $10^{-9}$, ~3 x $10^{-9}$, and ~4 x $10^{-9}$ (Table 5).

In conclusion, the promoter replacement provides support for the hypothesis, that the specific derepression of the stringent response should lead to specifically directed mutations, because a difference in transcription level alone can account for the difference in observed mutation rates in cultures with and without enhanced transcription.

Alternative explanations of the observed results were considered, tested and determined not to be capable of accounting for all the results. One explanation is that the *leuB*⁻ allele could be leaky and the increased transcription associated with the stringent response in CP78, or with IPTG induction in 78AL, could lead to increased production of a partially functional LeuB protein (isopropylmalate dehydrogenase, EC 1.1.1.85). Therefore, cells with increased transcription would benefit from increased leucine production and would be expected to have a growth advantage such that these cells would continue to replicate during leucine absence, even if at a very low rate. A growth advantage would result in a false-high calculated mutation rate because the actual number of cells undergoing mutagenesis would be greater than the number at the time cells were plated. A phenomenon similar to that proposed here has been implicated in the adaptive mutations observed in the *lacZ* system of Cairns and Foster (1991) by Galitski and Roth (1996).

This explanation is especially reasonable considering that the *leuB*$^{-}$ point mutation is a base-substitution and would be predicted to result in a functional LeuB enzyme some of the time either from mis-transcription or from mis-translation. A prediction inherent in this explanation is that cells with increased transcription of a leaky allele would have a growth advantage and their cell numbers should increase over time in the absence of leucine, even if only slightly, and that even if the allele is leaky if no growth advantage is incurred in the highly transcribed cells, then it is of no consequence in the calculation of mutation rates.

The prediction was tested in the recombinant strain, 78AL, by counting the number of viable cells from 10 different plates at each time point from each of 2 different 40 culture experiments: 1 experiment without IPTG and 1 with IPTG added at the end of growth (Figure 27). The cell numbers not only didn't go up over 72 h, but in fact in the IPTG induced cultures, the numbers may have decreased. These experiments are tricky to perform because revertant colonies begin to appear at about 40 h and if their numbers are high enough they can skew the viable count results. So in cases where the revertant numbers were very high (~100-fold higher than those with no revertants; on 4 IPTG plates and 5 non-IPTG plates), those plates were left out of the calculation. In a repeat of this experiment (Figure 28) there does seem to be a higher number of cells per culture at 96 h of the IPTG-induced cells but this is due to increased death in non-IPTG cultures and more revertants in the IPTG-induced cells. This does not interfere with the mutation rate calculations because the final rates are calculated at 96 h and any revertant colonies that are visible at 96 h must have originated prior to 30 h before being visible; this would put

the mutagenic events at no later than 66 h and at that time, there was no difference in cell number.

Leakiness is considered not to occur at a sufficient level in *leuB*$^-$ to produce a growth advantage in cells undergoing higher rates of transcription and therefore can not explain the observed results.

A second alternative explanation is that CP78 is more robust than CP79 so that at the time of mutagenesis there are fewer CP79 cells and the mutation rate is falsely calculated to be lower than it might actually be. CP78 is a more robust strain and CP79 cells do not recover well from starvation; however, Wright (1997) found an increased reversion rate in the CP79 compared to the CP78 strain -- in the *pyrD* gene (Figure 4). During leucine starvation, in CP78 (ppGpp$^+$) transcription of the leu operon increases while transcription of the *pyr* operon decreases; whereas in CP79 (ppGpp$^{def}$) transcription of the *leu* operon only increases slightly and transcription of the *pyr* operon increases. The mutation rates correlate well with the levels of transcription: *leuB*$^-$ reversion rate is higher in CP78 than in CP79, but *pyrD*$^-$ reversion rate is higher in CP79 than in CP78.

The mutations observed in this system, for the most part, occur without replication (during amino acid starvation). It is noted however that cell division must occur after an appropriate mutation in order for the mutation to become immortalized. It is possible that an appropriate mutation on the transcribed strand would lead to the expression of a functional enzyme and would therefore lead to the synthesis of the missing amino acid, thus allowing replication. There are several mechanisms that can be envisioned to participate in transcription-dependent mutagenesis but as none have yet been tested, they

are discussed here simply as a few possibilities. Because ssDNA is particularly vulnerable to mutagenesis (Lindahl and Nyberg, 1974; Frederico, et al., 1990) it is likely that the act of transcription leads to increased deaminations and possibly depurinations especially on the non-transcribed strand (Beletskii and Bhagwat, 1996). In non-replicating cells, a mutation on the non-transcribed strand has to become a mutation on the transcribed strand before the reverted allele can be expressed and provide enough product i.e. leucine, to support replication and immortalization of mutation. Mechanisms that might provide for such a transfer of mutation may involve repair mechanisms that during nutritional stress become more error-prone. Feng, et al. (1996) demonstrated that mismatch repair enzymes decrease in concentration during nutritional starvation. Experiments in which different repair enzymes are deleted from CP78, CP79 and 78AL will enable the testing of several of these possibilities. It is also possible that a damaged base on one strand will cause the complementary base to become damaged at a higher rate than base-paired bases (Frederico, et al., 1990).

Another possibility is that torsional stress created during high rates of transcription may lead to strand breaks that are repaired incorrectly. To test this possibility, a temperature-sensitive *gyrB* mutation could be introduced into 78AL and the effect of increased torsional stress on the *leuB*$^{-}$ reversion rates examined.

There are several interesting questions that follow from the work described here: First, how will *leuB*$^{-}$ reversion rates in 79AL (*relA2*) compare with 78AL (*relA*$^{wt}$) mutation rates? If the effect is truly transcription-dependent and ppGpp-independent, they should be the same unless the mutations happen 48 h after plating, then the mutation

rate in 79AL should be lower because of decreased viability of *relA2* strains after 24 h. If some 79AL cells are able to grow on the plates because of scavenging from dead cells, then it is possible that the mutation rate in 79AL with IPTG will be higher than in 78AL, because 78AL cells don't die on the plates until about 96 h after plating. Secondly, there appears to be a correlation between time of IPTG addition and the level of increase in mutation rate (Table 5). Is there a time limit to the ability of the starving cells to respond to induction? What is the maximum mutation rate that can be achieved with IPTG induction and is there a similar maximum under natural conditions with ppGpp enhanced transcription? It should be possible to determine when most of the induced mutations are occurring and this would make it possible to determine the mechanisms that are most responsible for the specifically directed mutations associated with the stringent response.

## REFERENCES

**Alexeyev, M.F.** (1995) Three Kanamycin Resistance Gene Cassettes with Different Polylinkers. *BioTechniques* **18:**52-56.

**Ausubel, F.M., Brent, R., Kingston, R.E., Moore, D.D., Seidman, J.G., Smith, J.A., Struhl, K.** (1994-1997) Current Protocols in Molecular Biology. John Wiley & Sons, Inc.

**Beletskii, A. and Bhagwat, A.S.** (1996) Transcription-Induced Mutations: Increase in C to T Mutations in the Nontranscribed Strand During Transcription in *Escherichia coli*, *Proc. Natl. Acad. Sci.* **93:**13919-13924.

**Brock, R. D.** (1971) Differential Mutation of the β-Galactosidase Gene of *Escherichia coli*. Mutation Research **11:**181-186.

**Cairns, J. and Foster, P.L.** (1991) Adaptive Reversion of a Frameshift Mutation in *Escherichia coli*. *Genetics* **128:**695-701.

**Cashel, M., Gentry, D.R., Hernandez, V.J. and Vinella, D.** (1996) The Stringent Response, in Neidhardt, F.C., ed. in chief, *Escherichia coli* and *Salmonella* Cellular and Molecular Biology, ASM Press, Washington, D.C.

**Chung, C.T., Niemela, S.L., and Miller, R.H.** (1989) One-Step Preparation of Competent *Escherichia coli*: Transformation and Storage of Bacterial Cells in the Same Solution. *Proc. Natl. Acad. Sci.* **86:**2172-2175.

**Datta, A., and Jinks-Robertson. S.** (1995) Association of increased spontaneous mutation rates with high levels of transcription in yeast. *Science* **268:**1616-1619.

**Feng, G., Tsui, H-C.T., and Winkler, M.E.** (1996) Depletion of the cellular amounts of the MutS and MutH methyl-directed mismatch repair proteins in stationary-phase *Escherichia coli* K-12 cells. *J. Bacteriol.* **178:**2388-2396.

**Fix, D.F. and Glickman, B.W.** (1987) Asymmetric Cytosine Deamination Revealed by Spontaneous Mutational Specificity in an $Ung^-$ Strain of *Escherichia coli*. *Mol. gen Genet.*, **209:**78-82.

**Frederico, L.A., Kunkel, T.A. and Shaw, B.R.** (1990) A Sensitive Genetic Assay for the Detection of Cytosine Deamination: Determination of Rate Constants and the Activation Energy. *Biochemistry*, **29:**2532-2537.

**Galitski, T. and Roth, J.R.** (1996) A Search for a General Phenomenon of Adaptive Mutability. *Genetics*, **143:**645-659.

**Gay, P., Le Coq, D., Steinmetz, M., Berkelman, T., and Kado, C.I.** (1985) Positive Selection Procedure for Entrapment of Insertion Sequence Elements in Gram-Negative Bacteria, *J. Bact.* **164:**918-921.

**Hengge-Aronis, R.** (1996) Regulation of Gene Expression during Entry into Stationary Phase, in Neidhardt, F.C., ed. in chief, *Escherichia coli* and *Salmonella* Cellular and Molecular Biology, ASM Press, Washington, D.C.

**Herman, R.K., and Dworkin, N.B.** (1971) Effect of gene induction on the rate of mutagenesis by ICR-191 in *Escherichia coli. J. Bacteriol.* **106:**543-550.

**Kolter, R. Siegele, D.A., and Tormo, A.** (1993) The Stationary Phase of the Bacterial Life Cycle. *Annu. Rev. Microbiol.* **47:**955-874.

**Lindahl, T. and Nyberg, B.** (1974) Heat-Induced Deamination of Cytosine Residues in Deoxyribonucleic acid, *Biochemistry*, **13:**3405-3410.

**Luria, S.E., and Delbrück, M.** (1943) Mutations of bacteria from virus sensitivity to virus resistance. *Genetics* **28:**491-511.

**Marchuk, D., Drumm, M., Saulino, A., and Collins, F.S.**(1991) Construction of T-Vectors, A Rapid and General System For Direct Cloning of Unmodified PCR Products. *Nucleic Acids Res.* **19:**1154.

**Metcalf, W.W., Jiang, W., Daniels, L.L., Kim, S.-K., Haldimann, A., and Wanner, B.L.** (1996) Conditionally replicative and conjugative plasmids carrying *lacZα* for cloning, mutagenesis, and allele replacement in bacteria. *Plasmid* **35:**1-14.

**Metzger, S., Schreiber, G., Aizenman, E., Cashel, M., and Glaser, G.** (1989) Characterization of the *relA1* mutation and a comparison of *relA1* with new *relA* null alleles in *Escherichia coli. J. Biol. Chem.* **264:**21146-21152.

**Ohman, D.E.** (1988) Experiments in Gene Manipulation. Prentice Hall, Inc., Englewood Cliffs, NJ. pp. 49-51.

**Sambrook, J., Fritsch, E.F., and Maniatis, T.** (1989) Molecular Cloning A Laboratory Manual, 2nd edition. Cold Spring Harbor Laboratory Press, NY.

**Savić, D.J., and Kanazir, D.T.** (1972) The effect of a histidine operator-constitutive mutation on UV induced mutability with the histidine operon of *Salmonella typhimurium. Molec. Gen. Genet.* **118:**30-45.

**Travers, A.** (1984) Conserved features of coordinately regulated *E. coli* promoters. *Nucleic Acids Res.* **12:**2605-2618.

**Wright, B.E.** (1996) The effect of the stringent response on mutation rates in *Escherichia coli* K-12. *Molec. Microbiol.* **19:**213-219.

**Wright, B.E.** (1997) Does Selective Gene Activation Direct Evolution?, *FEBS Letters*, **402:**4-8.

**Wright, B.E., Longacre, A., and Reimers, J.M.** (*in preparation*) Specifically Derepressed Operons Have Higher Mutation Rates in *E. coli* K12.

**Wright, B.E. and Minnick, M.F.** (1997) Reversion Rates in a *leuB* Auxotroph of *Escherichia coli* K-12 Correlate with ppGpp Levels During Exponential Growth, *Microbiology*, **143:**847-854.

**Zacharias, M., Göringer, H.U., and Wagner, R.** (1989) Influence of the GCGC Discriminator Motif Introduced into the Ribosomal RNA P2- and *tac* Promoter on Growth-rate Control and Stringent Sensitivity. *The EMBO J.* **8:**3357-3363.

# IMAGE EVALUATION TEST TARGET (QA-3)

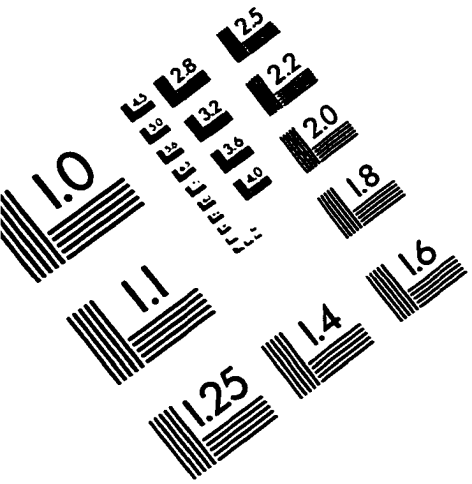


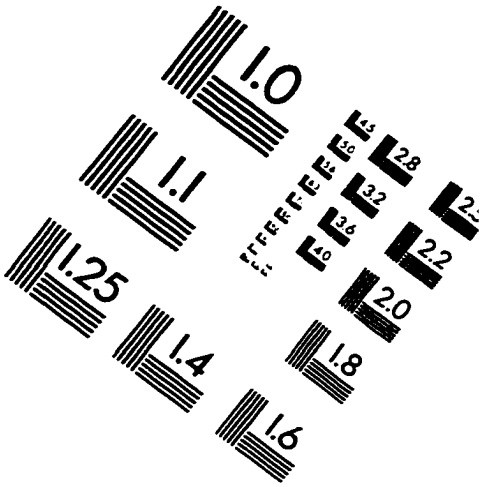


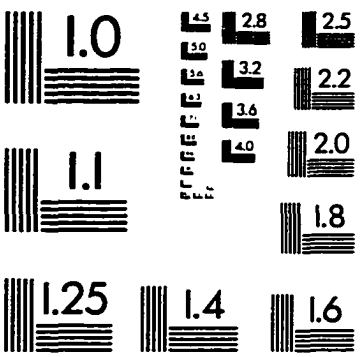


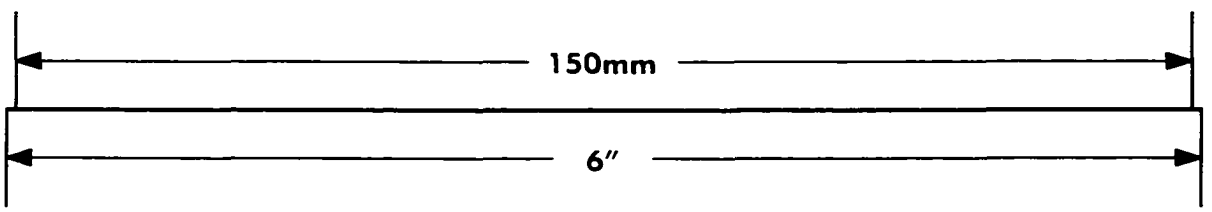


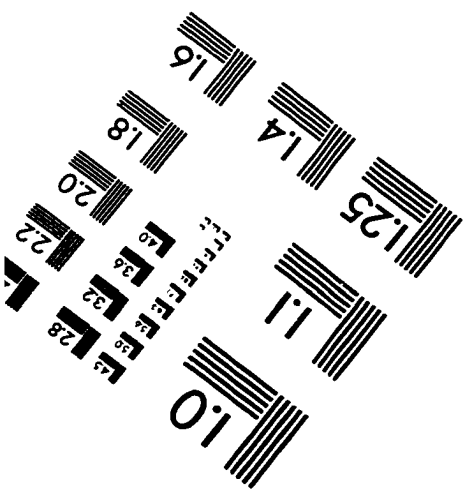


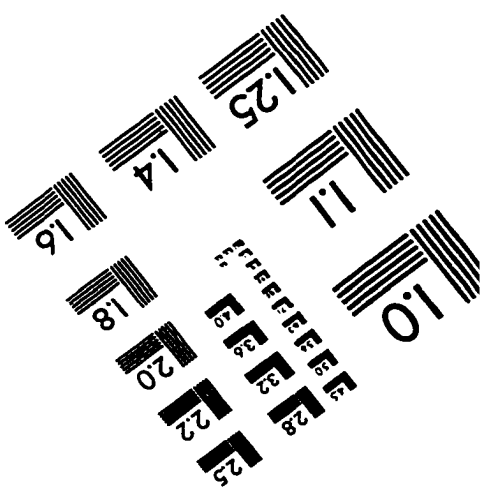


APPLIED IMAGE, Inc
1653 East Main Street
Rochester, NY 14609 USA
Phone: 716/482-0300
Fax: 716/288-5989